CHALMERS
UNIVERSITY OF TECHNOLOGY

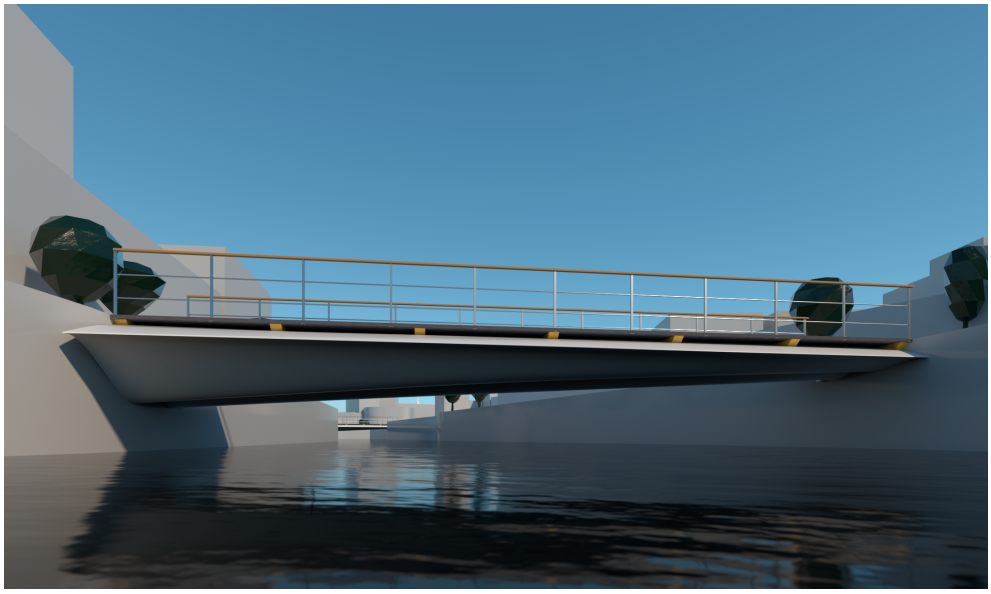

Reuse of decommissioned wind turbine blades in pedestrian bridges

An investigation of using wind turbine blades as structural members in pedestrian bridges.

Master's thesis in Master Program Structural engineering and Building technology

JOHANNA KULLBERG, DAVID NYGREN

Department of Architecture and Civil Engineering
CHALMERS UNIVERSITY OF TECHNOLOGY
Master's thesis ACEX30
Gothenburg, Sweden 2020

Master's thesis ACEX30

Reuse of decommissioned wind turbine blades in pedestrian bridges

An investigation of using wind turbine blades as structural members in pedestrian bridges.

JOHANNA KULLBERG, DAVID NYGREN

CHALMERS
UNIVERSITY OF TECHNOLOGY

Department of Architecture and Civil Engineering
Division of Structural Engineering
Lightweight structures
Chalmers University of Technology
Gothenburg, Sweden 2020

Reuse of decommissioned wind turbine blades in pedestrian bridges
An investigation of using wind turbine blades as structural members in pedestrian bridges

JOHANNA KULLBERG, DAVID NYGREN

© JOHANNA KULLBERG, DAVID NYGREN, 2020.

Supervisor: Georgi Nedev, Sweco Structures AB. Alann André, RISE
Examiner: Professor Reza Haghani Dogaheh, Department of Architecture and Civil Engineering

Department of Architecture and Civil Engineering
Division of Building Technology
Building Physics Group
Chalmers University of Technology
SE-412 96 Gothenburg
Telephone +46 31 772 1000

Cover: Design proposal of a pedestrian bridge where wind turbine blades are the main load bearing components.

Department of Architecture and Civil Engineering
Gothenburg, Sweden 2020

Reuse of decommissioned wind turbine blades
An investigation of using wind turbine blades as structural members in pedestrian bridges.
JOHANNA KULLBERG, DAVID NYGREN
Division of Structural Engineering, Lightweight structures
Chalmers University of Technology

Abstract

Wind energy is currently one of the fastest growing renewable energy sources. As a consequence, the amount of decommissioned wind turbine blades are expected to increase in a near future. The blades mainly consists of GFRP. The polymer in GFRP is most often a thermosetting polymer which, due to its complex composition, is both insoluble and infusible. As a result, waste management of the decommissioned blades are difficult and currently no viable sustainable recycling method of wind turbine blades exists. This thesis aims to investigate the possibilities to reuse the blades as structural members in pedestrian bridges. The blades are lightweight and high performing components and using the blades in bridges could lengthen the blades life cycle and handle a portion of the decommissioned turbine blades.

To achieve this a literature study was performed. This involved the theory of fibre reinforced plastics, the properties of the blades as well as guidelines and regulations on bridges provided in Eurocode and by Trafikverket. Together with experienced architects and engineers, different bridge concepts were developed. Based on the knowledge gained in the literature study, the concepts were evaluated in terms of aesthetics, simplicity of the construction, degree of maintenance as well as costs. The production method was also an important aspect considered as the part of the blade used in the bridge had a length of 20 m and a width of 3.6 m.

The final concept was further designed and a FE-model in BRIGADE/Plus were created. The FE-model showed that the deformation requirements were met but that the fundamental frequency were below 5 Hz. Further investigations are therefore needed in order to verify the acceleration.

Keywords: Wind turbine blades, GFRP, FRP, reuse, pedestrian bridge, sustainability, waste management.

Acknowledgements

We would like to acknowledge our supervisors Georgi Nedev at Sweco, Dr. Alann André at RISE and Prof. Reza Haghani Dogaheh at Chalmers for their enthusiasm and thoughtful guidance throughout the thesis. Also thanks to Dr. Martijn Veltkamp at FiberCore Europe who has supported us with great knowledge about building bridges in FRP. Furthermore, thanks to Anna Adamico at Anmet who generously shared their research. The thesis was carried out at Sweco Civil, Gothenburg. Thanks to them for creating a nice working environment and to all the colleagues for making us feel welcome.

We would also like to thank our opponents Viktor Norbäck and John Ek. By taking time and read our thesis they gave helpful feedback which developed the thesis further.

David Nygren and Johanna Kullberg, Gothenburg, June 2020

Contents

List of Figures

List of Tables

List of Acronyms

FE	Finite Element
FRP	Fibre Reinforced Polymer
GFRP	Glass Fibre Reinforced Polymer
CFRP	Carbon Fibre Reinforced Polymer
HMCF	High Modulus Carbon Fibres
HSCF	High Strength Carbon Fibres
ISAR	Inverse Syntetic Aperture Radar
PAN	PolycrylonitrilePAN
UD	Unidirectional

1
Introduction

According to the Swedish energy authority, Sweden's energy production should be 100% renewable by 2040 (Energimyndigheten, 2019). Wind energy, which is currently one of the fastest growing renewable energy sources is therefore expected to increase. The lifetime of a wind turbine is approximately 20-25 years, which will lead to a large amount of decommissioned turbines in a near future (Beauson and Brøndsted, 2016). According to Andersen et al., 2016, the annual amount of blade waste material is estimated to 28 100 tonne in 2034, in Sweden only. In Europe the amount is estimated to 50 000 tonne per year in 2022 (Beauson and Brøndsted, 2016). In figure 1.1, a simulation of the expected increase in blade waste until 2050 is shown. As can be seen, Europe will meet the end-of-life problem before the other regions as large scale wind farms was established here earlier.

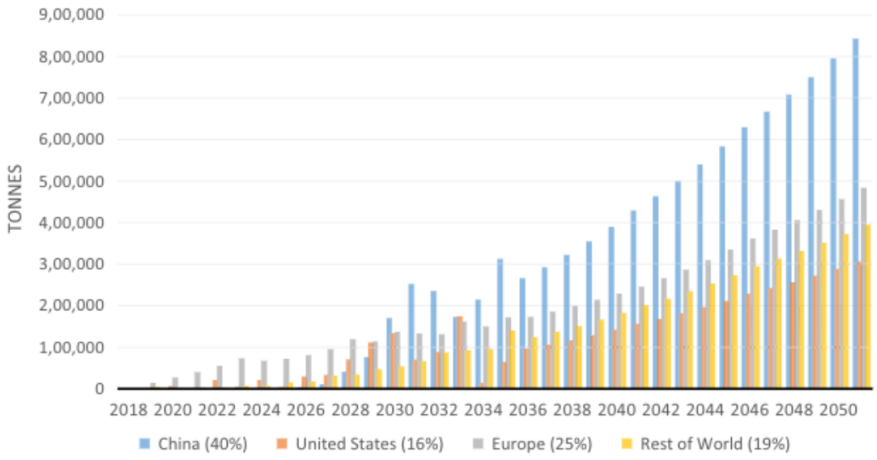

Figure 1.1: Estimated annual wind turbine blade waste projection, in tonnes. The assumption is based on data after 2014 with a moderate growth rate scenario. (Liu and Barlow, 2017).

The blades mainly consist of Glass Fibre Reinforced Plastics, GFRP. Currently there is no sustainable recycling method for these. In addition, new strict EU directives against landfill have been legislated which further complicates the waste management. If the end-of-life treatment is not taken care of in a sustainable way, wind energy is not a fully sustainable solution. Therefore, new solutions to take care of this growing issue must be developed. It is important to find cost effective and viable solutions to reuse these composites to increase the lifetime of the product. It

is mainly the possibilities to reuse wind turbine blades as structural members in a pedestrian bridge that will be evaluated in this theses. This could contribute to an increased circular economy which is one important aspect to reach the climate goals and thereby reduce the amount of emitted CO_2.

1.1 Aim

The aim of the master thesis is to create a bridge concept where wind turbine blades are the main structural and load bearing components.

1.2 Problem statements

First of all, different bridge concepts where wind turbine blades are the main load carrying structure will be investigated. To do so, it is important to learn about the material and to guarantee that the load carrying capacity fulfills the requirements. Different design proposals will be evaluated with the basis in the current regulations. A challenge within the project is to create a good model of a blade, as information of the dimensions and material composition is kept as classified information by the producers.

To easier get an overview of which problems that needs to be handled in order to achieve the general aim, following objectives has been listed.

- Characterization of the capacity of the material to ensure a safe design.
- Investigate the demands and requirements from the users as well as the regulations provided by Eurocode and Trafikverket.
- Investigation and development of different bridge concepts where wind turbine blades are the main load carrying structure.
- Create a FE-model of a blade to verify the feasibility of the design.

1.3 Method

Initially, a literature study was performed to gain knowledge regarding the blades in terms of its material composition as well as its mechanical properties. The requirements and demands on pedestrian bridges were also investigated in order to come up with reasonable bridge concepts. The approach was to come up with as many possible bridge concepts as possible. To improve this process a brain-storming session with Sweco Architects was arranged. This was a way to include additional aspects to the concepts, mainly in terms of aesthetics. To find the most suitable concept the advantages and disadvantages of each concept were listed. Based on these as well as consultation with experts, one final concept was chosen.

After one final concept was chosen, a FE-model was generated. The model were based on the SNL100-00 by Griffith and Ashwill, 2011. The blade was modelled

in Rhino 6 and then exported to BRIGADE/Plus where the FE-analysis was performed.

Finally, the bridge was further designed in terms of bridge deck, boundary conditions as well as all the crucial connections and details.

1.4 Limitations

Currently, the most commonly used wind turbine blade in Sweden is Vestas V90 (Carlstedt, 2016). These 2 MW turbines has a length of 44 m. The idea was therefore to base the design of the pedestrian bridge on this type of blades. However, secrecy from the producers has led to that the exact composition and dimension of these blades are not available. Instead the blade model used in this thesis is based on a blade called the SNL100-00 (Griffith and Ashwill, 2011). The SNL100-00 has a total length of 100 m and hence it was scaled down to half. A comparison with the 18.5 m long Vestas V27 (Abdillahi, 2011), shows that this assumption is conservative.

The bridge was assumed to be located in Sweden and the bridge will be designed after the requirements and regulations that apply here.

The study is done in a conceptual phase. Hence, the wanted level of detail is to see how the blade works when exposed to the loading that it would as a bridge. Thus, the blade material is through lamination theory modelled as an orthotropic homogeneous material, which does not give an exact response for each layer and fibre but shows the general behavior. For the same reason, the loads from service, bridge deck and other details are applied directly to the blade instead of modelling the bridge deck and all its connections and details.

2

Fibre Reinforced Polymers

The usage of Fibre Reinforced Polymers, FRP, within the field of civil engineering is on the rise. Due to the materials superior strength to weight ratio compared to conventional building materials, FRP offers a lot of advantages (Ascione et al., 2016). FRP are a composite material. The definition of a composite material is two or more materials, with different properties that creates a new material. The properties in the composite can be tailored to fully fit the specific requirements. Composites usually has a reinforcement material, known as the dispersed phase and a continuous material, the matrix. The material composition in FRP are, as the name reveals, fibres and polymers.

In wind turbine blades the dispersed phase consists of E-glass fibres and the matrix is a thermosetting polymer. Glass fibres provides high strength at an economically profitable cost to the composite, in comparison to the more expensive but more high performing carbon fibres. The thermosetting polymer can for instance be polyester, vinyl ester or epoxy based resin (Beauson and Brøndsted, 2016). Thermosetting polymers are in some extent incombustible which has led to a problematic waste management. However, thermosets are still widely used since they are cost-efficient compared to the more recyclable thermoplastic polymers.

2.1 Matrix

The matrix transfers the stresses between the fibres and works as a protective coating and resistance against the surroundings for the fibres. The matrix consists of resins, fillers and additives where the main part is resin (Potyrała et al., 2011). As previously mentioned, the resin in GFRP are most often a thermosetting polymer. A polymer, often referred to as plastics, is a chemical chain consisting of monomers. The thermosetting polymer is created by cross-linking of linear polymers. Cross-linking means that the polymer chains are bonding in other locations but the ends and thereby a three-dimensional network is created. The network is bonded by covalent bonded atoms. Due to this strong bonding the thermosets are both insoluble and infusible. These properties make it hard for the current waste management methods (Kulkarni, 2018), which is further described in section 2.8. Thermoplastic polymers would be a better option in terms of recycling but currently they are not an economically viable option. This is mainly due to the high viscosity of the unhardened thermoplastic polymer. It leads to a more complex production since they need to be molded at a higher temperature and pressure, and the production cost

is thus higher in comparison to thermosets. In addition, the thermoplastics generally show worse mechanical properties compared to the thermosets (Boogh and Mezzenga, 2000).

The most commonly used thermoset polymers are polyester, vinyl ester, phenolic and epoxy based resin (Potyrała et al., 2011). These are all examples of organic polymers. The choice of resin is mainly dependent on the desirable strength, stiffness, toughness and durability. The second order glass transition temperature also has a big impact in the choice of the resin. This is since a service temperature close to this temperature, will lead to significantly creep and loss of stiffness (Clarke, 1996). In addition to the resin, fillers are used in the matrix to reduce the amount of fibres and resin. This is an effective way of reducing the cost. Furthermore, additives are added to improve the performance of the matrix (Potyrała et al., 2011).

2.2 Fibres

The fibres constitutes the dispersed phase in the composite and can be compared to the reinforcement in concrete. The fibres are the component that contributes to the strength. The strength is proportional to the amount of fibres. This applies to a fibre volume of approximately 70% whereas after this there might be an insufficient amount of resin. An insufficient amount of resin might lead to dry areas and inadequate support for the fibres. The strength is also depending on the fibre-layout. Either the fibres can be continuous or discontinuous. If the fibres are continuous it means that the fibres have long aspect ratios, which describes the ratio between length and diameter of the fibres. The continuous fibres also have a preferred orientation which usually results in a higher strength and stiffness compared to the discontinuous fibre composites. In contrast the discontinuous fibre composites has short aspect ratios and a random orientation. In theory the discontinuous fibre composites could approach the same properties as continuous, but this is hard to perform in practice. This mainly depends on the difficulties to maintain the fibres aligned (Campbell, 2010). The two most commonly used fibres are glass and carbon, that are shown in Figure 2.1.

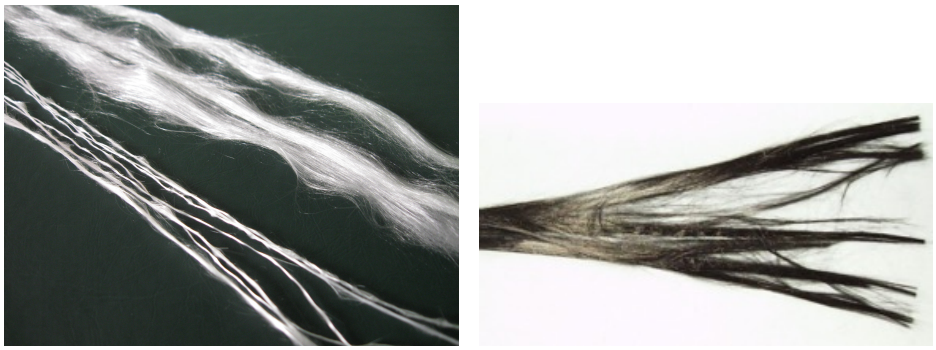

(a) Close up of glass fibres (b) Close up of carbon fibres

Figure 2.1: Continuous glass and carbon fibres (Wikipedia Commons, 2009).

2.2.1 Glass fibres

Continuous glass fibres are the most commonly used reinforcement in wind turbine blades, mainly due to the relatively low cost (Campbell, 2010). There are substantially two types of glass fibres, Electrical graded glass (E-glass) and Structural graded glass (S-glass). S-glass is far more expensive which has led to E-glass being generally used, even though S-glass fibres provides a higher strength. Besides the low cost of glass fibres its advantages are high tensile strength and chemical resistance. However, glass fibres have a lower tensile modulus compared to carbon fibres.

The process of making glass fibres is basically to expose the glass to high heat and then quickly cooling. The primary components in glass fibres are silica sand, limestone and boric acid. The raw materials are blended and then melted. The molten mix is extruded through bushings which generates the fibres. The fibres are then quickly cooled with water in order to prevent crystallization and an amorphous structure is created. In order to get proper compatibility with the matrix, a coupling agent is added. The coupling agent is dependent on the resin that will be used. Then they are collected and wound onto spools (Campbell, 2010). The main steps can be seen in Figure 2.2 and the finished product in Figure 2.1(a).

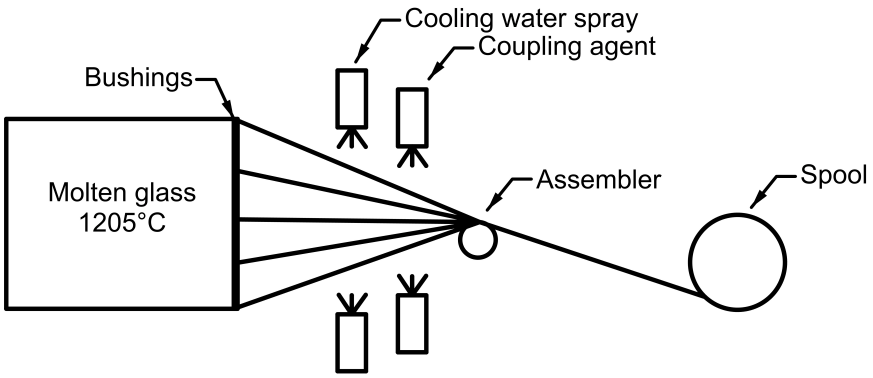

Figure 2.2: The production process of glass fibres.

2.2.2 Carbon fibres

Carbon fibres has a superior stiffness and strength-to-weight ratio compared to glass fibres. Therefore, carbon fibres are more suitable in larger blade constructions when these are desirable properties. The carbon fibres also have very good capacity in terms of fatigue and corrosion resistance. The disadvantages are mainly the increased cost and a lower damage tolerance in terms of ultimate strain (Campbell,

2010). The carbon fibres are shown in Figure 2.1(b).

The precursors used to create carbon fibres are either petroleum-based pitch, rayon or polyacrylonitrile, PAN. 90% of all carbon fibres are produced with PAN since the yield strength obtained is twice as big compared to the rayon produced fibres (Khayyam et al., 2020). In order to create the carbon fibres, the PAN copolymer is stretched and spun. To stabilize the bonding between the atoms the fibres needs to undergo a chemical alternation through oxidation. This process is executed at temperatures around 200-300°C. Thereafter the fibres are passing through two main processes. These are carbonization at 980-1595°C and finally graphitization at 1980-3040°C. In addition, the surface needs to be oxidized to create better bonding properties with the matrix (Campbell, 2010). The process of producing carbon fibres is both highly energy demanding and costly.

2.3 Production process

According to Ascione et al., 2016 the two most used production methods for FRP in civil engineering are pultrusion and Vacuum Assisted Resin Transfer Molding, VARTM. Wind turbine blades are often made with either VARTM or the prepreg method. VARTM is the most widely used whereas prepreg is the technology of choice by Vestas which is the largest producer of wind turbines for Sweden (Mishnaevsky et al., 2017). The choice of production process is mainly influenced by the economic and the intended usage. Depending on the required production volume, different techniques are more suitable than others. Alternative techniques that are commonly used are compression molding, filament winding and hand lay-up (Ascione et al., 2016).

2.3.1 Pultrusion

As the name reveals, pultrusion is a method consisting of simultaneous pulling and extruding. Pultrusion is a fully automated method. The first step in the manufacturing process involves fibre rovings that are pulled through a tension roller which intertwines the fibres. The fibres are then impregnated and saturated in resin. There are several kinds of resins but the most used in pultrusion is polyester. The saturated fibres are then pulled through a heated mold where the material is cured and formed. The formed composite is then continuously pulled by the reciprocating units. The last step in pultrusion is to cut the material into desirable lengths which is done by a so-called cut-off saw. Pultrusion is a resource saving, time and energy efficient production method and is therefore widely used (Joshi, 2012).

2.3.2 VARTM

VARTM is a manufacturing process which is performed in a closed mold. By pressurizing the mold into vacuum, the resin flows easier and is spread more evenly. The vacuum also contributes to a uniform compression which results in a consistent fibre volume fraction. Due to the limited pressure differences between the outer air

and inside the mold, it is important to have a resin with low viscosity. This is to get a sufficient flow of the resin. Another aspect to consider in VARTM is to avoid air leakages. Air leakages could cause inadequate resin flow and cause voids in the material. For high performance composites the mold needs to be heated in order for the resin to flow properly (Hsiao and Heider, 2012).

2.3.3 Prepreg

Prepreg is a technology developed by the aircraft industry that utilize fibres that are pre-impregnated with resin. Prepregs simplify the manufacturing process as the fibre sheets are workable and does not require extra resin (Wardle, 2000). For parts that have thickness variations, the prepreg technique are less keen to resin variations and defects. The prepreg production process could either be with an autoclave or an Out-Of-Autoclave, OOA. Using an autoclave ensures a higher production quality and a faster curing. The OOA prepregs removes the risk of the autoclave being a bottleneck, as well as it does not need the expensive autoclave oven. The prepreg fibres sheets are made of woven or knitted fabrics. The fibre sheets are coated in resin that is partially cured. These sheets are frozen to -18°C to stop the curing process and can be stored like this up to three months. As the fibres are to be put in their mold, they are first thawed to room temperature and cut into shape. As they have been positioned in the mold, a release film is laid on top along with a breather cloth that absorbs excess resin. For curing, the part is put in a vacuum bag or in an oven if it is an autoclave. During the curing the resin distributes itself evenly within the component (McIlhagger et al., 2015).

2.4 Laminate

Fibre reinforced polymers are considered an orthotropic material. This means that the composite has different properties in three different perpendicular directions. This is influenced by the orientation of the fibres (Campbell, 2010). In order to control the mechanical properties, the fibres are often arranged in laminates as a way of controlling the lay-up sequence. A laminate consists of several laminae, also known as a plies, that are bonded together and stacked on top of each other. A lamina is made of either unidirectional fibres, a mat or by a woven fabric combined with a matrix. By positioning the plies as laminates, the strength and stiffness can be optimized for specific load conditions. In Figure 2.3, two types of laminates are shown. The left picture shows a unidirectional laminate since all the plies are arranged in the same direction. The right picture describes a cross-plied stacking sequence, which gives the laminate a quasi-isotropic response (Potyrała et al., 2011). Due to the complex structure of the material, lamination theory is often used to analyse the behaviour. This is further described in subsection 6.2.1.

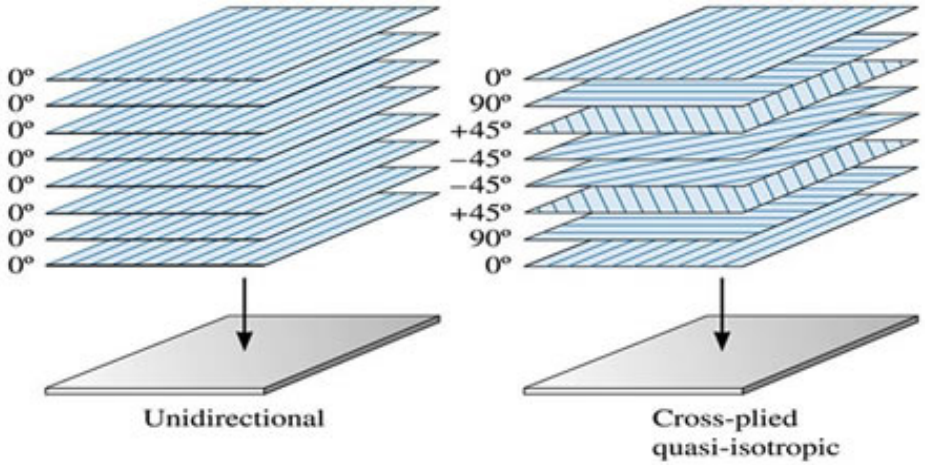

Figure 2.3: The lay-up of laminates. In the left picture all the fibres are arranged in the same direction which results in a unidirectional laminate. In the right picture the fibres are arranged with different fibre orientations which results in a cross-plied, quasi-isotropic laminate (Quartus Engineering, 2019).

2.4.1 Unidirectional lamina

The definition of a unidirectional lamina is that all fibres in the matrix are oriented along the same axis and the highest material properties is obtained in the direction of the fibres. In the other directions it is the matrix that determines the stiffness. This results in a highly orthotropic behaviour (Clarke, 1996). Since it is mainly the fibres that provides strength to the composite, the more fibres that are oriented in the load direction, the stronger it gets in that direction. The unidirectional stacking sequence hence results in maximized flexural strength in the fibre direction, but a lower capacity in the other directions.

2.4.2 Fabrics

Fabrics are often the base material used in a lamina. A fabric is created through assembly of long fibres to create a sheet. The fabric is categorized depending on the orientation of the fibres.

If a quasi-isotropic response is required, woven fabrics are an alternative. Even though the stiffness and strength in the main direction is lower compared to unidirectional laminae, woven fabrics are better if the direction of the loading is varying. The fabrics are created by interlacing yarns, with the horizontal fibres called warp and the transverse called weft. The angle between the warp and weft yarn is typically 90°(Gowayed, 2013). The fibres could be placed in many different patterns. Depending on the desired properties different weave methods are used. The most common are the plain, twill and satin weave styles and are described below. The weave styles have different amounts of crimp, which is the bending of fibres when they cross each other. Crimp can affect the mechanical properties. A too high level of crimp results in reduced mechanical properties.

2.4.2.1 Plain weave

A plain weave is characterized by a symmetrical pattern and uniform strength in both the in-plane directions. The pattern created is similar to that of a chessboard. This fabric has a high level of stability, meaning it is good at maintaining its weave angle and fibre orientation. The plain fabric is one of the more commonly used fabrics. The plain weave is suited for more simple shapes, as its stability makes it difficult to form. Furthermore, when it comes to thicker fabrics the level of crimp could be a problem. The pattern can be seen in Figure 2.4

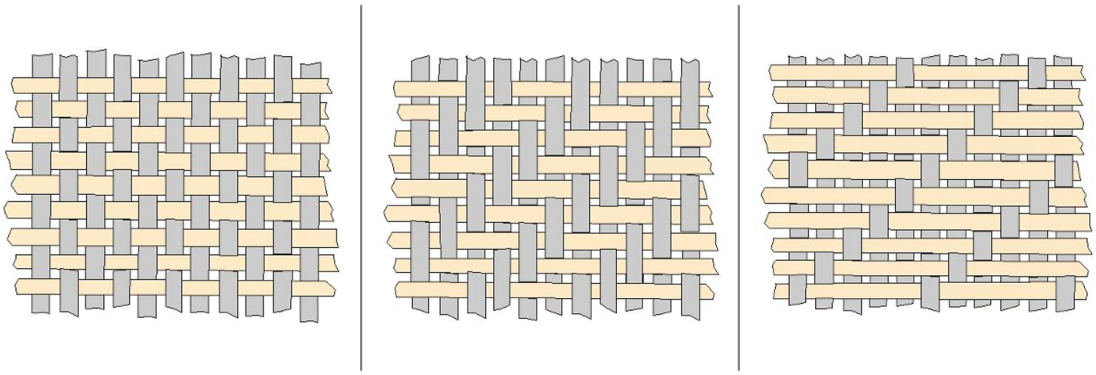

Figure 2.4: A plain (left), twill (middle) and satin (right) weave (Fibermax Composites, n.d.).

2.4.2.2 Twill weave

The twill fabrics are a middle ground between the plain fabric and the satin fabric. In contrast to the plain fabric, the twill is not as symmetrical. Instead of interlacing the warp and weft every other time, at least one warp is weaved under and above two or more wefts. This leads to a reduced crimp and hence a smoother surface, but also a lower stability and better formability than the plain weave. The weave pattern of the twill weave can be seen in Figure 2.4.

2.4.2.3 Satin weave

Satin weaves are produced with the aim of high formability and less intersections of warp and weft. Commonly there is between 4-8 fibres passed between each intersection, the pattern can be seen in Figure 2.4. This creates an asymmetric weave. If stacked in several layers, care must be taken in the direction of the fibres as it can lead to instability. The advantage of the satin weave is that it can be used in more complex parts because of its formability. The fabric has a smooth and seamless look. As the fibres in a satin weave runs longer, thicker fibres can be used without crimp.

2.5 Cores

In many FRP structures, a core is used in the middle of the FRP layers in order to optimize the structure. The core could either work as a form to the FRP composites, or as a structural core that is load bearing. The core could either be out of foam, honeycomb or a solid material. Together with the FRP laminates or woven fabrics, a sandwich construction is created. The structure becomes both stronger and stiffer compared to a laminate without a core and is characterized by its low weight. GFRP are placed under and above the core with structural adhesives in between. It is important that the adhesive layer is sufficient. Otherwise there is a risk of delamination due to the shear forces. By combining the materials as a sandwich structure the utilization of the materials are optimized (Reis and Rizkalla, 2008). Important properties for a structural core is for instance low density and high shear strength (Clarke, 1996). For non-loadbearing cores the high strength is not as necessary, but a sufficient thickness is needed in order to increase the bending stiffness.

2.5.1 Foam core

The foam is created by combining different sorts of plastics. Some commonly used plastics are polyurethanes, rigid polyvinyls and polymethacrylimides, PMI. One way to increase the structural properties of the foam is to add short glass fibres, reinforced foam. Another way is to create a sandwich structure out of the foam itself. The foam then has a solid surface with a cellular core, structural foam. The density of the foam is around 5 kg/m^3 (Clarke, 1996).

2.5.2 Honeycomb core

If a light-weight structure is desirable, honeycomb core could be a good alternative to achieve this. The shape of the core is typically hexagonal, similar to the natural beehive and hence the name, see Figure 2.5. The shape of the core reduces the needed material and hence the weight and cost. The honeycomb could either be made of Kraft paper or thermoplastics if a lower strength is acceptable. If the core needs to provide structural capacity, the core could instead be made of aluminium or FRP.

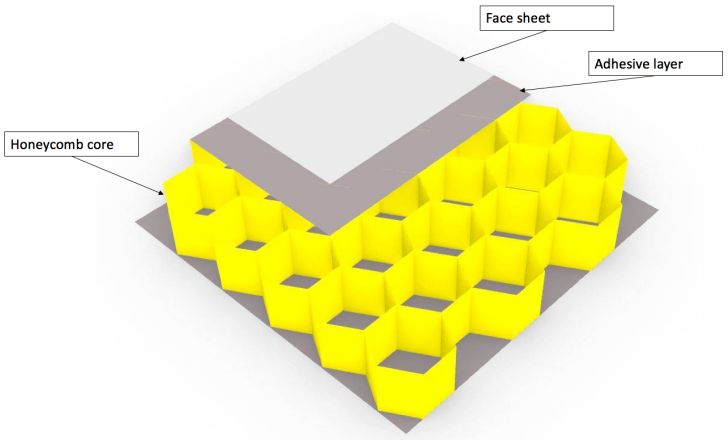

Figure 2.5: The shape of the honeycomb core. On top and bottom of the core the face sheet is placed with an adhesive layer in between.

2.5.3 Solid core

Due to the solid structure, the contact area between the core and the laminate becomes higher than in the honeycomb. This results in a higher distribution of the stresses. The most important parameters of a solid core in a sandwich structure is its weight and strength (Clarke, 1996). A widely used solid core is balsawood. Compared to foam cores, balsawood provides high compression and shear strength. Balsawood also provides a great resistance against fatigue. These advantages in combination with a low cost has led to balsawood being a widely used core material (Black, 2003).

2.6 Mechanical and physical properties

FRP are known for its high strength-to-weight ratio. A comparison between conventional building materials are shown in Table 2.1. One drawback with FRP are that they often show brittle behavior (Potyrała et al., 2011). This means that the material has an elastic response until collapse and insignificant plastic deformation takes place. This needs to be included in the design and according to Clarke, 1996, a serviceability limit state needs to be reached before the ultimate limit state.

The fibre volume fraction, type and orientation of the fibres as well as the matrix are all examples on factors influencing the thermal expansion coefficient. The coefficient is significantly higher in the transverse direction compared to the longitudinal. The thermal coefficient of the polymer is in the order of $100 * 10^{-6}$, which corresponds to an higher order compared to other commonly used building materials. Consequently, this needs to be considered when a hybrid structure is considered. Due to the properties of the polymer the composite receives a low thermal conductivity which also leads to good thermal insulating properties (Hollaway, 2010).

Table 2.1: Parameters for composite materials and commonly used construction materials (*CROW-CUR 96*, 2019), (Muniz and Bansal, 2009), (*SS-EN 1993-1-1*, 2005), (*SS-EN 14080*, 2013).

Material	Young's modulus [GPa]	Tensile strength [MPa]	Shear modulus [GPa]	Density [kg/m^3]
S-glass	86.9	4890	-	2460
E-glass	73.1	2750	30	2570
UD GFRP	20-40	520-1400	5.4	1920
HMCF	436	4210	27	1840
HSCF	238	3600	50	1790
UD CFRP	100-140	1020-2080	7.2	1310
Steel S355	210	490	81	7850
Timber GL30c	13	30	0.65	430

2.7 Durability

Depending on where the wind turbine is placed it is exposed to different types of surroundings. It can for instance be in a marine and moist environment which increases the risk of corrosion. It can be an alkaline environment which also influence the durability of the material. Besides the extreme wind that affects the blades it also has to resist UV-radiation, freeze-thaw cycles as well as lightning strikes.

When designing a structure, it is important to guarantee that the durability is sufficient. Some of the most important aspects according to Clarke, 1996 are:

- Intended use of the structure
- Required performance criteria
- Expected environmental conditions
- Intended maintenance during the lifetime of the structure

According to Potyrała et al., 2011, there is not enough documented data regarding the long-term effects of FRP composites. This results in an uncertainty regarding the durability. However, FRP are known to have good resistance against corrosion and their capacity to withstand harsh environments are proven to be good, compared to conventional building materials. The most crucial parameter in terms of durability is the capacity of the matrix to work as the protective coating to the fibres. In presence of moisture and corrosive environments the polymer is degrading, which eventually will affect the fibres (Potyrała et al., 2011). The glass fibres are especially sensitive to alkalies (Hollaway, 2010). An alkaline environment is one where the pH-value is higher than 7, a basic environment.

As previously described the polymer is composed by cross-linked polymers which are connected through covalent bonded atoms. The UV light is able to cleave these bonds. A consequence of this is embrittlement and yellowing. One way to reduce this effect is to add UV stabilizers in the polymer (Hollaway, 2010).

Studies on GFRP reinforcement bars exposed to long term aggressive environments has been done by D'Antino et al., 2018. These studies show that the exposure cause a significant reduction of the tensile strength. These aggressive environments are e.g. humidity, alkaline solutions and salt solutions. In alkaline environments, which is the most aggressive, only 20% of the residual tensile strength can be accounted for. According to D'Antino and Pisani, 2019, GFRP are a linear viscoelastic material and creep is expected. Because of this, long term loading should not exceed 40% of the tensile capacity. The deformation due to creep is generally small, because the relatively low Young's modulus and thus a small part of the tensile capacity is used. Most of the previous studies on creep comes from naval, mechanical and aeronautical applications. However, the FRP used in civil engineering shows better creep properties compared to these. This is mainly due to the fibres used having better viscous properties (Ascione et al., 2012).

2.8 Waste management of GFRP

The European waste framework directive has developed a waste hierarchy to handle the waste in a sustainable way (European Commission, 2019). According to the directive, the primary measure is to prevent the occurrence of waste. Otherwise, the waste should be reused, recycled, recovered and ultimately disposed, see Figure 2.6. Apart from preventing the waste, the different levels in the waste chain corresponds to the extracted value from the waste.

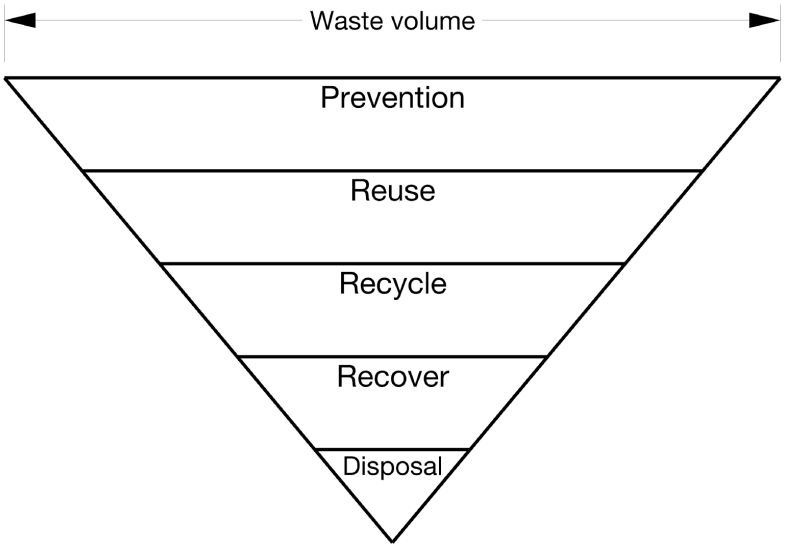

Figure 2.6: The waste hierarchy according to the European waste framework directive (European Commission, 2019).

GFRP consists of up to 75% thermosetting polymers which makes the recycling process complicated (Yazdanbakhsh et al., 2018). Due to its composition they are neither soluble nor fusible (Giorgini et al., 2016). In addition, if a sandwich structure is to be recycled, a mixed waste management is required due to the varying

materials. All these factors have led to that the existing waste management are having troubles to handle the GFRP waste in a sustainable way. In addition, the market price of new glass fibres is so low that there is no economic profit to use recycled fibres (Van Oudheusden, 2019). However, there are some industrial scale solutions that will be further explained.

There are mainly three reasons for replacing wind turbines. The first one is due to aging. The second reason is relative aging. This means that due to newer techniques the turbines could be more optimized and therefore they are out of age. The third and last case of decommission is recycling due to electricity certificate system. The aim of this certificate system is to increase the amount of produced energy. The national goal is to produce 48 TWh by 2030. Producers gains one certificate per MWh and by selling these they make an extra profit. This leads to an additional bonus to increase the production which is mainly done by increasing the size of the blades (Energimyndigheten, 2014). Consequently, many blades are replaced before they have reached the end of their life span.

2.8.1 Reuse

Reuse means to either extend the products lifetime, or to reuse it as something else by taking advantage of the products original design purpose. According to Beauson and Brøndsted, 2016, refurbishing is the most promising solution for decommissioned wind turbine blades. This solution is also consistent with the European waste hierarchy where reuse is the second best alternative. According to F. Sayer et al., 2009, the blades shows good mechanical properties after 18 years in service and refurbishment is therefore considered as a possible solution. In addition, handling the waste is an expense for the manufacturers and producers. To reuse the blades could instead lead to a secondary market. There is also a lot of labour involved in the production of new wind turbine blades. Thus, a secondary market that reuses old blades could instead be profitable.

To find a new application of the waste is contributing to a circular economy. This is desirable since it could limit the use of resources. A company in Poland, Anmet has done a full scale test of decommissioned blades (Appendix D). The results show that the blades still have a lot of capacity left. There is also a company in the Netherlands, Superuse-Studios, working on how to reuse the blades. In Figure 2.7 two suggestions of new applications for the blades can be seen. Other proposals of reuse will be further described and evaluated in chapter 10.

Figure 2.7: Playground and benches in Rotterdam designed by Superuse Studios made of decommissioned wind turbine blades. Photo: Denis Guzzo.

2.8.2 Recycling

Recycling is a process that converts waste material into new materials, that can be used instead of fresh raw materials. The different recycling methods could be divided into three main categories: mechanical, thermal and chemical recycling. However, almost all methods start with mechanical recycling. This is due to the size of the components that needs to be reduced before other recycling methods are applicable (Van Oudheusden, 2019).

2.8.2.1 Mechanical grinding

The intention with mechanical grinding is to divide the composite into its original components, fibres and resin. The method consists of three main processes: shredding, grinding and classifying. The first step, shredding, aims to divide the composite into smaller pieces. These pieces are then grinded. Finally, the fragments are classified in an attempt to distinguish the fibres and the matrix. The problem with mechanical recycling is that the process does not achieve a complete separation between the resin and the glass fibres (Ortegon et al., 2013). Therefore the result is classified as either a matrix rich powder or a fibre rich powder, mainly dependent on the sizes of the fractions (Vijay et al., 2016). In addition, the fibres have a significant loss of its mechanical properties (Yazdanbakhsh et al., 2018). However, the powder can be used in the cement industry to create cement kiln (Beauson and Brøndsted, 2016). Other suggestions for the shredded composites are to use it as reinforcement in concrete and polymer composite. This has however turned out to be very challenging since there is no adherence between the shredded composites and the new polymer. The reason is that the recycled fibres still are covered in old matrix material which complicates the new adherence.

Mechanical grinding is a cheaper recycling process compared to the other methods, mainly since no advanced equipment is needed. It also has the potential to handle large amounts of waste. The main drawback with grinding is the loss of strength and capacity of the fibres. Moreover, there is currently no profitable way of use the products created through grinding. The process also generates up to 40% waste

material that is of no use (Ierides et al., 2019).

2.8.2.2 Combustion

The process of combustion is to burn the material in a controlled environment and thereby a part of the embedded energy can be recovered. The process requires oxygen and the needed temperature is around 450-600°C. The energy could then be extracted as heat and electricity. Apart from the extracted energy, fibres and fillers are also an outcome. Due to the controlled burning process the fibres become less damaged but despite this the strength of the glass fibres are considerably reduced. At temperatures at 450°C the tensile strength is reduced with 50% and at 650°C the reduction is as high as 90% (Van Oudheusden, 2019). One of the main advantages with combustion is that the process can handle the composite even though the surface is painted or if it is a sandwich structure containing a core.

2.8.2.3 Pyrolysis

Pyrolysis is also a thermal recycling process but with the absence of oxygen. The process requires temperatures around 300-800°C which leads to a decomposition of the organic molecules (Vijay et al., 2016). Pyrolysis is an energy demanding process, in particular compared to mechanical grinding. The output of the process is gas and fibres. The gas could be burned and the fibres could be used as a new material. One major disadvantage is that the tensile strength of the fibres decreases with 50% after the thermal process (Kennerley et al., 1998). There is however an optimized technique called microwave pyrolysis. Microwave pyrolysis offers an easier control of the heating process which has led to a less damaged fibre. This could be a good solution to handle the GFRP but currently this method is not cost efficient (Ierides et al., 2019). Pyrolysis is better suited for carbon fibres which does not experience a large reduction of its mechanical properties and is more expensive to produce.

2.8.3 Recovery

Recovery means that the waste management results in a different application than it first was intended to, usually extracted energy. As can be seen in Figure 2.6, recovery is far down in the waste hierarchy. Considering the high strength material and remaining capacity in wind turbine blades, to only extract energy is considered a waste of potential.

2.8.3.1 Co-processing in a cement kiln

The idea of co-processing is to utilize waste as a resource in other industrial processes, and/or as an energy source, in this case in a cement-kiln. By burning the composite at a temperature of around 1050-2000°C the fibres are transformed into ash, while the resin works as fuel for the burning. The ash is then mixed with clinkers (Job, 2013). According to Vijay et al., 2016, co-processing is the most suitable method to handle the waste from the aerospace industry. The advantages with

co-processing are for instance the reduced carbon emissions compared to traditional cement production. One drawback is that the material value from the composite is lost. It is also a discussion whether co-processing contributes to the circularity. This is since the product is not in the original state and the remaining capacity of the fibres are not utilized.

2.8.4 Disposal

Disposal is the last measure in the waste hierarchy and means that the waste is either incinerated or sent to landfill. Through regulations and fees this alternative is intended to be an option that soon will not be viable.

2.8.4.1 Incineration

Incineration is a method similar to combustion which involves burning of the material, but not as controlled. The material is completely burned which leads to a high ash content and the only output is energy recovery and ash. The problem with burning of GFRP are that high temperatures are required since GFRP to some extent are incombustible. In addition, the ash content is very high which results in landfill after the combustion process (EWEA, n.d.). Incineration is far down in the waste hierarchy. Some energy can be recovered but 50-70% of the GFRP are left as ash that needs to be sent to landfill. Therefore, incineration should be avoided.

2.8.4.2 Landfill

Currently landfill is the cheapest waste option for GFRP (EWEA, n.d.), but according to the waste hierarchy it is the last measure that should be taken. This has led to legislation in order to make this alternative less attractive and in some countries, it is even illegal. The European commission states that *"Through a progressive increase of the existing targets on preparing for reuse and recycling of municipal waste and the elimination of recyclable waste from landfill corresponding to a maximum of 25% landfill by 2025, it should be ensured that economically valuable waste materials are progressively and effectively recovered through proper waste management and in line with the waste hierarchy."* (European Commission, 2019). Therefore, landfill is not a sustainable option and should not be seen as a solution. The issue with landfill was recently brought up in an article by C. Martin, 2020 from the US, where the majority of the blades goes to landfill. However, the American Energy Association does not consider it as a problem since the blades are landfill-safe and is an insignificant part of all waste that are being sent to landfill in the U.S.

Figure 2.8: Wind turbine blades being buried at Casper Regional Landfill. Photographer: Benjamin Rasmussen for Bloomberg Green (C. Martin, 2020).

3

Wind Turbine Blades

Theoretically, the optimal wind turbine blade is infinitely thin. Wind turbine blades are designed based on a combination of two things, an optimized aerofoil to increase the energy produced, as well as the structural strength and stiffness requirements. It is based on the same aerodynamical theories as airplane wings. Wind turbine blades are however much more aerodynamically efficient with a lift-to-drag ratio around 10 times larger than that of an airplane wing (Jamieson, 2011). The blades are typically hollow structures made of GFRP with a component to handle the shear forces. The shell is designed with focus on the aerodynamics to create one suction- and one pressure side (Sørensen et al., 2004). This is to get an as high lift-to-drag ratio as possible in order to maximize the efficiency. The size of the blades on the market is constantly growing, with the objective to maximize the energy to cost ratio (Greaves, 2016). Increasing the length is desirable since the power generated by a wind turbine is theoretically proportional to the square of the blade length.

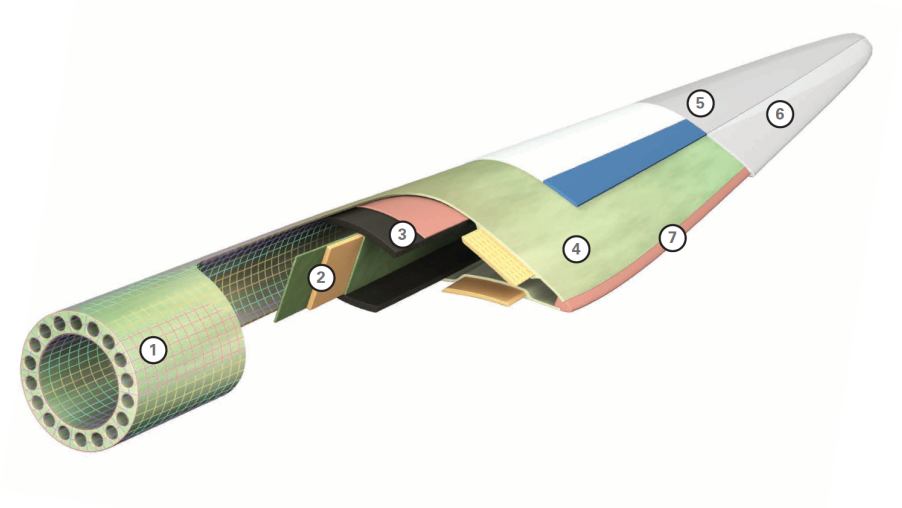

Figure 3.1: Terminology of the blades construction elements: 1. Blade root. 2. Shear web. 3. Spar cap. 4. Aerodynamic shell. 5. Blade coating. 6. Overlamination. 7. Bondline (Gurit, 2019).

3.1 Design and structure of the blade

The specific design of wind turbine blades is surrounded with a lot of secrecy from the manufacturers, as a good design gives a competitive edge. Design is done based

on of two things, aerodynamics and structural integrity. The main loads acting on the blades are gravity and inertia loads together with aerodynamic loads, with the prior two dominating more with increasing the size of the blades (M. F. Jensen and Branner, 2013). The mass of the blade is estimated to increase with length to the power of three (T. Ashwill and Veers, 2004). However, due to more efficient constructions of the longer blades, the increase of mass is closer to the power of 2.3 according to T. D. Ashwill, 2009. Structurally, there are two standard designs for the blades, with different ways to handle the bending moments and shear forces. The first option is with spar caps integrated in the shell and with one, two or three shear webs, see Figure 3.1. The other option is to use a box section, where the shell is left to be designed purely aerodynamically, see Figure 3.2 (Buckney et al., 2012).

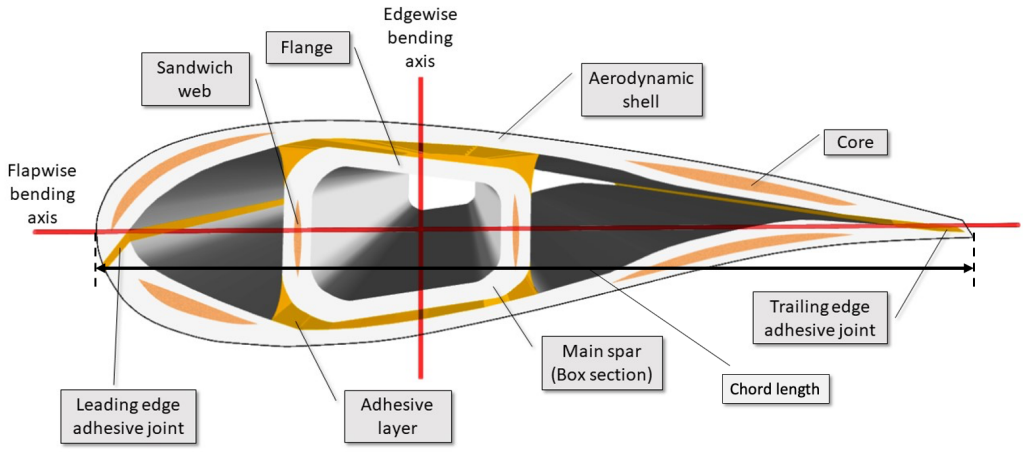

Figure 3.2: Terminology and description of a wind turbine blade.

The blade shell is typically constructed from a multi-axial fibre skin material and sandwich structure with a core, as can be seen in Figure 3.1 and Figure 3.2. The shear component is composed as a sandwich structure of $\pm 45°$ fibre laminates and a central core. The fibres are mainly glass fibres, but with an increasing amount of carbon fibres in the longer blades. The fibres are in a thermosetting polymer matrix. The core is either made of foam or balsa wood (Al-Khudairi et al., 2017). In the spar caps, that acts like the flange in a beam, the fibres are aligned longitudinally as maximized stiffness to bending is wanted in this direction. In the largest blades, carbon fibres are used in the blade spar and as local reinforcement to further increase the stiffness whilst maintaining a lower mass. The cores are used to increase the efficiency of the cross-section, as a structural core usually has low density and high shear strength. This increases the resistance to buckling and the second moment of area, letting the heavier and more expensive GFRP be used more optimal. In many blades, the spar caps have a constant width as it simplifies manufacturing (Greaves, 2016). Furthermore, the upper and lower blade shell as well as the shear component is usually made in two separate parts which are then glued together.

According to M. F. Jensen and Branner, 2013, the blades are not structurally fully optimized. The material strength is at a safety factor of 4, while buckling is at a factor of 1.2. Structural strength, such as failure are of the adhesive joints, web failure and transverse shear collapse are at a safety factor of 1. All large wind turbine blades must be subjected to full-scale testing to be certified. The tests should be done for flapwise bending, in upwind and downwind direction, as well as edgewise bending towards the leading and trailing edge directions. The tests should according to DNV, 2010 be composed of:

- Mass, centre of gravity, stiffness distribution and natural frequencies
- Static tests
- Fatigue load test
- Post fatigue static tests

Due to the design life of 25 years, the blades from the mid-nineties are the ones that will be decommissioned in a near future. A typical blade from the mid-nineties is around 50 m long, with a maximum chord width at around 10% of the length and a thickness-to-chord ratio varying from 27% at the root to 15% at the tip. Currently the most used wind turbine model in Sweden is Vestas V90-2MW. This model has a blade length of 44 m, maximum chord is 3.9 m, tip chord of 0.39 m and a weight of 6750 kg (Vestas, 2010). Vindstat.nu reports that as of February 2020, there were 4243 active wind turbines in Sweden of which 550 are of the V90-model, according to N-E. Carlstedt (personal communication, February 6, 2020).

3.1.1 Manufacturing process

The manufacturing process of wind turbine blade needs to be done in a precise way, as it has a great impact on the final performance of the blade. The process is labour heavy and the most commonly used method is the VARTM-method, although prepreg is also often used. The process of making wind turbine blades with the VARTM-method can be divided into six steps and is shown in Figure 3.3. The first step is to create a heated mould that has the outer shape of the blade. In the second step, dry layers of fibre fabrics are positioned and built up inside the mould. Thirdly, the laminate is infused with the resin through vacuum infusion into the heated mould. When the shell has dried, the shear webs are bonded to the shell. The shells are created in two parts, the pressure side and the suction side. After the shear web has been placed in one of the sides, the bottom and top shell is joined. When the joints have cured, the blade is demoulded and the outside is trimmed and polished (Bladena, 2019). Due to the elaborate steps in the process, all blades show minor differences in properties.

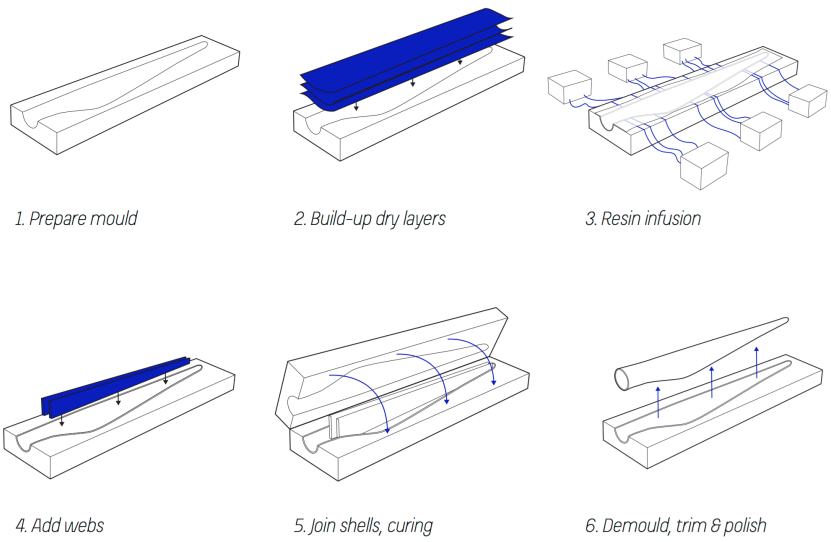

Figure 3.3: The main production steps in the blade manufacturing (Bladena, 2019).

3.1.2 Design loads

A wind turbine blade is modelled as a cantilever beam. The blades are exposed to several different loads, such as gravitational, aerodynamic, centrifugal, gyroscopic, ice and thermal loads. However, the magnitude of the gravitational, aerodynamic and the centrifugal forces are much larger than the others. The loads need to be considered in combination with the different operating conditions such as emergency braking, regular rotation, start-up and standing still. The intensity of the acting wind loads depends on both the geographical position, the height of the turbine and the shape of the blades. The five main design load cases becomes (Kong et al., 2005), (Greaves, 2016):

1. Standard wind speed condition during regular power production, in the area of 12.5 m/s
2. Standard wind speed condition with extreme gusts, in the area of an additional 9 m/s
3. Cut out wind speed condition, in the area of 25 m/s
4. Storm wind load condition, in the area of 55 m/s
5. Emergency braking

The most critical design case depends on the size of the turbines. For small turbines, the 50 year storm load is usually the most critical. Whereas for large turbines with a diameter of 70 m or more, the emergency braking is the most critical (Schubel and Crossley, 2012). At a sudden stop the rotating blades will have to be able to withstand huge inertia forces, most often in combination with large wind loads. The wind load cases are considering sudden changes in the wind direction of $\pm 40°$. The changing conditions and different loads cause large bending and twisting forces in the blades. This also means that design is done with time domain simulations for the wind turbine (Greaves, 2016). For the load cases that are dependent on

the wind load, the blades have to withstand flapwise bending. Here the deflection criterion is critical, as a too large deflection means that the blade risks hitting the tower. The emergency braking on the other hand causes edgewise bending, with the risk of the blade being damaged. The blades are designed with the spar caps positioned for resistance against flapwise bending, as they are positioned apart to have a larger second moment of area. To resist the edgewise bending, the bending axis inside are positioned inside the spar caps. As a result, the second moment of area is significantly reduced. In order to handle this, the longitudinal fibres are strategically positioned in the spar caps as a way to increase the efficiency. The flap- and edgewise loading can be seen in Figure 3.4.

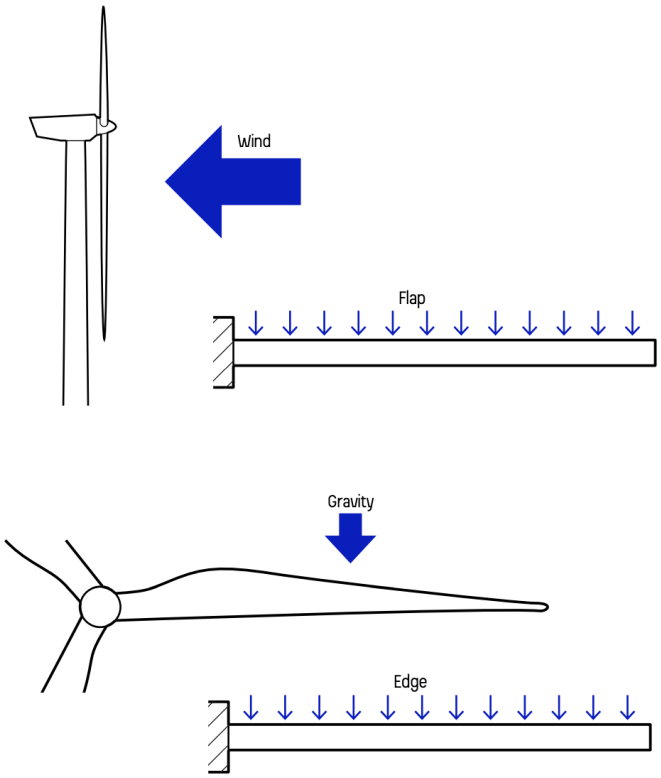

Figure 3.4: Flap- and edgewise loading for a wind turbine blade (Bladena, 2019).

3.1.3 Failure mechanisms

Due to the blades being an assembly of different parts it also has several different failure modes. Failure of the blades can be both stable and unstable, where the unstable failure mechanisms are the most dangerous (M. F. Jensen and Branner, 2013). The dominating design criteria is often the fatigue life. But there are also requirements for maximum strain of the fibres, surface stress limits and a minimum clearance between the blade tip and tower wall. This is specified by IEC, 1999 and Germanischer Lloyd, 2010.

Due to a design life of minimum 20 years of constant loading and unloading, fatigue is the most critical failure mode for turbine blades. According to F. Sayer et al.,

2009, the main influence on the fatigue is the number of rotations, turbulence and the wind history during the blades service life. The most sensible part to fatigue damage is the root of the blade. This owing to the large bending moments and the stress concentrations around the fasteners (M. F. Jensen and Branner, 2013). These stress concentrations are further increased by the edgewise forces that has been carried through curved panels, which causes out-of-plane deformations and peeling in the bond lines at the connection of the root. In a study done by Lee et al., 2015, a 56 m blade was tested until fatigue failure. This resulted in delamination failure at the blade root. The result was then redone in a FE-model to find the cause of the delamination. It was concluded that the load distribution in the root was different from what was calculated by conventional approaches under the assumption that the blade root can be modelled as a hollow circular cylinder. The cyclic motions of the blade shell cause alleviation and increase of load in different locations of the joint. This causes separation of the T-bolt joints and through this delamination.

According to M. F. Jensen and Branner, 2013, other common failure modes are:

- Failure in the spar caps: When the blade is subjected to bending moment, a flattening deformation can occur called the Brazier effect. This affects the blades spar caps. The effect of this can be both a transverse tension failure in the unidirectional layers close to the neutral axis or an inter-laminar shear failure between the different layers. It is the lack of transverse fibres and existence of imperfections in the matrix that enables this failure mode.
- Cross-sectional shear distortion: This is an elastic mechanism due to a combination of edge- and flapwise loads. The edge- and flapwise load combination is a common load combination during usage, coming from a combination of gravity, dynamic loads and wind loads. It is increasingly critical with size and weight of the blade (Branner, 2011).
- Failure in adhesive bondlines: Due to out-of-plane deformations, peeling stresses occur in the bondlines of the edge panels. These stresses can cause debonding between the upper and bottom shell in the trailing edge (Haselbach and Branner, 2016).
- Web failure: The shear webs collapse due to the compression forces that in some cases also are enhanced by the Brazier crushing forces and axial tension. The failure is initialized as face debonding of the outer skin in the shear web's sandwich structure (F. M. Jensen, 2009).
- Buckling: The instability phenomena buckling occur due to compression forces. This occurs in the core walls during flapwise loading or in the back edge of the blade during edgewise loads. Buckling of the blade can cause critical damage in the case of existing delamination imperfections, which then grows and can cause failure of the whole panel (M. F. Jensen and Branner, 2013). Buckling in the blade can occur both locally and globally.

3.2 Inspection methods

As previously described, the first step in the waste hierarchy is to prevent the waste. The blades have a relatively short lifetime of 20-25 years and one way to extend

this could be by performing regular inspections. This is also a way to guarantee a constant operation and to verify the service safety. According to G. Nilsson at Blade Solutions (personal communication, February 20, 2020), the most common deterioration of the blades is erosion. There are also some occasional design errors that could be a problem in terms of buckling of the fibres. Blade Solutions is a company working on inspecting and repairing blades.

3.2.1 Infrared thermography

With infrared thermography a thermal image can be created. This technique can for instance detect trapped air. The thermodynamic changes are due to the insulating effects that trapped air provides, which generates a reduced surface temperature. Other variations in the thermodynamic properties can be loss of internal contact or degeneration of components. This can be seen as hot spots (Yang and Sun, 2013). The technique can also detect impact damages (Chady et al., 2016). Infrared thermography provides a rapid and relatively simple examination of the blades. On the other hand, it is an expensive inspection method.

3.2.2 X-ray imaging

The X-ray imaging provides quantitative information based on the amount of photons absorbed. The process consists of an X-ray tube which produces photons that are moving towards the sample. The remaining photons are then propagating against an imager and finally a radiograph. A 2D image can then be seen which mainly depends on the density of the sample. High densities can be seen as dark grey areas while lower densities give a lighter grey. Thereby changes in the density can also be detected, mainly caused by internal delaminations or changes in the material properties (Yang and Sun, 2013).

3.2.3 Ultrasonic testing

The most commonly used non-destructive inspecting technique for composite materials is ultrasonic testing. By sending out high frequency sound waves, voids and cracks can be detected in the composite. This is since the sound waves will reflect when hitting a boundary and the reflection is then measured by a receiver. The defects can be identified as deviations from the norm. Classical defects that could be detected with ultrasonic testing are delamination, adhesive defects, broken fibres and lack of resin (Yang and Sun, 2013). High competence is needed to perform an ultrasonic test. Another drawback of the inspection technique is its limitation when it comes to uneven surfaces, for instance a bridge deck.

3.2.4 Terahertz testing

Terahertz radiation is within the frequency range from approximately 0.1 to 10 THz. Through the use of Terahertz imaging, defects such as voids, inhomogeneities between matrix and fibres, inclusion, delamination and surface roughness can be

detected (Chady et al., 2016). The terahertz radiation senses changes in the refractive index that describes the speed of light through a material. Another kind of Terahertz testing is Terahertz Inverse Synthetic Aperture Radar, ISAR. With this testing method scattering data is collected. The properties can then be described in a scattering matrix. The result is ISAR images that is quantified. From that evaluation the test is given a defect imaging score. ISAR can detect regions with a lack of resin and out-of-plane fibre wave defects (R. Martin, 2016), (R. Martin et al., 2016).

3.3 Remaining capacity

In accordance to the waste hierarchy the second measure is to reuse the material. This could be implemented for the blades to prolong their lifetime. In order to do so it is important to verify the remaining capacity to ensure a safe design. According to a recent study done by Anmet and Rzeszów University of Technology, it is shown that the decommissioned blades still possess a very high capacity (Appendix D). This was also confirmed by David Stien Pedersen, Senior Project Manager at Siemens Gamesa Renewable Energy (personal communication, February 10, 2020) and is a general consensus within the industry.

As previously described the main part of the blade that is severely affected by fatigue is the root section where stress concentrations around the bolts are critical. In addition, the blades can be exposed to irregular and unexpected events. This is something that can be detected when doing a visual inspection. It is therefore crucial to do a thorough inspection of the blades when they are prepared for reuse.

4
Design of a Pedestrian Bridge

When designing a pedestrian bridge there is a lot of aspects that needs to be handled. Most importantly it is all the regulations that needs to be followed. The regulations for the design of bridges are determined by Eurocodes, Transportstyrelsen (TSFS) and Trafikverket (Krav Brobyggande), where Transportstyrelsen mainly gives directions of how the Eurocodes should be interpreted and adapted in Sweden and Trafikverket with additional requirements and changes. Apart from the technical demands there are also demands from the client as well as the society. Furthermore, there are more specific demands which involves all the details that needs to be designed for a pedestrian bridge.

4.1 Technical demands

The most important Eurocodes concerning the general design of a pedestrian bridge and considered in this thesis are found in:

- *SS-EN 1990*, 2002 Eurocode: Basis of structural design
- *SS-EN 1991-1-1*, 2002 Eurocode 1: Actions on structures - Part 1-1: General actions - Densities, self-weight, imposed loads for buildings
- *SS-EN 1991-2*, 2003 Eurocode 1: Actions on structures - Part 2: Traffic loads on bridges

These are accompanied by the following national documents from Transportstyrelsen and Trafikverket:

- *Krav Brobyggande*, 2019 (TDOK 2016:0204) version 3.0
- *Råd Brobyggande*, 2019 (TDOK 2016:0203) version 3.0
- *TSFS*, 2018 Transportstyrelsens föreskrifter och allmänna råd om tillämpning av Eurokoder

Currently there are no Eurocodes for the design of FRP structures. Although it is set to be published in 2022. It has been under development for several years by researchers and engineers all over Europe. National guidelines does exist in some European countries, such as the Italian *"CNR DT 205*, 2007 *Guide for the Design and Construction of Structures made of Pultruded FRP elements"* and the Dutch *"CUR 96 Fibre Reinforced Polymers in Civil Load Bearing Structures"*.

4.1.1 Geometric guidelines

A combined bicycle and pedestrian bridge need to be wide enough to fit both of the user groups. According to Trafikverket, 2020b, a combined bicycle- and pedestrian road has to be at least 2.5 m wide. However, it is recommended to design them even wider. Göteborgs Stad, 2019 recommends 3.0 m - 4.0 m for a shared walkway & bike lane and 2.0 m + 2.4 - 4.8 m for a divided walkway and bike lane as seen in Figure 4.1. The recommended width is dependent on the intended usage, increasing with the expected amount of cyclists and their speed.

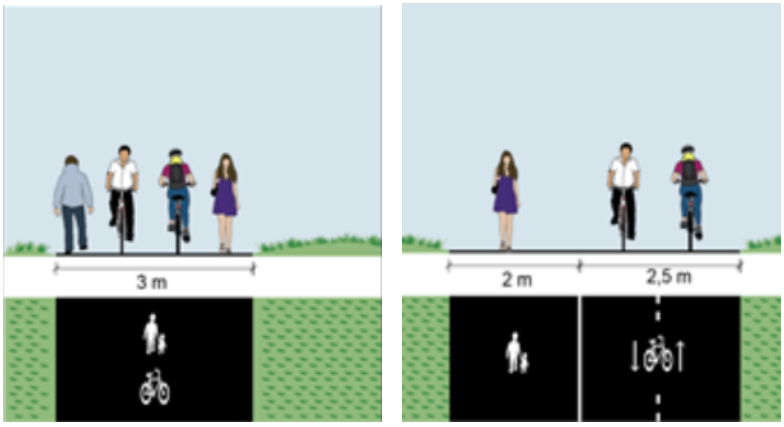

(a) Shared use path

(b) Divided walkway and bike lane

Figure 4.1: Width of a shared use path for bicycles and pedestrians (Göteborgs Stad, 2019).

The maximum allowed longitudinal inclination is 2%, due to accessibility, but can be exceeded up to 4% if motivated and accepted by the client. The bridge deck is required to have a handrail that has a minimum height of 1.4 m (Trafikverket, 2020a).

The Swedish road authorities, Transportstyrelsen, 2013 and Trafikverket, 2019, have requirements for the maximal width and length for transports on the roads. The maximum allowed length and width for a transport without an exemption is 24 m and 2.6 m respectively. With an exemption and proper marking this can be exceeded up to 30 m length and 3.1 m width. If a transport is required to exceed these limits, an escort by either the police or a road transport manager as well as a truck with bogie steering is required.

4.1.2 Safety classes, loads and load combinations

To determine the safety factors in the design, reliability classes are used. The class depends on the length of the bridge. If the span is below 15 m, safety class 2 shall be used, otherwise safety class 3 is used (*TSFS*, 2018).

The loads that needs to be considered are categorized as permanent, variable and exceptional loads. Self-weight of the structure and the decking are classified as permanent loads. Variable loads to be considered are crowd load (Ch. 4.3.5 & 5.3.2 in *SS-EN 1991-2*, 2003), load from service vehicles such as a snow clearing vehicle and emergency vehicles if decided by the client (Ch. 5.6.3 in *SS-EN 1991-2*, 2003), loads on the handrail (G.9.2.4 *Krav Brobyggande*, 2019), temperature- (*SS-EN 1991-1-5*, 2003), wind-(*SS-EN 1991-1-4*, 2005) and snow load (*SS-EN 1991-1-3*, 2003). The magnitude of the temperature-, wind- and snow load varies with the location of the bridge and could be found in *TSFS*, 2018. Exceptional loads must be considered if a risk of collision by road vehicles or trains are present. Directions for the load duration of the loads can be found in table 33.1 in *TSFS*, 2018.

A structure is designed for the serviceability limit state (SLS) and the ultimate limit state (ULS). FRP has high yield strength compared to stiffness, therefore the SLS requirements are in most cases governing the design. For SLS there are two requirements, deformation and acceptable acceleration which both are comfort criteria. The requirements for deflections are defined nationally and found in B.3.4.2 in *Krav Brobyggande*, 2019 as 1/400 of the span length. The acceleration criterion is defined in A2.4.3.2 in *SS-EN 1990/A1*, 2005. A verification of the acceleration needs to be done if the fundamental frequency for vertical vibrations are less than 5 Hz or the fundamental frequency for horizontal and torsional vibrations are less than 2.5 Hz. According to *SS-EN 1991-1-4*, 2005, wind loads are not included in the dynamic analysis for bridges with a span length below 40 m.

The guidelines for acceleration design can be found in *"Design of Lightweight Footbridges for Human induced Vibrations"* by Heinemeyer et al., 2009, that is an evolution of Eurocode 3. The difference between the dynamical analysis of the acceleration and the fundamental frequency is that the acceleration shows what is experienced on the structure. The acceleration accounts for the bridge damping properties, mass and pedestrian loading in the dynamic analysis. According to Heinemeyer et al., 2009, the critical frequency range is based on the natural frequencies of pedestrian loads. For vertical and longitudinal vibrations there are two frequency ranges and for lateral one range. The first vertical and longitudinal range is 1.25 - 2.3 Hz, this corresponds to the left leg to right leg of a person walking. The second is 2.5 - 4.6 Hz and includes the heel-toe action when walking. The lateral range is 0.5 - 1.2 Hz. The accelerations are calculated with harmonic load models and the loads depend on the expected amount of users of the bridge. *SS-EN 1990/A1*, 2005 recommends that the vertical acceleration should not exceed 0.7 m/s^2. Although, in *"Design of Lightweight Footbridges for Human induced Vibrations"* the acceleration criteria is divided in the four comfort classes as shown in Table 4.1.

Comfort class	Degree of comfort	Vertical $[m/s^2]$	Lateral $[m/s^2]$
CL1	Maximum	< 0.50	< 0.10
CL2	Medium	0.50 - 1.00	0.10 - 0.3
CL3	Minimum	1.00 - 2.50	0.3 - 0.8
CL4	Unacceptable discomfort	> 2.50	> 0.8

Table 4.1: Comfort classes within common acceleration ranges. Table 4-4 in *"Design of Lightweight Footbridges for Human induced Vibrations"* (Heinemeyer et al., 2009)

4.2 Detailing

The details of a bridge are of high importance and need to be thoughtfully designed. The choice of details has a great impact on the final result of the bridge, especially in terms of the amount of maintenance needed. The most important details that need to be solved are the connections between structural members, bridge deck and the fastening of the railing.

4.2.1 Bridge deck

The main purpose of the bridge deck is to create a walkable and accessible surface that can distribute the loads to the superstructure. This whilst fulfilling the requirements regarding inclination, width as well as the deformation mentioned above. In terms of maintenance it is crucial to keep the construction away from water. This means that the shape of the deck always needs to lead away the water.

4.2.2 Connections

The bridge deck and the load carrying members of the bridge needs to be connected. The way this connection needs to work depends on the decided structural system. If the bridge deck is a part of the structural system higher requirements are put on the connections between the main load carrying members and the deck. The connections for FRP are most often done with bolts or adhesives.

4.2.2.1 Bolted connections

A bolted connection is a joint that is easy to use on site for a fast and simple assembly. However, the connections are prone to cause stress concentrations as all the load is transferred in specific points. These stress concentrations can cause local damage around the bolt hole. FRP are especially keen to these damages because of their anisotropic and non-plastic behaviour. The damage shown around the bolt hole is either delamination or debonding.

There are several different failure modes for bolted joints in FRP. Shear-out failure, see Figure 4.2, is the most critical failure mode for the case of the close to unidirectional material in the spar caps of the blades (Mara, 2015). Shear-out failure is a

result of shear failure between the fibres and matrix and is commonly a consequence of a too short edge distance.

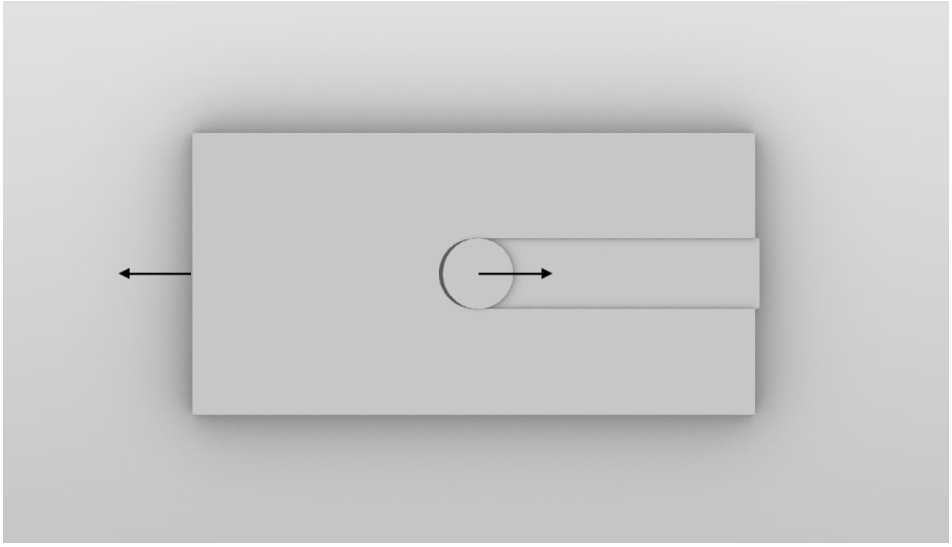

Figure 4.2: Shear-out failure in a bolted connection.

A bolted connection requires a hole, which means that drilling is required. The drilling needs to be precise and carried out with sharp tools to minimize delamination and spalling around the hole. Otherwise, this can lead to serious damage to the component. In order to get a connection that works properly, Fiberline, 2003 recommends using washers on both sides of the connection and that the bolt is placed inside a sleeve.

4.2.2.2 Adhesively bonded connections

Adhesively bonded connections use structural adhesives such as epoxies to create the joint. They need to work primarily in shear and compression to be efficient. This is due to the peeling and tensile strength that usually are considerably lower. To create a strong joint, eccentricities need to be avoided as these causes peeling stresses. Bonded joints create a stress distribution over the whole connection, but with some stress concentrations at the edges of the connection. A bonded joint can fail in three modes. Failure of the adherent material, failure of the adhesive or failure of the interface between the adhesive and adherent. A failure of the adherent material is ideal, but is hard to achieve as adhesive failure is predominant (Mara, 2015). In an adhesively bonded connection, the surfaces that are connected are of highest importance. The bonded components need to have the same geometry and have their surface layer roughened. In order to get maximum bond strength, the bond line should be thin. The surfaces need to be clean from contaminants to create a connection that works as intended. Due to this, adhesively bonded connections are preferred to do inside a workshop.

4.3 Client and Societal demands

A finalized project is full of compromises and prioritizing between different demands and stakeholders. The main demands from the clients are usually to create a sustainable and cost-efficient bridge that requires small amounts of maintenance. In a study done in the PANTURA Project, road authorities and bridge owners in Europe were asked what their main demands are for bridges. Their answer can be seen in Table 4.2.

Table 4.2: Priorities set by road authorities and bridge owners for new construction and maintenance activities for bridges (Reza Haghani Dogaheh, 2013), (Mara et al., 2014).

New construction	**Maintenance activity**
1. Low initial costs	1. Minimization of traffic disruption
2. Low maintenance costs	2. Minimum application time
3. Short construction time	3. Low initial costs
4. Minimize traffic disruption	4. High long-term performance
5. Minimize life-cycle costs	5. Low maintenance costs
6. Minimize environmental impact	

While the client demands are more constant, the societal demands come of increasing importance with the amount of people affected by the bridge. Within a city a more architecturally challenging design could be justified at a higher cost. In a residential area or an area where the bridge crosses a road with frequent traffic, a higher prefabrication grade can be desirable to minimize the disturbance. Creating a sustainable solution requires multiple things, with the main focus on being environmentally in both a global and a local scale. The global scale affects factors such as CO_2-emission while the local scale consider things as minimizing the disturbance to the existing ecosystem. In addition to the environmental focus, sustainability also includes social and economical aspects (Mara et al., 2014). All these factors should be considered and it is desirable that the new bridge fulfils as many of these demands as possible.

Almost all pedestrian bridges in Sweden are built with the conventional building materials timber, concrete and steel. Bridges in FRP is uncommon in Sweden, only a few has been built. However, in other parts of Europe it is more common. According to Jan Kroon at FiberCore Europe, it is hard to introduce composite bridges into the market as the client does not have prior knowledge of using the material. This is noticed as there is no routines for how to evaluate the proposal which is further hindered due to the absence of a code in Sweden. In addition, the initial investment cost is often a barrier for selection of this solution. However, as stated in Mara et al., 2014, FRP can be economically profitable if considering the whole life-cycle. This has to do with the simple and fast assembly as well as low maintenance costs.

5
Conceptual design

In a master thesis made by Stijn Speksnijder, 2018, different solutions to find a new application for the decommissioned wind turbine blades were evaluated. Several interesting and promising suggestions were presented. The first idea was to build a transmission tower. The root of the blade should then be used as a foundation to the tower. The second idea was a pedestrian bridge, with the blades as load carrying members. Wind turbine blades are designed to withstand shear stresses along its entire length, a property that is useful in this type of bridges. The third proposed solution was a ventilation shaft and the fourth proposal were an urban micro-climate. By doing a proper evaluation of all these proposals, the pedestrian bridge was concluded to be the most promising concept. Another article published by Russell and Irel, 2019, concluded that *"wind blades have the good potentials to be used as structural members in pedestrian bridges, providing an alternative and environmentally friendly solution to the disposal of wind blades when they are decommissioned"*. Based on these conclusions as well as the knowledge from the literature study, this thesis will discuss and evaluate different bridge concepts in order to find the most suitable.

The approach is to find as many promising concepts as possible and then evaluate them. The pros and cons with each concept will be analysed and finally the most promising concept will be investigated and further designed. The process was initiated by a brainstorming session together with Sweco Architects. For this session, 25 cm long blades were 3D printed in order to get a better understanding of its shapes and dimensions. They are shown in Figure 5.1 As the evaluation and design proceeded, consultation was given by experienced engineers.

Figure 5.1: 3D-printed blade with a length of 25 cm.

Generally, all the concepts will have a 4 m wide bridge deck as is the recommended width for a shared pedestrian and bicycle way in accordance to Göteborgs Stad, 2019. They will all span 20 m, which is a common span length for pedestrian bridges.

5.1 Concept one

The first concept is to use four blades oriented to carry the load in the edgewise direction as shown in Figure 5.2 and Figure 5.3. Beams will be placed transversely between the blades to make the blades work as a unit. By placing the blades with a c-c distance of 1500 mm the total width of the bridge becomes 4500 mm. On top of the blades the 4000 mm wide bridge deck will be placed.

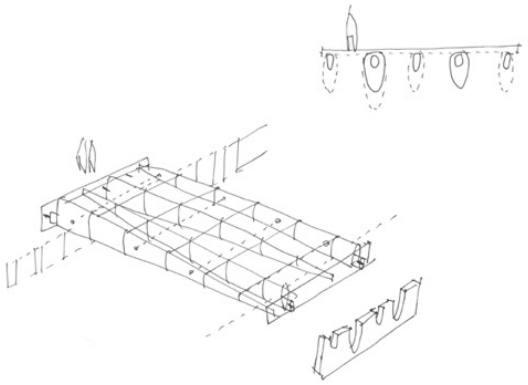

Figure 5.2: Sketch of bridge concept one. Architect: Pege Hillinge, Sweco.

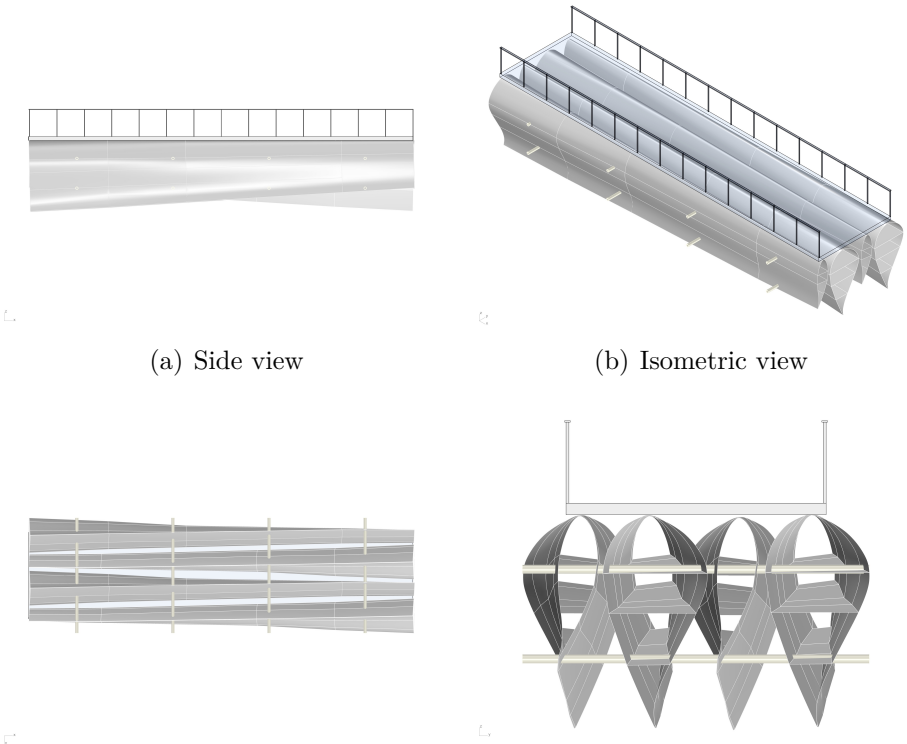

(a) Side view

(b) Isometric view

(c) Bottom view

(d) Cross-sectional view

Figure 5.3: Concept one as drawn in Rhino.

5.1.1 Advantages

By placing four blades in this direction a robust bridge is created. This is since the strength from more blades could be utilized than if they were positioned flapwise. A bridge that uses more blades for the same width also means that more blades are taken care of. This is desirable as finding a purpose for the decommissioned blades is the origin of the problem. The vertical positioning of the blades also creates a bridge that clearly shows the spectacular load carrying members that the blades are.

5.1.2 Difficulties

The main disadvantage with this bridge concept is the construction height. By placing the blades like this the full chord width of the blades needs to be considered, which is approximately four meters. Even if the smallest part of the blades is used, the chord length would still be around two meters. The conclusion drawn from this is that the blades should be positioned in the flapwise direction instead to reduce the construction height. Another drawback with this concept is the orientation of the spar caps and shear webs. The webs are designed to take shear forces and by this placement their structural intention is not used in an optimal way. A crucial detail with this concept is the connection between the blades to make them work as a unit. These connections need to handle high stresses and will be complicated and time consuming to produce.

5.2 Concept two

The second concept is to use two blades as beams and placing the bridge deck on top of the beams. This is a quite intuitive and similar concept to the one that was evaluated in the master thesis from Stijn Speksnijder, 2018. The blades are in contrary to concept one placed in the flapwise direction. This results in a lower construction height and a better utilization of the original design intention of how the loads are to be carried. As can be seen in Figure 5.4, the blades are placed in the opposite direction to each other to keep the cross section as constant as possible. The idea is to separate the blades and make sure that they do not work as a unit. This results in higher demands on the bridge deck but no cross-beams or connection between the two blades are needed.

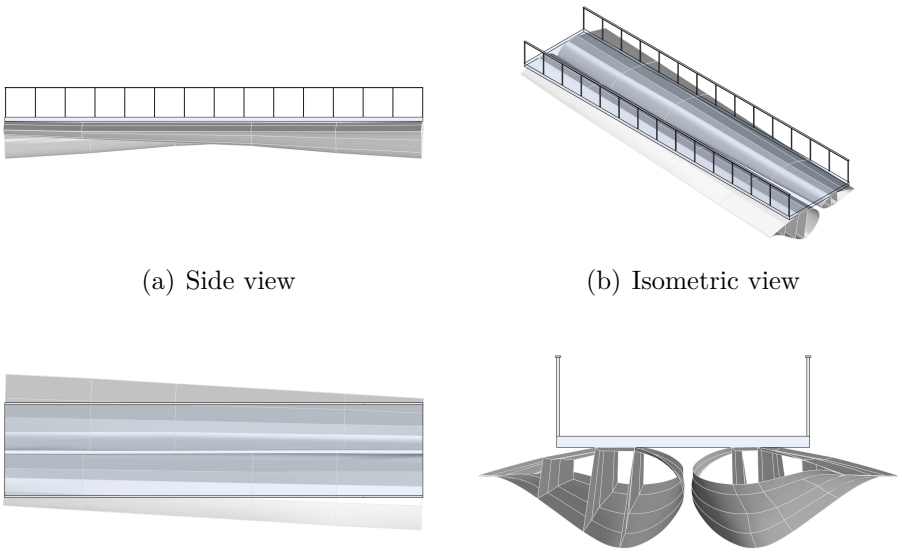

(a) Side view

(b) Isometric view

(c) Top

(d) Cross-sectional view

Figure 5.4: Concept two as drawn in Rhino.

5.2.1 Advantages

The main advantage with this concept is a simple construction with a relatively low construction height. The blades are also positioned in a way that highly utilize their design intention. Furthermore, there is no connection between the blades which simplifies the construction.

5.2.2 Difficulties

As the blades have a changing cross section and are positioned in the opposite direction of each other, the cross section of the bridge will be asymmetric. This means that the blade will deflect more on one side of the bridge deck than the other and torsional forces in the bridge deck are introduced. Furthermore, due to the uneven shape of the blades the connection to the bridge deck becomes even more complicated.

5.3 Concept three

The third concept is a cable-stayed bridge created out of four blades, as in Figure 5.5 and Figure 5.6. The blades are leaning towards each other connected with a shear-key to transfer shear forces between the blades and making them work together. In order to transfer the moment forces to the abutments, the blades have a clamped connection at their root. The bridge deck will be connected to the superstructure with cables attached to the blades. The cables can be connected on the side of the deck or in the middle of the deck to create two lanes.

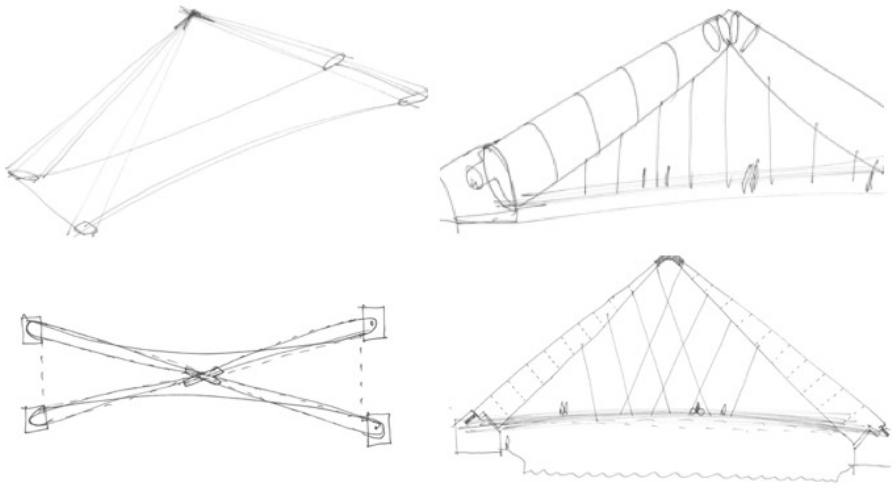

Figure 5.5: Sketch of bridge concept three. Architect: Pege Hillinge, Sweco.

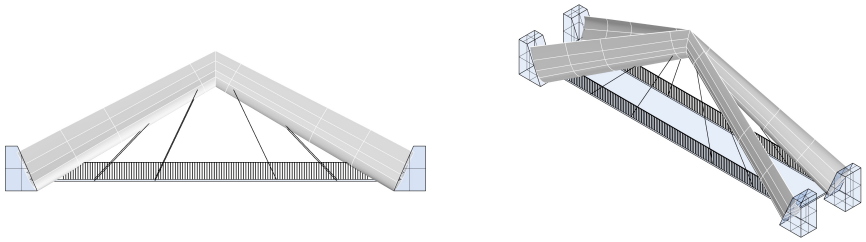

(a) Side view

(b) Isometric view

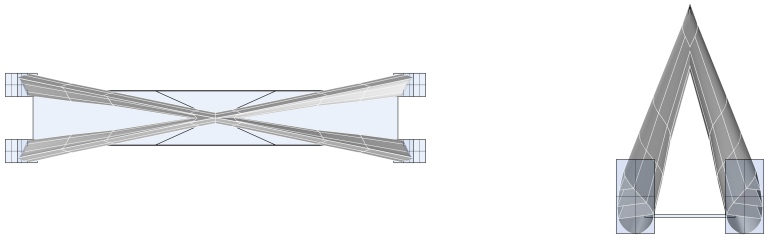

(c) Top view

(d) Cross-sectional view

Figure 5.6: Concept three as drawn in Rhino.

5.3.1 Advantages

Concept three is a large construction and could be quite spectacular with an innovative design. This construction allows for longer span lengths as the blades can be used as cantilevers as they were designed for. As the structural system is positioned above the bridge deck, this concept does not intrude on the space beneath the bridge. This space is often limited and thus an advantage for this concept.

5.3.2 Difficulties

Out of all the concepts, this is probably the most complex solution. In this concept there are several crucial details that needs to be handled. The connections between the blades as well as the connections with cables and bridge deck are difficult and expensive to produce, maintain and inspect. In addition, large bending moments needs to be handled in the abutments due to the long lever arms and the fixed connection. This would lead to heavy abutments, most likely out of concrete, producing large CO_2-emissions. This could however be overseen depending on the purpose of the bridge but as this thesis aims to find a sustainable solution this is not an acceptable argument.

5.4 Concept four

The fourth concept is an attempt to create a slender structure. This concept is similar to concept two, although this connects the same section out of four blades to create a more constant and lower cross section, see Figure 5.7 and Figure 5.8. By placing the blades with the flat end upwards, a lower construction height is achieved. This is also how the blades were designed and the construction is therefore assumed to be working in an optimized way. In an early version of this concept the thicker parts were placed in the middle of the span. This was done since the largest bending moment is acting here when having a simply supported bridge. The main problem with this solution was the connection between the four blades that would be placed in the position of maximum bending moment. This will then have to be a very rigid and complicated detail. Therefore, the concept was reconsidered. By changing the boundary conditions and position of the blades this was solved. Instead the ends will be clamped to the foundation and the middle part will be connected through a shear joint. By having this kind of joint between the blades, no bending moment is transferred here and the connections becomes easier to accomplish.

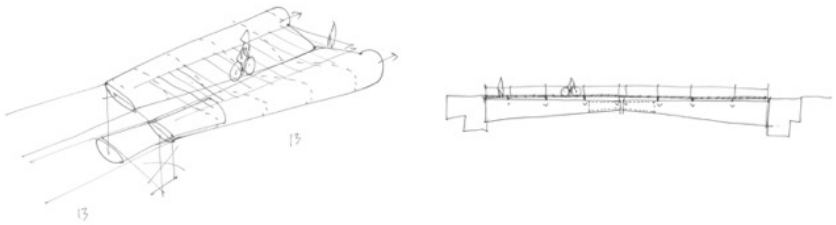

Figure 5.7: Sketch of bridge concept four. Architect: Pege Hillinge, Sweco.

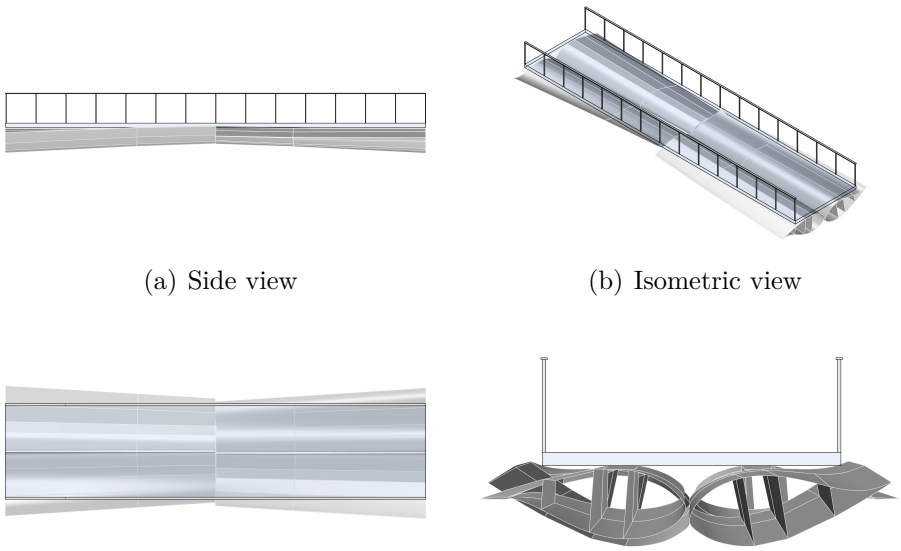

(a) Side view

(b) Isometric view

(c) Top view

(d) Cross-sectional view

Figure 5.8: Concept four as drawn in Rhino.

5.4.1 Advantages

As a more optimized part of four blades are used, this concept has the lowest construction height out of all the concepts. This is the main advantage with this concept. Since the blades are joined together, transportation of the blades to the site will also be simplified due to the thinner and shorter components.

5.4.2 Difficulties

The main disadvantage and difficulty with this concept is the supports at the ends of the bridge. Clamped foundations are a more complex and expensive solution compared to having a simply supported bridge. In this case the clamped foundation would be on both sides of the bridge which is not optimal from an economically point of view. Furthermore, all blades are made to rotate in the same direction. Due to this, the cross sections of the blades that are connected at the middle will be in different directions of each other, complicating the connection.

5.5 Concept five

Concept five is developed from concept two and four. The similarity to concept two is the utilization of only two blades that spans the whole length. By using the whole length, the joint in the middle section could be avoided and the concept becomes less complex. From concept four the position of the blades is used with the thicker parts on one side and the smaller on the other. In Figure 5.9 the position of the blades are shown. The thick end of the blade is clamped to the abutment while the narrow end has a roller support. By using these boundary conditions, the maximum

bending moment is where the blades have the largest cross section and thus have a higher capacity. The idea with this concept is that the two blades are working as two separate beams.

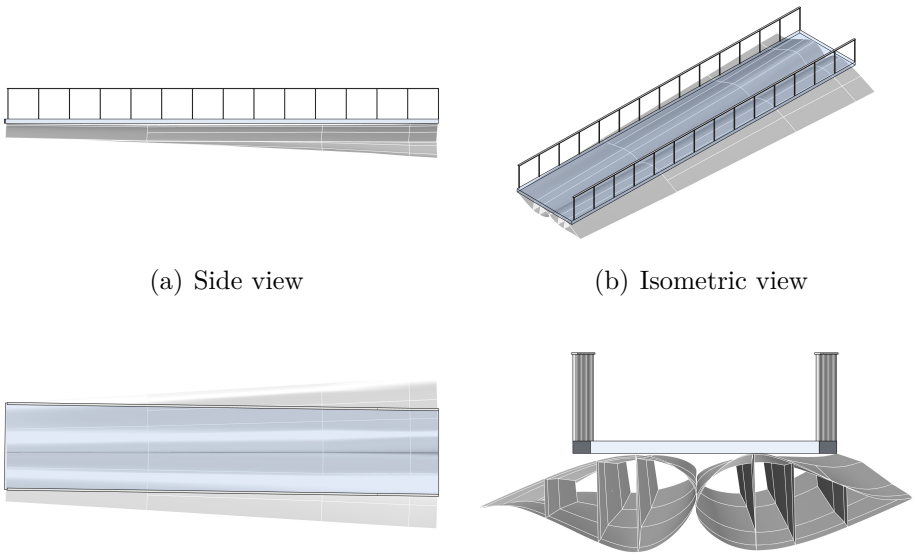

(a) Side view

(b) Isometric view

(c) Top view

(d) Cross-sectional view

Figure 5.9: Concept five as drawn in Rhino.

5.5.1 Advantages

The main advantage with concept five compared to concept four is that the connection in the middle of the span is no longer needed. This saves labour and the bridge becomes more economically attractive. In addition, this concept is just clamped on one side which simplifies the construction. By having these boundary conditions, the bending moment curve follows the cross section of the blades which is an efficient way of utilizing the material.

5.5.2 Difficulties

The disadvantage compared to concept four is that the transportation length is increased. Furthermore, the construction height of the bridge is increased since a larger part of the blade is used. In addition, the clamped foundation is an expensive and complicated solution. In comparison to concept four, where two clamped foundations are used the price is lower here. However, the single clamped foundation needs to handle the bending moment from twice the span length. This still requires large and expensive foundations with a complicated connection to the blade. As a result of the two blades working separately the demands on the bridge deck is increased.

5.6 Concept six

Concept six is a further development from the second concept in terms of the position of the blades. The difference between them is that the blades are attached to each other, see Figure 5.10. This is done in order to make them work as a unit. By removing a part of the shell, the shear webs can be connected directly to each other. They will be joined by either bolts or bonded with an adhesive. The bridge is intended to be simply supported.

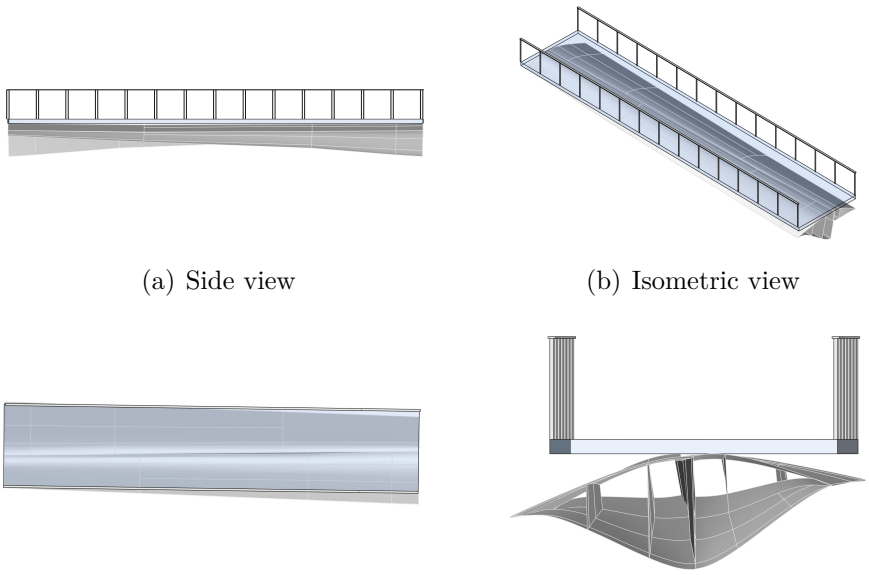

(a) Side view

(b) Isometric view

(c) Bottom view

(d) Cross-sectional view

Figure 5.10: Concept six as drawn in Rhino.

5.6.1 Advantages

The two straight surfaces could be joined together making the two blades working together. This leads to a simpler design of the bridge deck. As in concept five the advantage is that no joint is needed in the middle of the span length.

5.6.2 Difficulties

To be able to join the blades with an adhesive, the two shear webs need to be completely planar to each other. This is since high grade adhesives are most efficient in very thin layers. The other option is to use bolts, which instead requires labour inside the blade where space is limited. As in concept five the construction height is higher. An additional complication is that both the intended fastening lines between the deck and blades are in the spar cap of the blades, that are now in the centre. Thus, the deck need to span longer transversely. When the deck is loaded close to the railing, the lever arm is long and causes large bending moments that the deck to blade connection needs to handle.

5.7 Selection

Apart from the technical demands described in chapter 4, there are several different aspects that need to be considered before one final concept could be chosen. One of the factors that have great impact in the decision making is the costs. This is an aspect that will play an important role in this project as well. Furthermore, one of the objectives in this project is to find a concept which is easy to build, requires low maintenance and does not require a lot of additional material apart from the blades. Another important parameter is the design of the bridge. Not only in terms of the structural design but also aesthetically. In Aalborg, where a similar project is carried out, the design was criticised for looking like the blades were put in the nature as a form of disposal. Therefore, it is important that the bridge looks thoughtfully designed. On the other hand, it is an interesting idea to still see that the structural components are made out of wind turbine blades since they are spectacular pieces.

When choosing one final concept it is important to include as many relevant aspects as possible. A life cycle perspective is therefore applied where factors as initial cost, transportation, production method, usage and maintenance are roughly evaluated for each concept. With this in mind, concept one was eliminated in an early stage due to the unrealistic construction height. Concept three, the suspension bridge, where also eliminated early on due to its complex details. These details would probably have led to an advanced production process as well as high construction and maintenance costs. The remaining concepts, two and four, were then further evaluated and improved to find the most promising alternative. This process resulted in two new concepts, five and six. After consultation with experts and discussions between the authors, concept six was eliminated and five was chosen. The connection of the two blades in concept six was analysed as too complicated to construct and thus the concept was eliminated. The fifth concept is the concept with the least complicated details and modifications to the blades as well as the simplest structural system. This is economically favourable as the production and maintenance costs will be kept low. The detailed design of the fifth concept will be further analysed.

5.8 Construction

As the final concept is chosen all the details needs to be further analysed and designed. This involves how and where the bridge will be assembled, how it is affected by the transportation, how to handle the boundary conditions as well as all the crucial connections. The final construction and details will be presented in chapter 7.

5.8.1 Assembly

When it comes to the assembly there is mainly two alternatives. Either the bridge could be assembled and prepared in a workshop or it could be built on-site. If the first case was to be chosen, i.e. to build the whole bridge in a workshop, the construction process could be more effective as well as more controlled. A controlled environment is especially crucial when using adhesive joints. On the other hand, the

transportation of the bridge is of greater importance. First of all, there is a risk that the connections and other details will be damaged during transportation. Secondly, an increase in size makes the transportation more difficult.

The other alternative is to build the bridge on-site. This will simplify the transportation process but the assembly might be more complicated. The environment is not as controlled as in a workshop and the access might be more limited to certain parts. Despite this, the assembly could be adapted for the site of the bridge and it is easier to customize the solution. However, a customized production process increases the cost.

Another aspect in terms of the assembly is the handling of the blades when decommissioned. Due to their sizes it is desirable that the blades are cut to its final size as soon as they are decommissioned since this will simplify the transportation.

5.8.2 Transportation

As mentioned in subsection 4.1.1, the guidelines regarding transportation without an exemption is a length of 24 m and a width of 2.6 m. The final dimensions of one blade is a length of 20 m, a width of 3.6 m and a height of 1.8 m. The final bridge concept has a span length of 20 m and a width of approximately 7 m and a total height of approximately 2 m. The conclusion that can be drawn from these dimensions are that due to the width of the bridge a transportation of the completed bridge will be complicated. It is also highly dependent on where the bridge will be located since the access at the site might be limited. Therefore, the bridge will mainly be assembled on-site.

5.8.3 Boundary conditions

Before the analysis was made the main concern was the dynamic in terms of a critical natural frequency. Based on this together with the bending moment curve, the boundary conditions were set to be clamped in the thicker side of the blade and pinned in the other. However, a clamped foundation is an expensive solution since it requires a large foundation, complex details and skilled labour. Instead, the bridge was set to be simply supported to create a material efficient and economically attractive solution.

5.8.4 Bridge deck

The selection of a bridge deck depends on multiple important factors such as structural demands, weight, initial cost and maintenance demands. These factors control what design and material is suitable for this specific bridge. This concept aims to be a way of handling the waste from decommissioned wind turbine blades and hence the whole concept should be sustainable. This involves a lot of aspects but one of the most important one is always the cost. Both the initial cost but also the cost in terms of maintenance. It is also important to include the end-of-life thinking in the choice of bridge deck as this is a growing issue. Apart from these requirements

the bridge deck needs to be connected for both tension and compression in order to transfer the loads.

The materials studied as a bridge deck were FRP, steel, aluminium and timber. Timber was eliminated in an early stage due to the high construction height that would make the bridge unreasonably high. Aluminium was also discarded, mainly due to its high initial cost. In the end, FRP was chosen due to many reasons. First of all, FRP is a strong and lightweight material that lowers both the mass as well as the construction height. Secondly the production process is easy as the decks are prefabricated and the cost could thereby be reduced and partially compensate for the high initial cost. Additionally, the maintenance costs are low. Compared to steel, FRP has a lower initial carbon footprint but the main challenge is the waste management. If a thermosetting polymer is used the ability to reuse as well as recycle is limited. It might be contradictory to add a material that has the same problems as the blade bridge is intended to solve. On the other hand, the bridge will serve a purpose that could reduce the use of additional materials. In addition, the waste management is simplified by using similar materials in the whole bridge.

Bridge decks made of GFRP are most often pultruded elements that are available in different cross sections. The most commonly used are either an I-section or a closed box section. For this concept a box section was used as it simplifies the connections between the deck and the blade. Furthermore, a closed section reduces the wear caused by the surrounding environment and reduces the need for maintenance. On top of the bridge deck an acrylate will be used in order to achieve a suitable walking and biking surface.

5.8.5 Railing

The railing will be made of FRP. This is mainly in order to keep the self-weight low and the material in the bridge concept consistent. For a bridge which allows bicycles, the railing needs to have a minimum height of 1400 mm and the distance between the posts need to be 2000 mm according to TRVK Bro 11 (Trafikverket, 2011). The railing is mounted on top of the bridge deck with a bolted connection. There is one plate on each side of the deck that connects the post. The plates distribute the forces and hence lowers the stress concentrations on the deck.

5.8.6 Connectors

Wind turbine blades have a very irregular shape and thus something to fill the void between flat bridge deck and the blades is required. This can be done by casting on-site using the blades as a mould, 3D-scanning the blades and produce the part off-site or cutting a solid block to fit. Different ways of doing the connections are described in subsection 4.2.2. In Table 5.1, a comparison between bolted connections and bonded connections are done.

Table 5.1: Comparison between bolted and bonded connections.

	Bolted connection	Bonded connection
Production time	Low	High
Production difficulty	Medium	High
Stress concentrations	High	Low
Mid layer requirement	Low	High

The component that will be used between the deck and blades is polyurethane cast on site and connected with bolts. This is a simple process without the need of expensive equipment and materials, as the component that fills the void only needs to carry compression forces. If an adhesive connection were to be used, the bonded joint would have been required on both sides of the void component and required to handle tension forces. Furthermore, the void component needs to be able to transfer all the loads between the deck and blades, whereas for a bolted connection only the compression forces will act on the void component. This reduces the demands of the void component, ensuring a simpler manufacturing process. Polyurethane is a versatile polymer that can be given a wide range of properties. The properties change with the combination of the forming agents: prepolymers, curatives and additives. With the right mixture a material of good compression strength and hardness is created (PSI Urethanes, 2020). Polyurethane is castable in a mould, and typically fully cured after 14 days depending on the added curing agents. The polyurethane bonds with other plastics when casted. Because the polyurethane is castable the component can be created when the blades are placed, and the production is simplified.

6
Modelling

The first step when creating a Finite Element model is to define what the model should be able to describe and how precise the results need to be. A more detailed model gives a more precise result. However, a higher level of detail has a higher computational cost and is more time consuming to create. It is important to verify the FE-model with hand calculations to get an estimation of the result. In that way the result from the FE-model can be predicted, understood and analysed in a better way as well as addressing the limitations in the model.

In this thesis, the FE-program used was BRIGADE/Plus where the 3D-model was imported from Rhino 6. Rhino 6 was used due to the complex geometry of a wind turbine blade and a more accurate model of the blade could be created with the more advanced tools in it. The FE-model was done as one blade with loads applied on the spar cap of the blade. Symmetry was utilized and thus only half the bridge was modelled.

The initial idea was to work with the most common wind turbine in Sweden, Vestas-V90. Due to much of the material being classified, the amount of information regarding this blade was not sufficient. Instead a model from Sandia National Laboratories was used in order to reduce the amount of assumptions in the model. The blade model used is the SNL100-00 from Griffith and Ashwill, 2011. The SNL100-00 has a length of 100 m and a chord length (see Figure 3.2) of 7.628 m. The length of Vestas-V90 is 44 m with a maximum chord length of 3.9 m. In order to get a similar blade to the Vestas-V90, the SNL100-00 was scaled down to half. The length-to-chord ratio for the SNL100-00 is 16% larger compared to the Vestas-V90. Using the SNL100-00 is thus an assumption on the safe side since the blade is modelled with a smaller chord than in reality. When it comes to estimations of the material thickness the approach was not as straight forward. This mainly depends on that the thickness is not given for the Vestas-V90 and thus it is harder to draw accurate assumptions. To account for this a parametric study was performed where the thickness varied between one half to a quarter of the SNL100-00 and a range of results were obtained.

6.1 Element type

Shell elements were used for the FE-model as they are known to be the most efficient elements in terms of computational time. The shell element is a mathematical

simplification of a solid element and should according to the *BRIGADE/Plus User's Manual*, 2018 be used when *"one dimension (the thickness) is significantly smaller than the other two dimensions and in which the stresses in the thickness direction are negligible"*. If the thickness of the part is too large, solid elements should be used as the shell elements gives an inaccurate solution of through thickness stresses. These stresses are important to consider for composites as they can cause delaminations and cracks in the matrix (Akin, 2009). However, the thickness-to-length ratio for the blade is very low and this will not have an impact on the results.

6.2 Material properties

As described in chapter 2, fibre reinforced polymers possesses orthotropic material properties. These properties need to be considered in the model as well, since it can have significant impact on the output. The material type was set to Lamina in BRIGADE/Plus. The properties applied to the model is shown in Table 6.1.

Table 6.1: Equivalent material properties used in the finite element model. Calculated in Appendix A and obtained from Griffith and Ashwill, 2011.

Part of the blade	$E_x[GPa]$	$E_y[GPa]$	$G_{xy}[GPa]$	$\nu_{xy}[-]$	$\rho[kg/m^3]$
Spar cap	26.37	10.04	3.11	0.32	1920
Shell	8.98	5.42	1.93	0.36	1780
Trailing edge	25.23	9.33	2.51	0.31	909
Shear web	10.19	8.55	6.59	0.49	877

The materials were modelled as linear elastic because the stress on the material is expected to be low and serviceability the governing factor. A linear elastic model is accurate when having small elastic strains.

6.2.1 Lamination theory

Depending on what is desired to be modelled and the level of detail, different techniques are used to model the composites. They are separated into three main categories and are shown in Figure 6.1:

- Microscopic modelling: Microscopic model of the composite with the fibres and matrix as separate materials.
- Layered modelling: The composite is modelled as composite layup with each ply having a specific orientation and material properties.
- Smeared modelling: The composite is modelled as one homogeneous material of an equivalent strength.

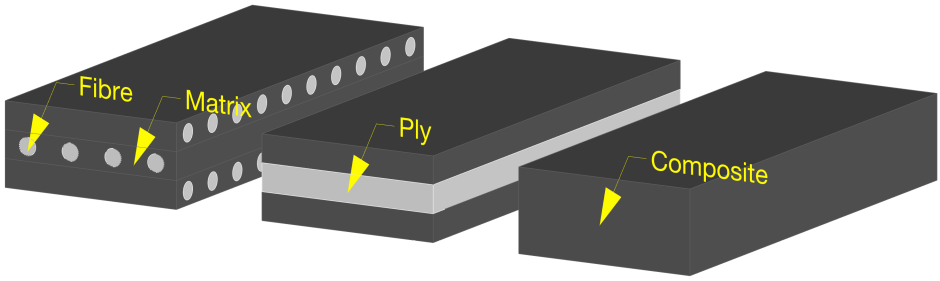

Figure 6.1: From the left: Microscopic modelling, Layered modelling, Smeared modelling.

In this thesis, the blade is modelled as a lamina of a homogeneous material of equivalent strength. This is done because it is the large-scale behaviour of the blade that is of interest. The equivalent material properties of the blade are thus estimated using classical lamination theory. Classical lamination theory is used to analyse the behaviour of a composite material in a simplified manner. Important simplifications are that the layers are perfectly stacked, straight segments remain straight in the deformed shape and that the layers are thin and work in an in-plane state of stress. In lamination theory all plies have specific material properties, orientations and thicknesses. This can then be combined to represent one laminate with its equivalent properties through a series of coupling relations. *Structural Design of Polymer Composites* by Clarke, 1996 was used as the source for the equations.
The fundamental equation of lamination theory is:

$$\begin{Bmatrix} N \\ M \end{Bmatrix} = \begin{bmatrix} A & B \\ B & D \end{bmatrix} \begin{Bmatrix} \epsilon_0 \\ \kappa \end{Bmatrix} \tag{6.1}$$

with the membrane stiffness matrix

$$A = \sum_{k=1}^{N} [Q']^k t_k \tag{6.2}$$

the membrane- flexural coupling matrix

$$B = \frac{1}{2} \sum_{k=1}^{N} [Q']^k Z_k^2 - Z_{k-1}^2 \tag{6.3}$$

and the flexural stiffness matrix

$$D = \frac{1}{3}\sum_{k=1}^{N}[Q']^k Z_k^3 - Z_{k-1}^3 \tag{6.4}$$

where N is the normal force, M the bending moment, ϵ_0 is the laminate midplane strains, κ the curvature of the laminate, t_k is the thickness of the lamina and Z the position of the lamina from the mid-plane of the laminate.

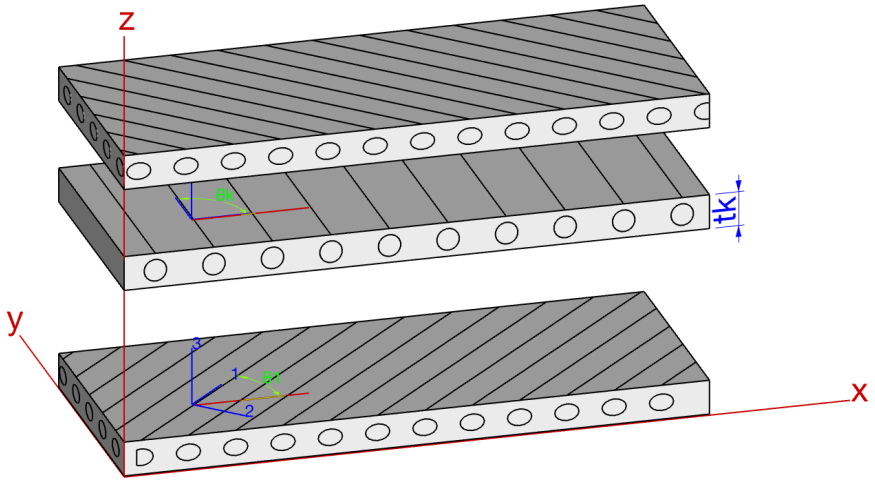

Figure 6.2: Orientations of the layup theory. Shows the global coordinate system (x, y, z) in red and the local coordinate systems (1, 2, 3) in blue, thickness of a lamina t_k and the angle between the principal axis and the local axis θ_k.

$[Q']^k$ is the transformed reduced stiffness matrix for the layer. The reduced stiffness matrix Q contains each layers material properties.

$$Q = \begin{bmatrix} \frac{E_{11}}{1-\nu_{12}\nu_{21}} & \frac{\nu_{21}E_{11}}{1-\nu_{12}\nu_{21}} & 0 \\ \frac{\nu_{12}E_{11}}{1-\nu_{12}\nu_{21}} & \frac{E_{22}}{1-\nu_{12}\nu_{21}} & 0 \\ 0 & 0 & G_{12} \end{bmatrix} \tag{6.5}$$

In order to transform the reduced stiffness matrix to the global system, the transformation matrix $\tilde{T}(\theta)$ is used.

$$\tilde{T}(\theta) = \begin{bmatrix} m^2 & n^2 & 2mn \\ n^2 & m^2 & -2mn \\ -m*n & m*n & m^2-n^2 \end{bmatrix} \tag{6.6}$$

where $m = cos(\theta)$ and $n = sin(\theta)$ and θ is the angle between the lamina's principal direction and the laminate's principal direction. From the membrane stiffness matrix, the equivalent membrane elastic constants solved for as:

$$E_{N.xx} = \frac{1}{A_{11}^{-1} * t_{laminate}} \quad (6.7a) \qquad E_{N.yy} = \frac{1}{A_{22}^{-1} * t_{laminate}} \quad (6.7b)$$

$$\nu_{N.xy} = \frac{A_{12}^{-1}}{A_{11}^{-1}} \quad (6.7c) \qquad \nu_{N.yx} = \frac{A_{12}^{-1}}{A_{22}^{-1}} \quad (6.7d)$$

$$G_{N.xy} = \frac{1}{A_{66}^{-1} * t_{laminate}} \quad (6.7e)$$

From the flexural stiffness matrix, the equivalent bending elastic constants are solved for as:

$$E_{M.xx} = \frac{12}{D_{11}^{-1} * t_{laminate}^{3}} \quad (6.8a) \qquad E_{M.yy} = \frac{12}{D_{22}^{-1} * t_{laminate}^{3}} \quad (6.8b)$$

$$\nu_{M.xy} = \frac{D_{12}^{-1}}{D_{11}^{-1}} \quad (6.8c) \qquad \nu_{M.yx} = \frac{D_{12}^{-1}}{D_{22}^{-1}} \quad (6.8d)$$

$$G_{M.xy} = \frac{12}{D_{66}^{-1} * t_{laminate}^{3}} \quad (6.8e)$$

6.3 Loads and load application

The loads were calculated in accordance to Eurocode and Krav Brobyggande. The calculations are shown in Appendix C and the final loads are shown in Table 6.2. The variable loads and the self-weight from the bridge deck are added on the spar cap as seen in Figure 6.3. The loads are applied to the spar cap in this way to simulate where the loads on and from the bridge deck are carried down.

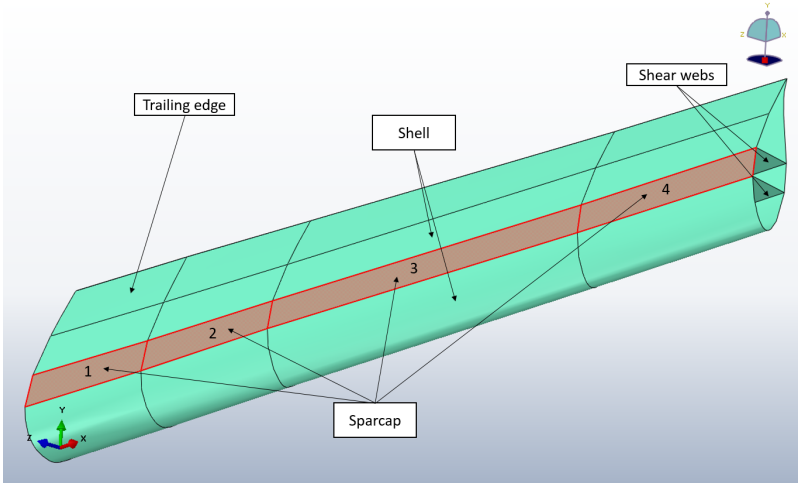

Figure 6.3: The loads were applied on the four sections of the spar cap.

6.3.1 Static general analysis

With a static general analysis, the deformation were controlled against the requirement 1/400 of the span length. This is a requirement for the serviceability limit state and a comfort criterion. According to B.3.4.2.2, *Krav Brobyggande*, 2019, only the variable loads are used to check the deflection requirement. The loads applied can be seen in Table 6.2. The loads were based on the frequent load combination. For a FRP structure, the SLS governs the design as the yield strength of the material is high in comparison to the Young's modulus. Therefore, only the SLS is checked.

Table 6.2: Loads applied to the model in BRIGADE/PLUS, calculated in Mathcad, see Appendix C.

Position of the spar cap	1	2	3	4
Live load [kPa]	5.4	6.1	7.0	7.6

6.3.2 Frequency analysis

The frequency analysis is done with linear perturbation theory. The natural frequency depends on the mass and stiffness of the structure. A higher stiffness increase the frequency and a higher mass decrease the frequency, see Equation 6.9.

$$f_n = \frac{\pi}{2}\sqrt{\frac{EI}{mL^4}} \tag{6.9}$$

All permanent loads have an influence on the natural frequency of the blade. Therefore, the permanent loads from the deck, wearing layer, polyurethane and railing were applied as an increased density of the spar cap. The stiffness contribution from the bridge deck were neglected as no composite action between the deck and blades are intended. Accounting for the additional self-weight while neglecting its stiffness contribution is a conservative assumption as it decreases the fundamental frequency. If the vertical frequency is lower than 5 Hz, a verification of the comfort criteria regarding acceleration of the deck needs to be done.

6.4 Boundary conditions

The boundary conditions for the bridge were set to simply supported. The thick end of the blade was modelled with a pinned support whilst the thin end were modelled with a roller support. The vertical displacement was only fixed in the bottom part of the blade where the bearing will be attached. The boundary conditions were applied in the initial step of the model, before the loads were applied. In order to avoid local frequency modes in the blade, a tied constraint was applied to the cross sections on both ends. This is further described in Appendix C.

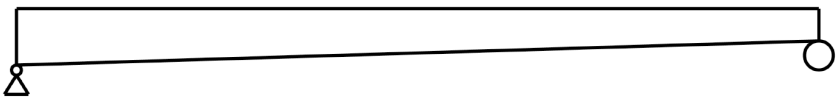

Figure 6.4: Boundary conditions of the bridge.

6.5 Mesh

Due to the complex geometry of the blade some simplifications were done. The blade was created from cross-sections with lofts between them. These sections needed some minor geometrical simplifications in order to get the mesh to work properly. To simplify the geometry, the spar cap was straightened but this is assumed to have a negligible effect on the results.

The mesh was generated on the basis of a sensitivity study. The convergence study can be seen in Appendix C. The mesh was generated with the free top-down meshing technique which according to *BRIGADE/Plus User's Manual*, 2018, is the most flexible technique that can be used on most shapes. However, the free meshing technique provides the least amount of manual control on the mesh to correct potential errors. The element shape was set to quad-dominated. The approximate global element size was set to 50 mm which created 83800 elements. This was true for both the static general analysis and the frequency analysis.

7
Results

The results are based on the outcome obtained from the conceptual design phase and the FE-model. From the conceptual phase the final design of the bridge including the important details will be presented. The results from the FE-model is a control of the designed bridge in terms of comfort criteria.

7.1 Conceptual design

The final design resulted in a bridge where the blades are positioned to carry the vertical loads in the flapwise direction. Both blades span the whole length and are parallel to each other. This is shown in Figure 7.1 and Figure 7.2. The bridge deck is a pultruded FRP deck with a box section. The deck is 80 mm high and spans between the polyurethane components. The components are placed with a cc-distance of 2000 mm and fills the void between the blades and the deck. The deck is connected to the blades with bolts fastened from the inside of the blades through the polyurethane and the spar cap. This is shown in Figure 7.3. The railing will also be made of FRP and attached to the deck through a bolted connection with plates on both sides. The posts are placed with a distance of 2000 mm and the height of the railing is 1400 mm. The connection between the railing and the bridge deck is shown in Figure 7.3. On top of the bridge deck there is an acrylate wearing layer with a thickness of 5 mm.

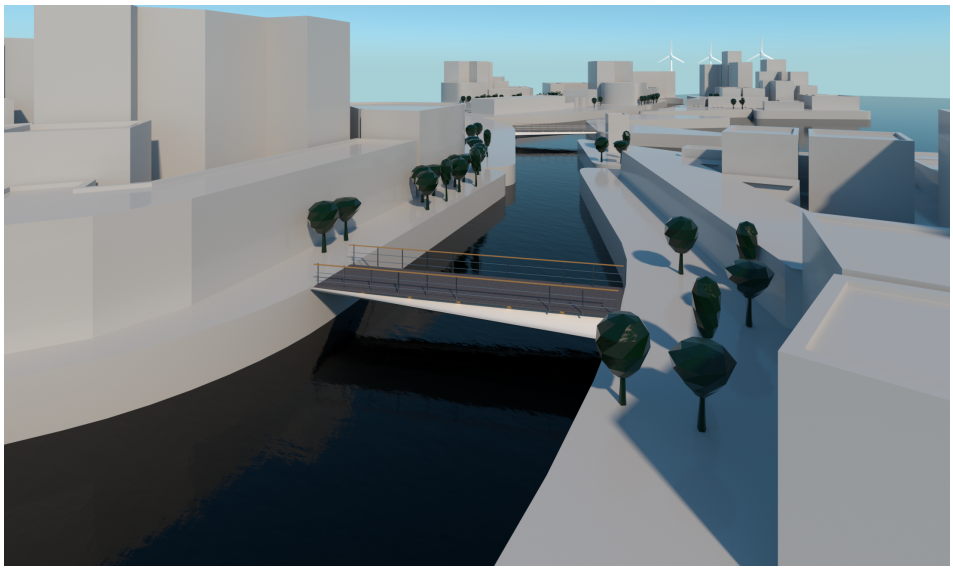

Figure 7.1: Illustration of the final design.

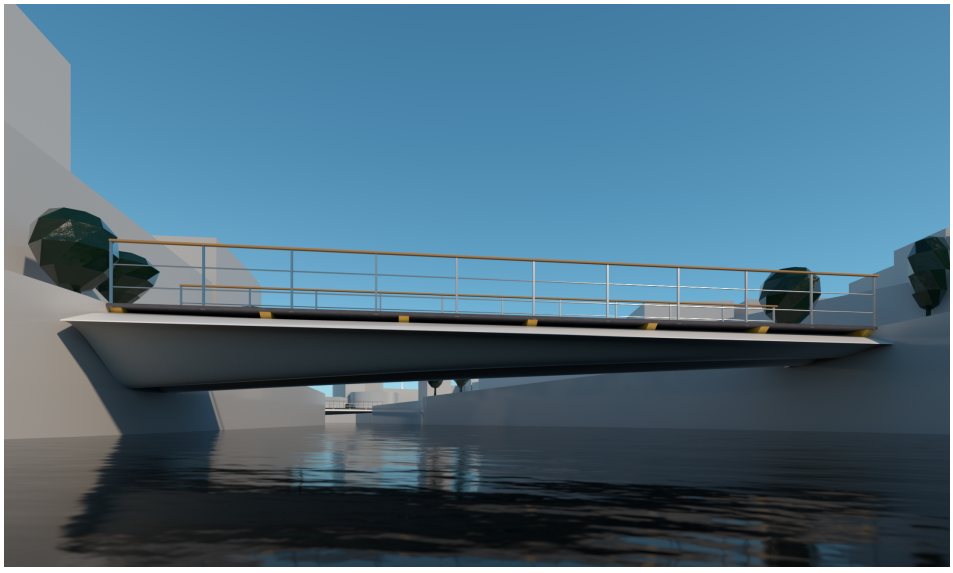

Figure 7.2: Illustration of the final design.

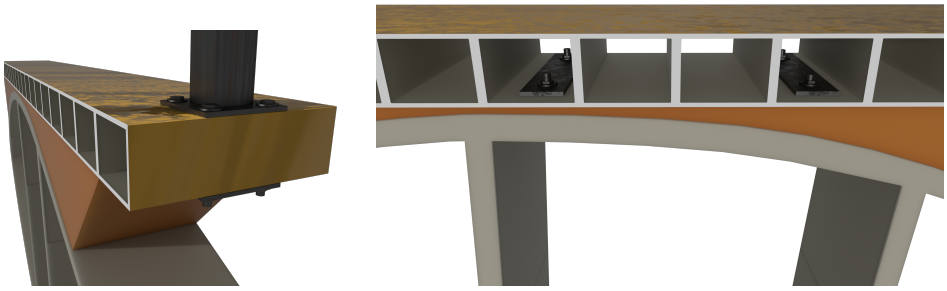

(a) Connection of the railing to the bridge deck.

(b) Connection of the bridge deck to the blade.

Figure 7.3: Connections between the bridge deck, railing and blade.

The bridge will be simply supported and a detailed illustration of the bearing is shown in Figure 7.4. The blade is placed on the bearing and in order to maximise the contact surface, the upper plate will be shaped after the blade. The roller support consists of an elastomeric bearing. This support allows for rotations and horizontal displacement. This movement is important mainly due to thermal expansion caused by temperature variations. The pinned support also consists of an elastomeric bearing but it is restrained to allow for horizontal forces to be transferred.

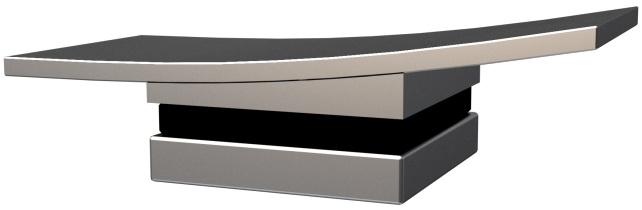

Figure 7.4: An elastomeric bearing designed to support a blade.

In order to minimize the need for maintenance, the ends of the blades will be sealed. This is to avoid water intrusion as well as vermin penetrating the blade and cause structural damage to the bridge. In addition, they work as stiffeners to the structure to prevent local buckling modes near the supports. The seal will be done using bolts so that access to the inside still is possible, if needed.

7.2 FE-model

In Table 7.1 the results obtained from the FE-model in BRIGADE/Plus are shown, calculated with 25%, 33% and 50% of the material thickness in the SNL100-00. The deformation is calculated in the vertical direction for the serviceability limit state using a frequent load combination. In Figure 7.5, the deflection is shown. The frequency calculated is the fundamental frequency of the bridge and is shown in Figure 7.6.

Table 7.1: Deflection and fundamental frequency obtained from BRIGADE/Plus. Thickness is in relation to the SNL100-00.

Thickness [%]	**Deflection** [mm]	$\mathbf{f_1}$ [Hz]
25	27.5	3.4
33	19.0	3.5
50	12.8	3.9
Requirement	≤ 50.0	≥ 5.0

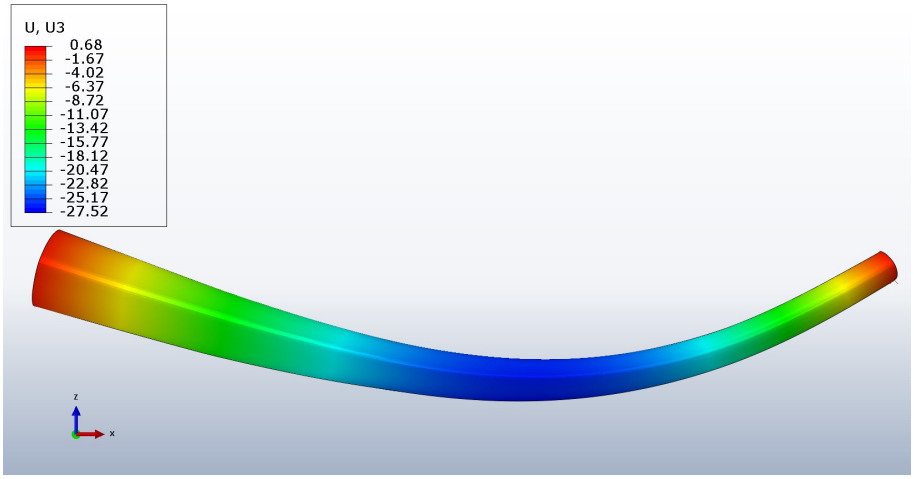

(a) Deflection with 25% of material thickness.

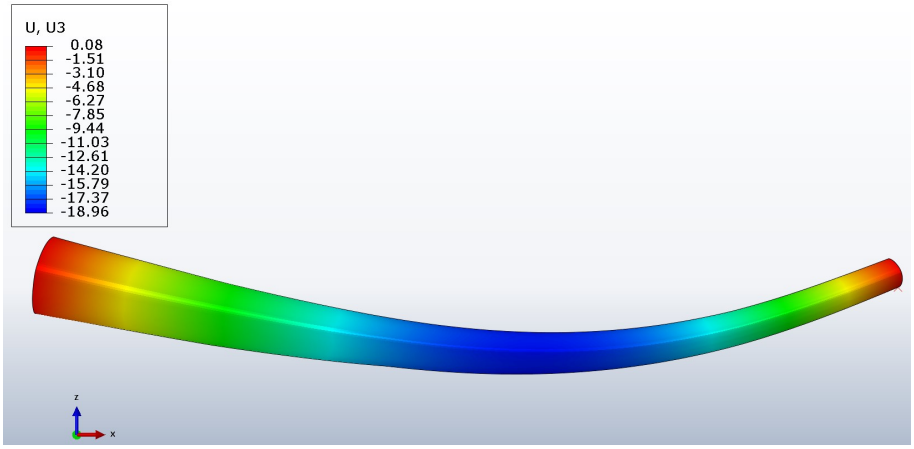

(b) Deflection with 33% of material thickness.

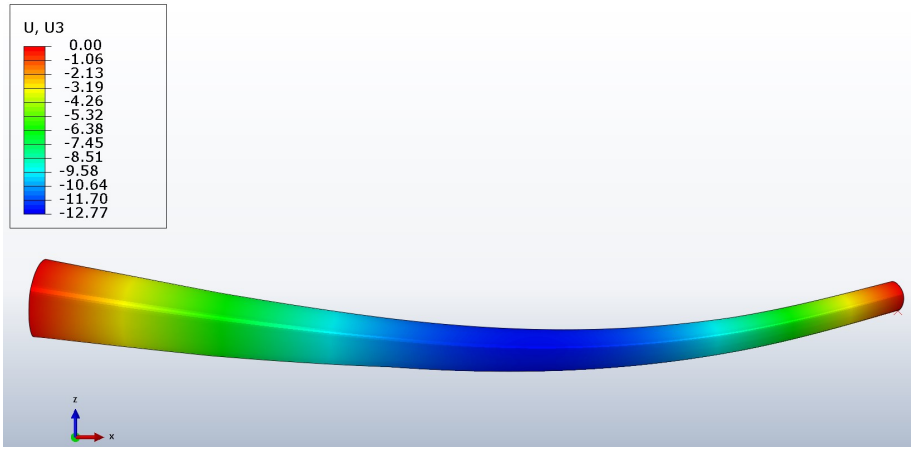

(c) Deflection with 50% of material thickness.

Figure 7.5: Contour plots of vertical deflection. The deflection is measured in mm. Scale factor 100.

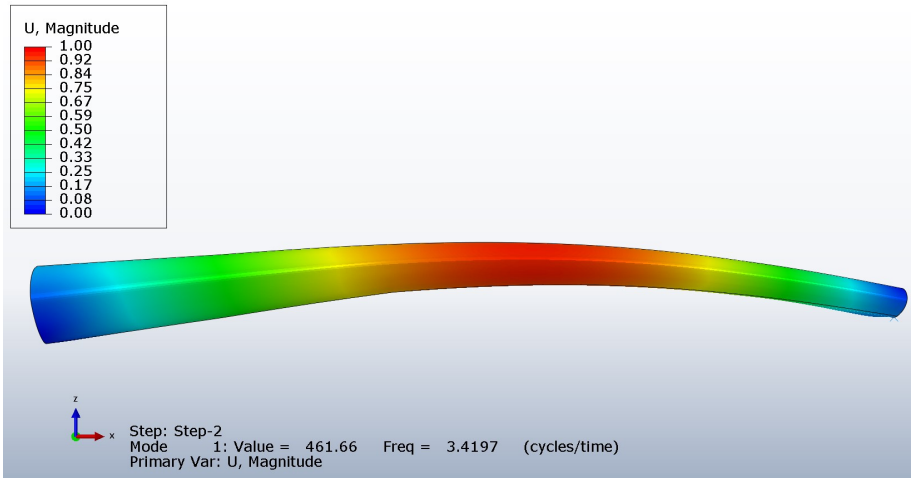

(a) Fundamental frequency with 25% of material thickness.

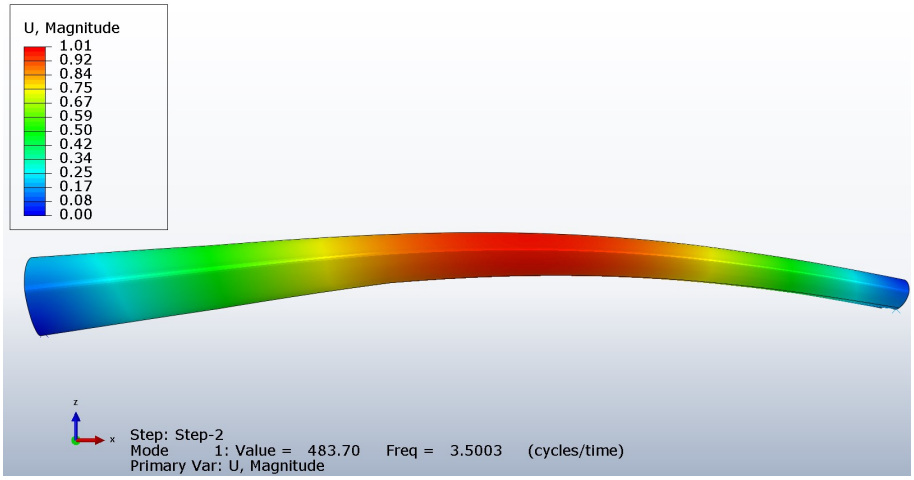

(b) Fundamental frequency with 33% of material thickness.

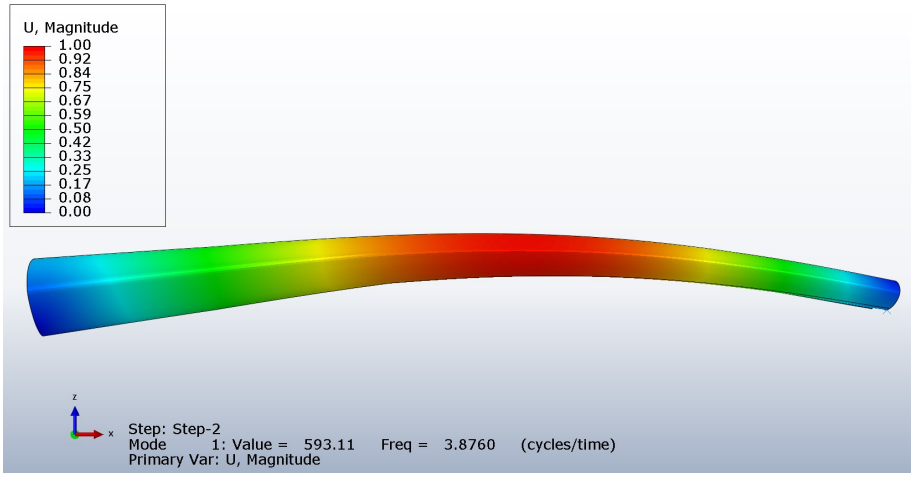

(c) Fundamental frequency with 50% of material thickness.

Figure 7.6: Contour plots of fundamental frequency. The frequency is measured in Hz. Scale factor 1000.

8
Discussion

The initial idea in this project was to use the blades from the most common wind turbine in Sweden, Vestas V90. However, the high level of confidentiality from the producers lead to that a different approach had to be used. The blade model used was a model from Sandia Laboratories, created by researchers. The differences in thinking between what is valued for researchers and companies can result in differences in the final product. The lack of information also led to a lot of assumptions in the blade model as it was scaled down. In order to cover for the uncertainties, a parametric study with variation of the material thickness was performed. This gave a range of results that shows the possibilities of the concept, despite all unknowns. Another uncertainty regarding the model is that the material data for the GFRP is based on an unused material. The blade intended for the bridge is assumed to have been in use for approximately 20 years. However, recent research done by Anmet and conversations with people in the field, all indicates that the knock-down factor on mechanical properties such as strength and stiffness is not significant.

The material was modelled as a homogeneous material. This means that the exact response for each layer and fibre is not calculated but the general behaviour of the structure is investigated. The main reason for this was that the thesis aimed at providing a conceptual design of a pedestrian bridge and hence it is the general behaviour that is of interest. As there is no client or specific location of the bridge, the level of detailing cannot be developed further. In addition, the report from Sandia Laboratories did not provide more information regarding the material properties. The level of detail is therefore considered sufficient for this conceptual study.

The serviceability limit state analysis showed two things, that the deflection criteria was fulfilled with margin and that the fundamental frequency was below 5 Hz. As the fundamental frequency was low, the acceleration needs to be checked. The requirement is that the acceleration should be kept low and if this is not fulfilled, changes to the structure are needed in order to reduce it. This can be done by increasing the stiffness, adding mass, changing the boundary conditions or installing dampers.

The natural frequency obtained from the FE-model were highly dependent on how the boundary conditions were applied. This is since the support conditions affects the shape of the modes. It was therefore crucial to make them as realistic as possible. As the fundamental frequency were too low it was also analysed if it would be sufficient if the boundary conditions were changed to the initial idea, clamped

in one end and a roller support in the other. It proved to be effective and doubled the frequency. However, a fully clamped connection is in reality not achievable as some rotation still will occur which lowers the frequency. In addition, the clamped solution is not economical as it requires a lot of labour and material. Thus, other solutions to increase the fundamental frequency should still be investigated.

When it comes to the selection of the blade section it could have been done differently. First of all the span length, 20 m, was chosen in an early stage as this is a common length for pedestrian bridges. The length influences the frequency of the bridge with a potency of two, where a larger span leads to a lower frequency. A shorter length could therefore be an effective way of increasing the fundamental frequency. In terms of the cross section a rather large section of the blade was chosen. The construction height was 1.9 m and due to this the bridge is not suitable at all locations as there are often limitations on free height. On the other hand, a smaller cross section leads to a lower frequency which in this case is not desirable. Finding a balance between span length, construction height and acceleration will be important.

Even though reusing the blades in bridges extend the lifetime of the blades, the problematic waste management still exists after the bridges are decommissioned. Developing methods to recycle the material in a viable way is therefore still crucial. Sustainable solutions, as wind energy, should include a circular way of thinking. If the waste management of wind turbine blades is not solved, a part of their role as a sustainable alternative is lost. It is also remarkable that such a sustainable and promising solution as wind energy has not acknowledged this issue until recently. The circular way of thinking needs to be adapted for a material to be a long-term solution. Hence, the solution to this problematic waste management is not only to find a way to reuse the blades, but also to find a solution that considers the end-of-life in an early stage.

The wind industry claims that an increased length of the blades leads to a significant increase in the produced energy. This is true, but there are other difficulties that comes with larger blades. Larger blades mean a bigger challenge in terms of the waste management of the decommissioned blades, as the larger blades often contains both glass and carbon fibres. It also requires bigger foundations, more complicated transports and so on. These factors should all be included and considered before increasing the sizes. Once again, it is important to have a lifecycle thinking and include as many aspects as possible before decisions are taken.

The confidentiality in the design of the blade is problematic in order to actually reuse blades in bridges. Due to insurance reasons and client demands, calculations and models generally need to be reviewed by an external part for the design to be approved. The blade bridge that is planned to be built in Aalborg has stalled due to this problem. If the turbine blade producers are not sharing their confidential information and take responsibility of the reuse of the blades, an alternative needs to be found. Maybe where the blade producers share a generic model with the correct equivalent material properties to a reviewer with a confidentiality agreement. This

could be one way of establishing a middle ground.

The solution to handle the blades at their end of life in a wind turbine has to be desired by the blade manufacturers. This can either be forced through legislation or through the desire from the producers to become a truly sustainable energy alternative. The producers are the ones that have the possibilities to develop a composite that is possible to recycle. The producers are the ones that have all the information about the blades, with a very high level of detail. If they truly desire to be sustainable, sharing the general information of the composition of a blade should not be an issue.

9
Conclusion

The conclusions are based on the objectives stated in section 1.2.

The first objective was to characterise the remaining capacity of the material in order to ensure a safe design. This was more challenging than expected. The high level of classified information from the producers in combination with limited amount of research of decommissioned blades complicated this. However, data from tests of used blades was given from Amnet (Appendix D). According to this research along with conversations with people in the field, the reduction in the capacity from service is limited and hence not considered in the thesis. More importantly, there can be localized damage from lightning strikes, collisions with birds and rough climate. These damages can affect the structural behaviour but through visual inspection they can be detected. Either these damaged blades can be repaired, or the blade discarded. These damages are therefore assumed to be negligible.

The next objective was to investigate the demands from the users as well as the regulations provided by Eurocode and Trafikverket. It was concluded that the regulations in terms of geometric guidelines, safety classes and load combinations are well stated. Also, the demands from the clients are constant and unitary. The societal demands are on the other hand not as constant. This could be a challenge in a real project and hence this needs to be investigated.

A brainstorming session were arranged in order to investigate and develop different bridge concepts. 3D blades were printed to improve this process. This was valuable as it is easier to imagine something if you can hold and see the blade. The session resulted in several interesting bridge concepts. It was extra rewarding as architects were a part of this since an additional aspect were added to the bridges. The conceptual design phase resulted in one final concept that was chosen and further designed. In the end it was the concept that had the least complicated details and modifications to the blades as well as the simplest structural system that was chosen. This is economically favourable as the assembly is quick and production as well as maintenance costs can be kept low.

The last objective was to create a FE-model of a blade to verify the feasibility of the design. A working model was created. It showed that the deflection requirements were met but that the fundamental frequency was below the requirement. Thus, a verification of the comfort criteria on accelerations must be performed.

The aim of the master thesis was to create a bridge concept where wind turbine blades are the main structural and load bearing components. Based on the results obtained and knowledge gained, building bridges out of decommissioned wind turbine blades is considered to be a promising solution.

10
Suggestion for further studies

This project was a conceptual study and further investigations needs to be done. There is still significant need for detailed calculations, investigation of the remaining capacity of the blades and fatigue damage from usage of the blades. There is especially a need of a further investigation in terms of the dynamics as the fundamental frequency were too low.

The design of the bridge that were presented in section 7.1 are suggestions on how to solve the most crucial details and connections. These are conceptual ideas that requires further design and calculations. In terms of the support, the solution requires a custom made bearing. This is an expensive option and further studies should be done to find a more standardized solution. For example, the bearing could be a polyurethane component shaped as the blade to have a standardized bearing. In combination with the design of the bearing, the end stiffener for the blade should be designed in order to handle transverse forces and avoid local buckling.

This project aimed at finding a bridge concept where wind turbine blades are the main structural and load bearing components. As a lot of blade waste is expected in a near future, this solution will not be enough to handle all the waste. Therefore, other possible solutions of reusing the blades are needed and could be further investigated. Throughout the project several suggestions were encountered and are listed below:

- In Aalborg a bicycle shed has been built out of a decommissioned wind turbine blade (Energy Supply DK, 2020). The project was a collaboration together with the blade producer Siemens Gamesa. From this the idea to build other types of sheds were born. This could be a good way to reuse the large quantities of decommissioned blades. For instance, the substitute booths at football stadiums could have a similar design. Similarly, bus stops could be designed. In order to move further with these proposals, it is required to do investigations in terms of the load bearing capacities. An investigation in terms of surface treatments would also be necessary.
- Similar to the above mentioned sheds, a roof construction could be built. For instance, in pavilions or in simple housing as the shape of the blades remind of these roof constructions. This would take advantage of the widths of the blades as they will cover a large part. Similar investigation as above are then needed. Furthermore, there will be a challenge to solve the attachment between the blade and the superstructure in a good way.

- In an article published by BBC News, 2020, the problem of the decommissioned wind turbine blades was addressed. In the article, a company called Global Fibreglass Solutions is interviewed that has created something called EcoPly. This is small pellets created from fibreglass composites. The pellets could then be used in waterproof boards for the construction industry or in injectable plastics. Suggestions for further studies is to investigate whether this is a sustainable solution and how profitable it is compared to reuse. A comparison between the current waste management could also be done.
- As the blades are hollow they could be used as floating devices. This could be utilized in floating constructions such as piers or in wave energy. A roughly made calculation supports this claim as they are much lighter than water. This would need to be further investigated in order to verify if the blades are suitable to be placed in water as well as the design of these solutions.
- As described in section 2.8 and in Figure 2.7, playgrounds and benches have been built in Rotterdam. This is an interesting idea as the blades original shape is used in the design. This proposal could also be further investigated and the production process of these could be optimized and hence more economically attractive.

(a) Bicycle shed in Aalborg (Energy Supply DK, 2020)

(b) Bench in Rotterdam. Photo: Deniz Guzzo

(c) Playground in Rotterdam. Photo: Deniz Guzzo

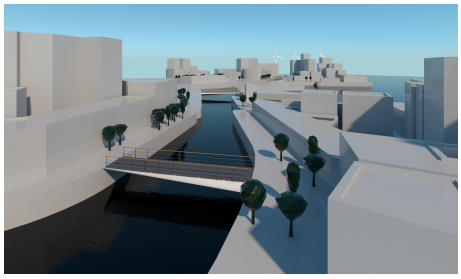

(d) Bridge concept

Figure 10.1: Examples of reuse of wind turbine blades.

Bibliography

Abdillahi, A. M. (2011). *Modellering av NACA 63* (tech. rep.). Universitetet i Stavanger.

Akin, J. E. (2009). *Finite Element Analysis Concepts via SolidWorks* (tech. rep.). Rice University. Houston, Texas.

Al-Khudairi, O., Hadavinia, H., Little, C., Gillmore, G., Greaves, P., & Dyer, K. (2017). Full-scale fatigue testing of a wind turbine blade in flapwise direction and examining the effect of crack propagation on the blade performance. *Materials*, *10*(10). https://doi.org/10.3390/ma10101152

Andersen, N., Eriksson, O., Hillman, K., & Wallhagen, M. (2016). Wind turbines' end-of-life: Quantification and characterisation of future waste materials on a national level. *Energies*, *9*(12). https://doi.org/10.3390/en9120999

Ascione, L., Caron, J.-F., Godonou, P., van IJselmuijden, K., Knippers, J., Mottram, T., Oppe, M., Gantriis Sorensen, M., Taby, J., & Tromp, L. (2016). Prospect for New Guidance in the Design of FRP. *EUR 27666 EN*, 172. https://doi.org/10.2788/22306

Ascione, L., Berardi, V. P., & D'Aponte, A. (2012). Creep phenomena in FRP materials. *Mechanics Research Communications*. https://doi.org/10.1016/j.mechrescom.2012.03.010

Ashwill, T. D. (2009). *Materials and Innovations for Large Blade Structures: Research Opportunities in Wind Energy Technology* (tech. rep.). www.awea.org

Ashwill, T., & Veers, P. (2004). *Innovative Design Approaches for Large Wind Turbine Blades Final Report* (tech. rep.). Sandia National Laboratories. http://www.ntis.gov/help/ordermethods.asp?loc=7-4-0#online

BBC News. (2020). What happens to all the old wind turbines? https://www.bbc.com/news/business-51325101

Beauson, J. ; & Brøndsted, P. (2016). Wind Turbine Blades: An End of Life Perspective. *Citation*, 421–432. https://doi.org/10.1007/978-3-319-39095-6{_}23

Black, S. (2003). Getting To The Core Of Composite Laminates. https://www.compositesworld.com/articles/getting-to-the-core-of-composite-laminates

Bladena. (2019). *The Blade Handbook*.

Boogh, L., & Mezzenga, R. (2000). Processing Principles for Thermoset Composites, In *Comprehensive composite materials*. Elsevier. https://doi.org/10.1016/b0-08-042993-9/00221-7

Branner, K. (2011). *Wind turbine blade testing under combined loading ReliaBlade-Prediction of Structural Blade Reliability and Application to Cost Effective Blades by Digital Twins View project DARWIN-Drone Application for pi-*

oneering Reporting in Wind turbine blade INspections View project (tech. rep.). https://www.researchgate.net/publication/287760066

BRIGADE/Plus User's Manual. (2018). Scanscot Technology.

Buckney, N., Green, S. D., Pirrera, A., & Weaver, P. M. (2012). Wind turbine blade structural efficiency. *Collection of Technical Papers - AIAA/ASME/ASCE/AHS/ASC Structures, Structural Dynamics and Materials Conference*, (April). https://doi.org/10.2514/6.2012-1502

Campbell, F. C. (2010). *Structural Composite Materials*. https://books.google.se/books?hl=sv&lr=&id=D3Wta8e07t0C&oi=fnd&pg=PR1&dq=Campbell,+F.C.+(2010).+Structural+Composite+Materials.+ASM+International.+Ohio,+USA.&ots=T-1ceDY9td&sig=H_WqjXPN0Z_hPV028fmQeU2Ilsk&redir_esc=y#v=onepage&q&f=false

Carlstedt, N.-e. (2016). *Vindkraftverk > 50 kW* (tech. rep.). Energimyndigheten.

Chady, T., Sikora, R., Lopato, P., Psuj, G., Szymanik, B., Balasubramaniam, K., & Rajagopal, P. (2016). Metody nieniszczacego badania łopat turbin wiatrowych. *Przeglad Elektrotechniczny*, *92*(5), 1–4. https://doi.org/10.15199/48.2016.05.01

Clarke, J. (1996). Structural Design of Polymer Composites.

CNR DT 205 (tech. rep.). (2007). NATIONAL RESEARCH COUNCIL OF ITALY ADVISORY COMMITTEE ON TECHNICAL RECOMMENDATIONS FOR CONSTRUCTION.

CROW-CUR 96 (tech. rep.). (2019).

D'Antino, T., Pisani, M. A., & Poggi, C. (2018). Effect of the environment on the performance of GFRP reinforcing bars. *Composites Part B: Engineering*, *141*, 123–136. https://doi.org/10.1016/j.compositesb.2017.12.037

D'Antino, T., & Pisani, M. A. (2019). Long-term behavior of GFRP reinforcing bars. *Composite Structures*, *227*. https://doi.org/10.1016/j.compstruct.2019.111283

DNV. (2010). *STANDARD DESIGN AND MANUFACTURE OF WIND TURBINE BLADES, OFFSHORE AND ONSHORE WIND TURBINES* (tech. rep.). https://doi.org/DetNorskeVeritas

Energimyndigheten. (2014). Elcertifikatsystemet är ett marknadsbaserat stödsystem. Läs mer om systemet här. https://www.energimyndigheten.se/fornybart/elcertifikatsystemet/om-elcertifikatsystemet/

Energimyndigheten. (2019). Sveriges energi- och klimatmål. https://www.energimyndigheten.se/klimat--miljo/sveriges-energi--och-klimatmal/

Energy Supply DK. (2020). Vindmøllevinge får nyt liv på Aalborg Havn. https://www.energy-supply.dk/article/view/699757/vindmollevinge_far_nyt_liv_pa_aalborg_havn

European Commission. (2019). Directive 2008/98/EC on waste (Waste Framework Directive). https://ec.europa.eu/environment/waste/framework/

EWEA. (n.d.). *Research note outline on recycling wind turbine blades* (tech. rep.). European Wind Energy Association.

F. Sayer, F. Bürkner, M. Blunk, A. M. van Wingerde, & H.-G. Busmann. (2009). *Influence of Loads and Environmental Conditions on Material Properties over the Service Life of Rotor Blades* (tech. rep.).

Fiberline. (2003). *Fiberline Design Manual* (tech. rep.).

Fibermax Composites. (n.d.). Weaving styles and patterns of fabrics for composites. http://www.fibermax.eu/index_files/weavingstylesandpatterns.htm

Germanischer Lloyd. (2010). *Regulations for the certification of wind energy conversion system.* (tech. rep.). Hamburg. www.gl-group.com/GLRenewables

Giorgini, L., Giorgini Professor, L., Leonardi, C., Mazzocchetti Assistant Professor, L., Zattini, G., Sp, C., Montanari Curti Spa, I., Cristian Tosi Curti Spa Divisione Energia, I., & Tiziana Benelli Assistant Professor, I. (2016). Massimo Cavazzoni Pyrolysis of Fiberglass/Polyester Composites: Recovery and Characterization of Obtained Products. https://doi.org/10.5937/fmet1604405G

Göteborgs Stad. (2019). Teknisk Handbok. https://tekniskhandbok.goteborg.se/

Gowayed, Y. (2013). Types of fiber and fiber arrangement in fiber-reinforced polymer (FRP) composites, In *Developments in fiber-reinforced polymer (frp) composites for civil engineering*. Elsevier Inc. https://doi.org/10.1533/9780857098955.1.3

Greaves, P. (2016). Design of offshore wind turbine blades, In *Offshore wind farms: Technologies, design and operation*. Elsevier Inc. https://doi.org/10.1016/B978-0-08-100779-2.00006-4

Griffith, T., & Ashwill, T. (2011). *SANDIA REPORT The Sandia 100-meter All-glass Baseline Wind Turbine Blade: SNL100-00* (tech. rep.). Sandia National Laboratories. Albuquerque, New Mexico. https://energy.sandia.gov/wp-content/gallery/uploads/113779.pdf

Gurit. (2019). Composite materials for Wind Energy. www.gurit.com

Haselbach, P. U., & Branner, K. (2016). Initiation of trailing edge failure in full-scale wind turbine blade test. *Engineering Fracture Mechanics*, *162*, 136–154. https://doi.org/10.1016/j.engfracmech.2016.04.041

Heinemeyer, C., Butz, C., Keil, A., Schlaich, M., Goldack, A., Trometer, S., Lukić, M., Chabrolin, B., Lemaire, A., Martin, P.-O., Cunha, Á., & Caetano, E. (2009). *Design of Lightweight Footbridges for Human Induced Vibrations* (tech. rep.).

Hollaway, L. C. (2010). A review of the present and future utilisation of FRP composites in the civil infrastructure with reference to their important in-service properties. Elsevier Ltd. https://doi.org/10.1016/j.conbuildmat.2010.04.062

Hsiao, K.-T., & Heider, D. (2012). Vacuum assisted resin transfer molding (VARTM) in polymer matrix composites, In *Manufacturing techniques for polymer matrix composites (pmcs)*. Elsevier. https://doi.org/10.1533/9780857096258.3.310

IEC. (1999). *Wind turbine generator systems-Part 1: Safety requirements Aérogénérateurs-Partie 1: Spécifications de sécurité* (tech. rep.). http://www.iec.ch

Ierides, M., Reiland, J., & Dierckx, A. (2019). Wind turbine blade circularity: Technologies and practices around the value chain. *WindEurope Conference & Exhibition 2-4 April 2019, Workshop on blade disposal*, 1–38.

Jamieson, P. (2011). *Innovation in Wind Turbine Design*. John Wiley; Sons. https://doi.org/10.1002/9781119975441

Jensen, F. M. (2009). *Ultimate strength of a large wind turbine blade*. Roskilde, Denmark, Risø National Laboratory.

Jensen, M. F., & Branner, K. (2013). Introduction to wind turbine blade design, In *Advances in wind turbine blade design and materials*. https://doi.org/10.1533/9780857097286.1.3

Job, S. (2013). Recycling glass fibre reinforced composites - History and progress. *Reinforced Plastics*. https://doi.org/10.1016/S0034-3617(13)70151-6

Joshi, S. (2012). The pultrusion process for polymer matrix composites, In *Manufacturing techniques for polymer matrix composites (pmcs)*. Elsevier. https://doi.org/10.1533/9780857096258.3.381

Kennerley, J. R., Kelly, R. M., Fenwick, N. J., Pickering, S. J., & Rudd, C. D. (1998). The characterisation and reuse of glass fibres recycled from scrap composites by the action of a fluidised bed process. *Composites Part A: Applied Science and Manufacturing*, *29*(7), 839–845. https://doi.org/10.1016/S1359-835X(98)00008-6

Khayyam, H., Jazar, R. N., Nunna, S., Golkarnarenji, G., Badii, K., Fakhrhoseini, S. M., Kumar, S., & Naebe, M. (2020). PAN precursor fabrication, applications and thermal stabilization process in carbon fiber production: Experimental and mathematical modelling. Elsevier Ltd. https://doi.org/10.1016/j.pmatsci.2019.100575

Kong, C., Bang, J., & Sugiyama, Y. (2005). Structural investigation of composite wind turbine blade considering various load cases and fatigue life. *Energy*, *30*(11-12 SPEC. ISS.), 2101–2114. https://doi.org/10.1016/j.energy.2004.08.016

Krav Brobyggande (tech. rep.). (2019). Trafikverket.

Kulkarni, G. S. (2018). Introduction to Polymer and Their Recycling Techniques, In *Recycling of polyurethane foams*. Elsevier. https://doi.org/10.1016/b978-0-323-51133-9.00001-2

Lee, H. G., Kang, M. G., & Park, J. (2015). Fatigue failure of a composite wind turbine blade at its root end. *Composite Structures*, *133*, 878–885. https://doi.org/10.1016/j.compstruct.2015.08.010

Liu, P., & Barlow, C. Y. (2017). Wind turbine blade waste in 2050. *Waste Management*, *62*, 229–240. https://doi.org/10.1016/j.wasman.2017.02.007

Mara, V. (2015). *Development of connections for fibre reinforced bridge elements and an analysis of sustainability* (Doctoral dissertation). Chalmers tekniska högskola.

Mara, V., Haghani, R., & Harryson, P. (2014). Bridge decks of fibre reinforced polymer (FRP): A sustainable solution. *Construction and Building Materials*, *50*, 190–199. https://doi.org/10.1016/j.conbuildmat.2013.09.03

Martin, C. (2020). Wind Turbine Blades Can't Be Recycled, So They're Piling Up in Landfills - Bloomberg. https://www.bloomberg.com/news/features/2020-02-05/wind-turbine-blades-can-t-be-recycled-so-they-re-piling-up-in-landfills

Martin, R. (2016). Analysis of Polarimetric Terahertz Imaging for Non-Destructive Detection of Subsurface Defects in Wind Turbine Blades.

Martin, R., Baird, C. S., Giles, R. H., Niezrecki, C., & Lowell, M. (2016). Terahertz ISAR and x-ray imaging of wind turbine blade structures. https://doi.org/10.1117/12.2218616

McIlhagger, A., Archer, E., & McIlhagger, R. (2015). Manufacturing processes for composite materials and components for aerospace applications, In *Polymer composites in the aerospace industry*. Elsevier Inc. https://doi.org/10.1016/B978-0-85709-523-7.00003-7

Mishnaevsky, L., Branner, K., Petersen, H. N., Beauson, J., McGugan, M., & Sørensen, B. F. (2017). Materials for wind turbine blades: An overview. MDPI AG. https://doi.org/10.3390/ma10111285

Muniz, I., & Bansal, A. (2009). *Assessment of the performance of FRP materials for construction application* (tech. rep.). Trans-IND.

Ortegon, K., Nies, L. F., & Sutherland, J. W. (2013). Preparing for end of service life of wind turbines. *Journal of Cleaner Production*, *39*, 191–199. https://doi.org/10.1016/j.jclepro.2012.08.022

Potyrała, P. B., Ramón, J., & Rius, C. (2011). *PROJECTE O TESINA D'ESPECIALITAT Títol Use of Fibre Reinforced Polymer Composites in Bridge Construction. State of the Art in Hybrid and All-Composite Structures* (tech. rep.).

PSI Urethanes. (2020). What is thermoset polyurethane? https://psiurethanes.com/what-is-thermoset-polyurethane/

Quartus Engineering. (2019). COMPOSITES 101. https://www.quartus.com/resources/composites-101/

Råd Brobyggande (tech. rep.). (2019). Trafikverket.

Reis, E. M., & Rizkalla, S. H. (2008). Material characteristics of 3-D FRP sandwich panels. *Construction and Building Materials*, *22*(6), 1009–1018. https://doi.org/10.1016/j.conbuildmat.2007.03.023

Reza Haghani Dogaheh. (2013). *Needs for maintenance and refurbishment of bridges in urban environments Low-disturbance sustainable urban construction* (tech. rep.).

Russell, G., & Irel, N. (2019). Analysis and Design of a Pedestrian Bridge with Decommissioned FRP Windblades and Concrete, (June), 1–5.

Schubel, P. J., & Crossley, R. J. (2012). Wind turbine blade design. *Energies*, *5*(9), 3425–3449. https://doi.org/10.3390/en5093425

Sørensen, B. F., Jørgensen, E., Debel, C. P., Jensen, F. M., Jensen, H. M., Jacobsen, T. K., & Halling, K. M. (2004). *Improved design of large wind turbine blade of fiber composites based on studies of scale effects (Phase 1)* (Vol. 1390). https://doi.org/Ris{\o}-R-1390(EN)

SS-EN 14080 (tech. rep.). (2013). SIS. https://www.sis.se/std-98579

SS-EN 1990 (tech. rep.). (2002). SIS. www.sis.se

SS-EN 1990/A1 (tech. rep.). (2005). SIS. www.sis.se

SS-EN 1991-1-1 (tech. rep.). (2002). SIS.

SS-EN 1991-1-3 (tech. rep.). (2003). SIS. www.sis.se

SS-EN 1991-1-4 (tech. rep.). (2005). SIS. www.sis.se

SS-EN 1991-1-5 (tech. rep.). (2003). SIS.

SS-EN 1991-2 (tech. rep.). (2003). SIS. www.sis.se

SS-EN 1993-1-1 (tech. rep.). (2005). SIS. www.sis.se

Stijn Speksnijder. (2018). *Reuse of wind turbine blades in a slow traffic bridge* (tech. rep.).

Trafikverket. (2011). *TRVK Bro 11*.

Trafikverket. (2019). Villkor. https://www.trafikverket.se/for-dig-i-branschen/vag/Transportdispens/Villkor/

Trafikverket. (2020a). *Krav - VGU, Begrepp och grundvärden* (tech. rep.). Trafikverket.

Trafikverket. (2020b). *Krav - VGU, Vägars och gators utformning*. Trafikverket.

Transportstyrelsen. (2013). Dimensioner. https://www.transportstyrelsen.se/sv/vagtrafik/Yrkestrafik/Gods-och-buss/Matt-och-vikt/Dimensioner/

TSFS (tech. rep.). (2018). Transportstyrelsen.

Van Oudheusden, A. A. (2019). *Recycling of composite materials* (tech. rep.).

Vestas. (2010). General Specification V90–1.8/2.0 MW 50 Hz VCS. www.vestas.com

Vijay, N., Rajkumara, V., & Bhattacharjee, P. (2016). Assessment of Composite Waste Disposal in Aerospace Industries. *Procedia Environmental Sciences*, *35*, 563–570. https://doi.org/10.1016/j.proenv.2016.07.041

Wardle, M. W. (2000). *Polymer Matrix Composites* (tech. rep.). www.cubictechnology.com

Wikipedia Commons. (2009). Glass_Fiber.jpg. https://upload.wikimedia.org/wikipedia/commons/3/31/Glass_Fiber.jpg

Yang, B., & Sun, D. (2013). Testing, inspecting and monitoring technologies for wind turbine blades: A survey. https://doi.org/10.1016/j.rser.2012.12.056

Yazdanbakhsh, A., Bank, L. C., & Tian, Y. (2018). Recycling Mechanical Processing of GFRP Waste into Large-Sized Pieces for Use in Concrete. https://doi.org/10.3390/recycling3010008

A

Appendix: Lamination theory

```
%% Appendix B:Lamination theory
% Calculation of equivalent laminate properties. Reference:
% Clarke, J. (1996). Structural Design of Polymer Composites.
clc
clf
clear all
close all

% Properties for TE Reinforcement %

EL=[27.7; 41.8; 3.44 ; 41.8; 27.7]*10^9;     % [Pa]
ET=[13.65; 14.0; 3.44; 14.0; 13.65]*10^9;    % [Pa]
GLT=[7.2; 2.63; 1.38; 2.63; 7.2]*10^9;       % [Pa]
vLT=[0.39; 0.28; 0.3; 0.28; 0.39];           % [-]
a=0*pi/180;                                  % Rad

th = 0;                              % Fiber angle from normala axis
N = 5;                               % Number of layers
h =[5; 30; 60; 30; 5]*10^-3;         % Thickness of laminas
HH = sum(h);                         % Total thickeness of the laminate
A=zeros(3);D=A;B=A;
for i=1:N

    % Reduced Compliance Matrix for glass
    SLT = [1/EL(i) -vLT(i,1)/EL(i) 0;
          -vLT(i)/EL(i) 1/ET(i) 0;
           0 0 1/GLT(i)];            % Reduced Compliance Matrix
    QLT = inv(SLT);                  % Reduced Stiffness Matrix (Eq 4.50)
    hi=0;
    a=((-1)^i)*th; % Since for Tbar theta=-theta
    hi=-HH/2+sum(h(1:i)); hj=hi-h(i);
    m=cos(a); n=sin(a);
```

```
33      Tbar=[ m^2 n^2 2*m*n;
34             n^2 m^2 -2*m*n;
35            -m*n m*n m^2-n^2]; % Transformation Matrix
36      Qp=Tbar * QLT;
37      A=A+(Qp*(hi-hj));          % Membrane stiffnes matrix (Eq
            4.51)
38      D=D+(1/3)*Qp*(hi^3-hj^3);% Flexural stiffness matrix  (
            Eq 4.53)
39  end
40
41  a = inv(A); d = inv(D);
42  % Equivalent membrane elastic constants (Eq 4.54)
43  Exx = 1/(HH*a(1,1));
44  Eyy = 1/(HH*a(2,2));
45  Gxy = 1/(HH*a(3,3));
46  vxy = -a(1,2)/a(1,1);
47  vyx = -a(1,2)/a(2,2);
48
49
50  % Equivalent bending elastic constants (Eq 4.55)
51  Exx_M = 12/(HH^3*d(1,1));
52  Eyy_M = 12/(HH^3*d(2,2));
53  Gxy_M = 12/(HH^3*d(3,3));
54  vxy_M = -d(1,2)/d(1,1);
55  vyx_M = -d(1,2)/d(2,2);
56
57
58  Constant = {'Membrane'; 'Bending'};
59  Ex       = [Exx; Exx_M];
60  Ey = [Eyy; Eyy_M];
61  G = [Gxy; Gxy_M];
62  v_xy = [vxy; vxy_M];
63  v_yx = [vyx; vyx_M];
64  Trailingedge = table(Constant, Ex, Ey, G, v_xy, v_yx)
65
66
67  % Properties for Spar cap %
68  EL=[27.7; 41.8; 41.8; 27.7]*10^9;
69  ET=[13.65; 14.0; 14.0; 13.65]*10^9;
70  GLT=[7.2; 2.63; 2.63; 7.2]*10^9; % Pa
71  vLT=[0.39; 0.28; 0.28; 0.39]; a=0*pi/180; % Rad
72
73  th = 0;                        % Fiber angle from normala axis
74  h =[5; 30; 30; 5]*10^-3;       % Thickness of laminas
75  N = length(h);                 % Number of layers
76  HH = sum(h);                   % Total thickeness of the
```

```
    laminate
A=zeros(3);D=A;B=A;
for i=1:N
    % Reduced Compliance Matrix for glass
    SLT = [1/EL(i) -vLT(i)/EL(i) 0;
          -vLT(i)/EL(i) 1/ET(i) 0;
           0 0 1/GLT(i)];              % Reduced Compliance
              Matrix

    QLT = inv(SLT);                    % Reduced Stiffness
       Matrix
    hi=0;
    a=((-1)^i)*th;                     % Since for Tbar theta=-
       theta
    hi=-HH/2+sum(h(1:i)); hj=hi-h(i);
    m=cos(a); n=sin(a);
    Tbar=[ m^2 n^2 2*m*n;
           n^2 m^2 -2*m*n;
          -m*n m*n m^2-n^2]; %Transformation Matrix
    Qp=Tbar * QLT;
    A=A+(Qp*(hi-hj));
    D=D+(1/3)*Qp*(hi^3-hj^3);
end

a = inv(A); d = inv(D);
% Equivalent membrane elastic constants
Exx = 1/(HH*a(1,1));
Eyy = 1/(HH*a(2,2));
Gxy = 1/(HH*a(3,3));
vxy = -a(1,2)/a(1,1);
vyx = -a(1,2)/a(2,2);

% Equivalent bending elastic constants
Exx_M = 12/(HH^3*d(1,1));
Eyy_M = 12/(HH^3*d(2,2));
Gxy_M = 12/(HH^3*d(3,3));
vxy_M = -d(1,2)/d(1,1);
vyx_M = -d(1,2)/d(2,2);


Constant = {'Membrane'; 'Bending'};
Ex       = [Exx; Exx_M];
Ey = [Eyy; Eyy_M];
G = [Gxy; Gxy_M];
v_xy = [vxy; vxy_M];
v_yx = [vyx; vyx_M];
```

```
Sparcap = table(Constant, Ex, Ey, G, v_xy, v_yx)

% Properties for Shear web %
EL=[27.7; 13.6; 0.256; 13.3; 27.7]*10^9;
ET=[13.65; 13.3; 0.256; 13.6; 13.65]*10^9;
GLT=[7.2; 11.8; 0.022; 11.8; 7.2]*10^9; % Pa
vLT=[0.39; 0.51; 0.3; 0.51; 0.39]; a=0*pi/180; % Rad

th = 0;                    % Fiber angle from normala axis
h =[5; 30; 80; 30; 5]*10^-3;  % Thickness of laminas
N = length(h);                  % Number of layers
HH = sum(h);               % Total thickeness of the laminate
A=zeros(3); D=A; B=A;
for i=1:N
    % Reduced Compliance Matrix
    SLT = [1/EL(i) -vLT(i)/EL(i) 0;
          -vLT(i)/EL(i) 1/ET(i) 0;
          0 0 1/GLT(i)];
    QLT = inv(SLT);                % Reduced Stiffness Matrix
    hi=0;
    a=((-1)^i)*th; % Since for Tbar theta=-theta
    hi=-HH/2+sum(h(1:i)); hj=hi-h(i);
    m=cos(a); n=sin(a);
    Tbar=[ m^2 n^2 2*m*n;
           n^2 m^2 -2*m*n;
          -m*n m*n m^2-n^2]; %Transformation Matrix
    Qp=Tbar * QLT;
    A=A+(Qp*(hi-hj));
    D=D+(1/3)*Qp*(hi^3-hj^3);
end

a = inv(A); d = inv(D);
% Equivalent membrane elastic constants
Exx = 1/(HH*a(1,1));
Eyy = 1/(HH*a(2,2));
Gxy = 1/(HH*a(3,3));
vxy = -a(1,2)/a(1,1);
vyx = -a(1,2)/a(2,2);

% Equivalent bending elastic constants
Exx_M = 12/(HH^3*d(1,1));
Eyy_M = 12/(HH^3*d(2,2));
Gxy_M = 12/(HH^3*d(3,3));
vxy_M = -d(1,2)/d(1,1);
vyx_M = -d(1,2)/d(2,2);

```

```
Constant = {'Membrane'; 'Bending'};
Ex       = [Exx; Exx_M];
Ey = [Eyy; Eyy_M];
G = [Gxy; Gxy_M];
v_xy = [vxy; vxy_M];
v_yx = [vyx; vyx_M];
Shearweb = table(Constant, Ex, Ey, G, v_xy, v_yx)



% Properties for Shell %
EL=[27.7; 3.5; 27.7]*10^9;
ET=[13.65; 3.5; 13.65]*10^9;
GLT=[7.2; 0.022; 7.2]*10^9; % Pa
vLT=[0.39; 0.3; 0.39]; a=0*pi/180; % Rad
h =[5; 60; 5]*10^-3;  % Thickness of laminas

th = 0;                    % Fiber angle from normala axis
N = length(h);                    % Number of layers
HH = sum(h);               % Total thickeness of the laminate
A=zeros(3); D=A; B=A;
for i=1:N
    % Reduced Compliance Matrix
    SLT = [1/EL(i) -vLT(i)/EL(i) 0;
          -vLT(i)/EL(i) 1/ET(i) 0;
          0 0 1/GLT(i)];
    QLT = inv(SLT);                % Reduced Stiffness Matrix
    hi=0;
    a=((-1)^i)*th; % Since for Tbar theta=-theta
    hi=-HH/2+sum(h(1:i)); hj=hi-h(i);
    m=cos(a); n=sin(a);
    Tbar=[ m^2 n^2 2*m*n;
           n^2 m^2 -2*m*n;
          -m*n m*n m^2-n^2]; %Transformation Matrix
    Qp=Tbar * QLT;
    A=A+(Qp*(hi-hj));
    D=D+(1/3)*Qp*(hi^3-hj^3);
end

a = inv(A); d = inv(D);
% Equivalent membrane elastic constants
Exx = 1/(HH*a(1,1));
Eyy = 1/(HH*a(2,2));
Gxy = 1/(HH*a(3,3));
vxy = -a(1,2)/a(1,1);
vyx = -a(1,2)/a(2,2);
```

```
211
212 % Equivalent bending elastic constants
213 Exx_M = 12/(HH^3*d(1,1));
214 Eyy_M = 12/(HH^3*d(2,2));
215 Gxy_M = 12/(HH^3*d(3,3));
216 vxy_M = -d(1,2)/d(1,1);
217 vyx_M = -d(1,2)/d(2,2);
218
219 Constant = {'Membrane'; 'Bending'};
220 Ex       = [Exx; Exx_M];
221 Ey = [Eyy; Eyy_M];
222 G = [Gxy; Gxy_M];
223 v_xy = [vxy; vxy_M];
224 v_yx = [vyx; vyx_M];
225 Shell = table(Constant, Ex, Ey, G, v_xy, v_yx)
226
227 Exx
228 Exxx = A(1,1)/HH
```

B

Appendix: Bridge deck

Bridge deck

$w_x := 1.9m$ *Iterated span length of the bridge deck.*

$L_x := 20m$ *Total span length as in figure 2.*

$b := 604.3mm$ *Values taken from figure 3.*

$h := 80mm$

$mass := 11.2\frac{kg}{m}$

$I := 6.82 \cdot 10^6 mm^4$

$E := 17140MPa$

$$q_{fk} := \begin{cases} 5\frac{kN}{m^2} & \text{if } 2\frac{kN}{m^2} + \frac{120\frac{kN}{m}}{w_x + 30m} \le 5\frac{kN}{m^2} \\ 5\frac{kN}{m^2} & = 5 \cdot \frac{kN}{m^2} \end{cases}$$ *Iterated depending on w_x*

$$w_x := \left(\frac{384 \cdot E \cdot I}{400 \cdot 5 \cdot q_{fk} \cdot b}\right)^{\frac{1}{3}} = 1.951 \cdot m$$

$w_x := 1.9m$ *This is the maximum span length for the bridge deck.*

$$\delta_{requirement} := \frac{w_x}{400} = 4.75 \cdot mm \qquad \delta_{max} := \frac{5 q_{fk} \cdot b \cdot w_x^4}{384 \cdot E \cdot I} = 4.386 \cdot mm$$ *OK*

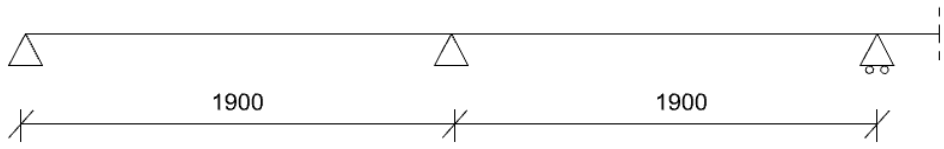

Figure 1: 1900 mm is the maximum length that the bridge deck could span.

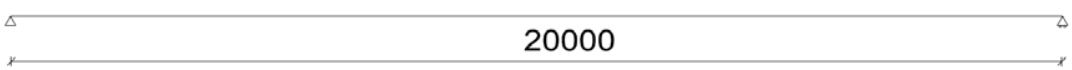

Figure 2: Total span length of the bridge

Structural Component Mechanical Properties (minimum)

PROPERTIES	ASTM TEST METHOD	VALUE ksi (N/mm²)
Flexural Strength, LW	D790	24.5 (168.9)
Flexural Strength, CW	D790	8.2 (56.5)
Flexural Modulus, LW	D790	885.0 (6101.9)
Flexural Modulus, CW	D790	646.0 (4454.0)
Tensile Strength, LW	D638	31.1 (214.4)
Tensile Modulus, LW	D638	2486.0 (17140.4)
Short Beam Shear, LW	D2344	3.19 (22.0)
Note: All values are minimum ultimate properties from coupon tests.		

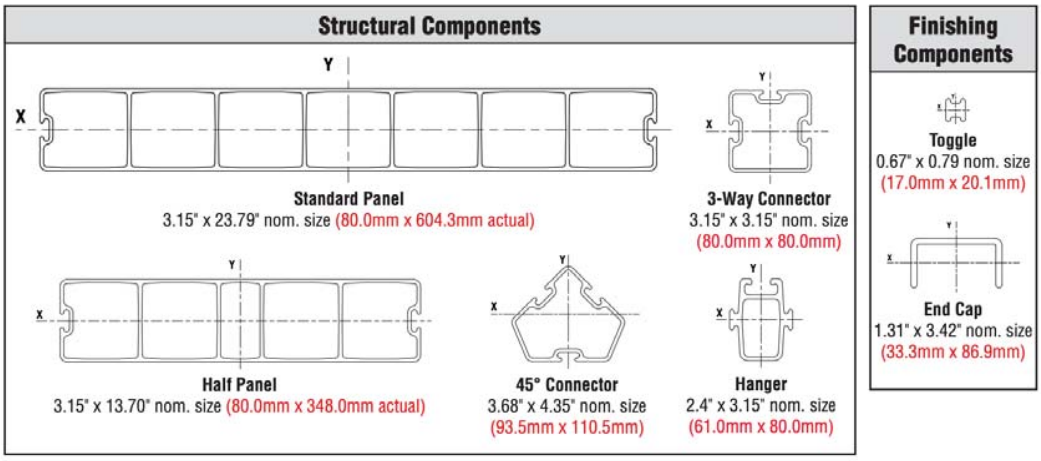

Section Properties

SHAPE	WEIGHT LB/LIN. FT (KG/M)	I_x IN⁴ (MM⁴)	S_x IN³ (MM³)	r_x IN (MM)	I_y IN⁴ (MM⁴)	S_y IN³ (MM³)	r_y IN (MM)	A IN² (MM²)	Aw_x IN² (MM²)	Aw_y IN² (MM²)
Panel	7.22 (11.19)	16.39 (6.82×10^6)	10.41 (1.71×10^5)	1.31 (33.16)	510.28 (2.12×10^8)	21.45 (0.167×10^6)	7.28 (185.00)	9.62 (6206)	3.13 (2020)	6.49 (4186)

Figure 3: Strength parameters and geometry of the bridge deck.

C

Appendix: Modelling

Modelling

The material data is taken from the SANDIA REPORT: "The Sandia 100-meter All-glass Baseline Wind Turbine Blade: SNL100-00" and calculations of the equivalent material properties can be seen in Appendix: Lamination Theory. A parametic study was performed due to uncertainties regarding the thickness. Calculations were done for three different thicknesses (25%, 33% and 50% of the total thickness), hence three analysis were performed for the SLS analysis as well as the frequency analysis.

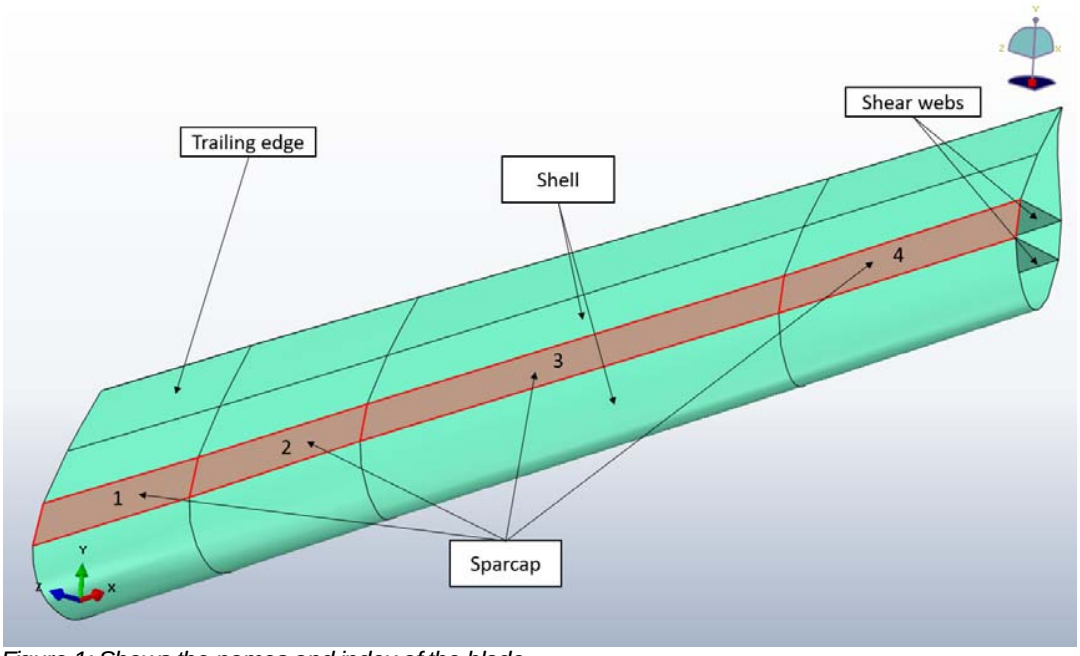

Figure 1: Shows the names and index of the blade.

The strength parameters are reduced due to temperature, humudity and fatigue in accordance to "Prospect for new guidance in design of FRP" Table 2.4. The conversion factor is applied in both the momentary deformation as well as in the comfort analysis.

$$\eta_c := \eta_{ct} \cdot \eta_{cm} \cdot \eta_{cf} \quad (2.6)$$

$\eta_{ct} := 1.0$

$\eta_{cm} := 0.8$

$\eta_{cf} := 0.9$

$\eta_c := \eta_{ct} \cdot \eta_{cm} \cdot \eta_{cf} = 0.72$

$$X_d := \eta_c \cdot \frac{X_k}{\gamma_M} \quad (2.3)$$

$\gamma_M := 1.0$

SparCap E-LT-5500/EP-3

$$\rho_{sc} := 1920\frac{kg}{m^3} = 1.92 \times 10^{-9}\cdot\frac{tonne}{mm^3}$$

$$E_{xsc} := \frac{\eta_c}{\gamma_M}\cdot 3.6621\cdot 10^{10}Pa = 2.637 \times 10^{4}\cdot MPa$$

$$E_{ysc} := \frac{\eta_c}{\gamma_M}\cdot 1.3947\cdot 10^{10}Pa = 1.004 \times 10^{4}\cdot MPa$$

$$G_{sc} := \frac{\eta_c}{\gamma_M}\cdot 4.3221\cdot 10^{9}Pa = 3.112 \times 10^{3}\cdot MPa$$

$$v_{xysc} := 0.3214$$

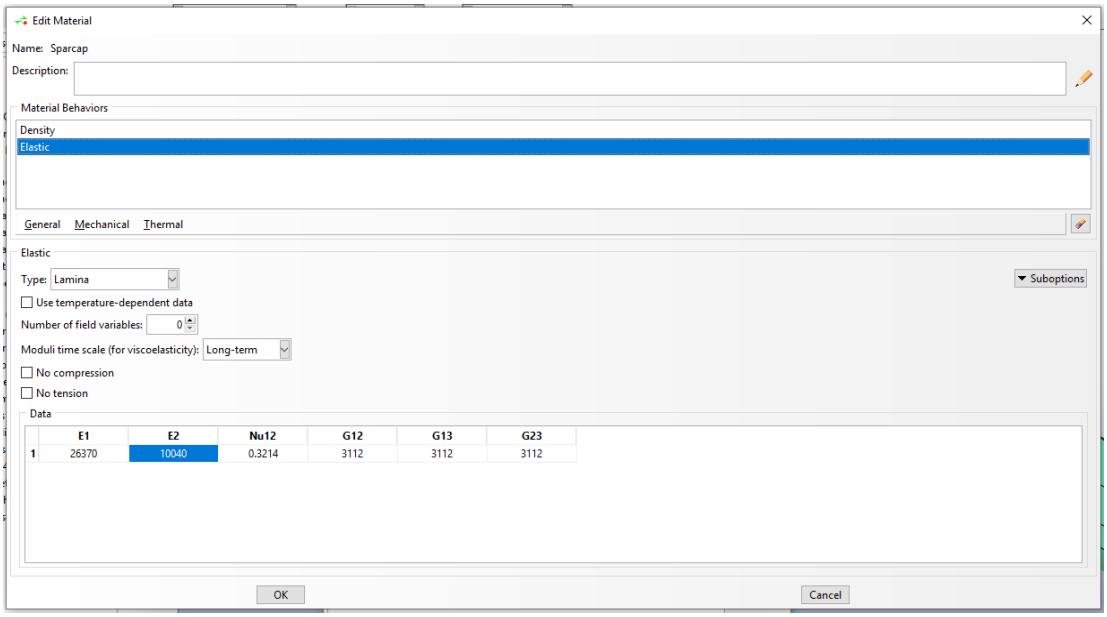

Figure 2: The material parameters were defined as elastic and the type used was lamina.

25%

$$t_{0.25sc1} := 30.9mm$$

$$t_{0.25sc2} := 28.8mm$$

$$t_{0.25sc3} := 24.5mm$$

$$t_{0.25sc4} := 18.6mm$$

33%

$$t_{0.3sc1} := 41.2mm$$

$$t_{0.3sc2} := 38.3mm$$

$$t_{0.3sc3} := 32.7mm$$

$$t_{0.3sc4} := 24.8mm$$

50%

$$t_{0.5sc1} := 61.8mm$$

$$t_{0.5sc2} := 57.5mm$$

$$t_{0.5sc3} := 49mm$$

$$t_{0.5sc4} := 37.3mm$$

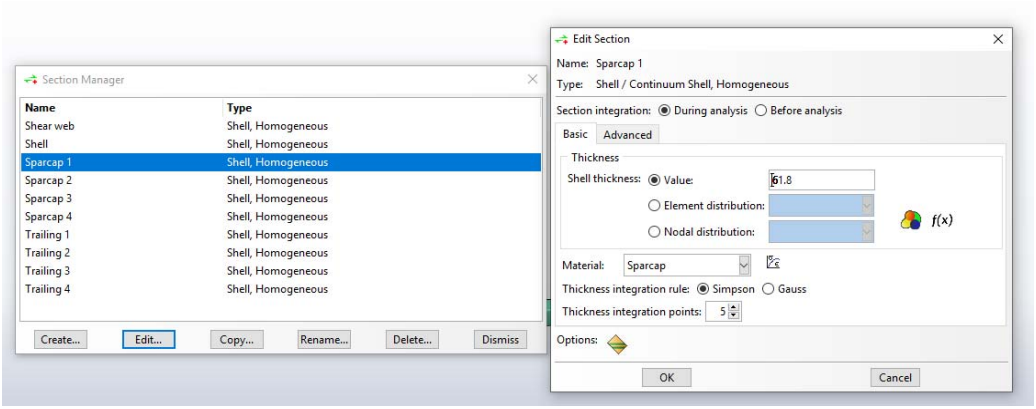

Figure 3: In the section manager the thicknesses and material of each part was defined. Since calculations were done for three different thicknesses (25%, 33% and 50% of the total thickness), three analyses were made.

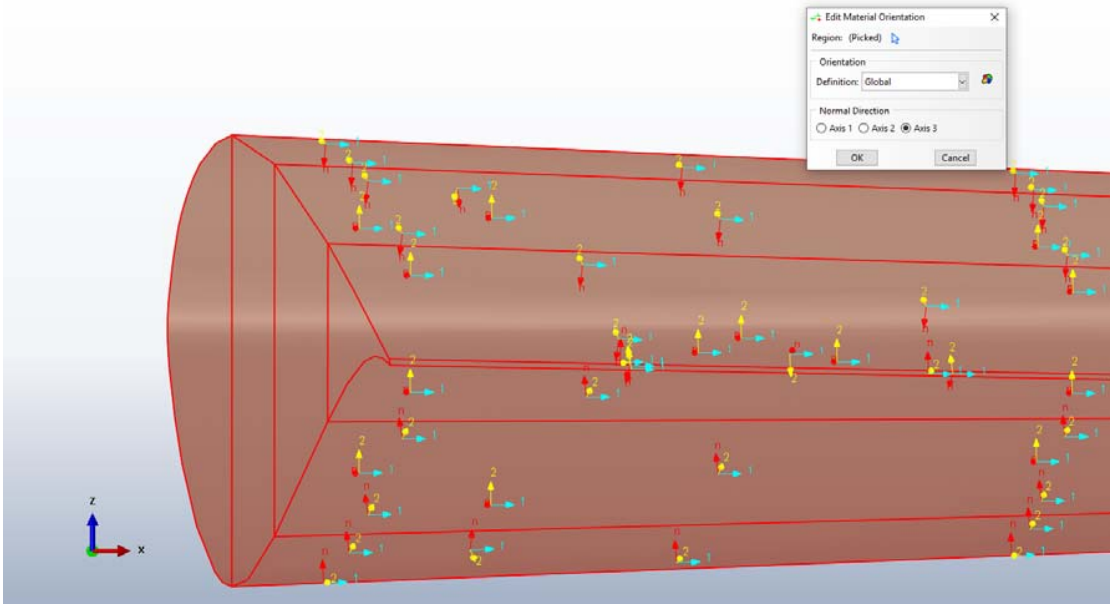

Figure 4: The material orientation was set to "Axis 3".

Shell Saertex/EP-3

$$\rho_{sh} := 1780\frac{kg}{m^3} = 1.78 \times 10^{-9}\cdot\frac{tonne}{mm^3}$$

$$E_{xsh} := \frac{\eta_c}{\gamma_M}\cdot 1.2474\cdot 10^{10}Pa = 8.981 \times 10^{3}\cdot MPa$$

$$E_{ysh} := \frac{\eta_c}{\gamma_M}\cdot 7.2813\cdot 10^{9}Pa = 5.243 \times 10^{3}\cdot MPa$$

$$G_{sh} := \frac{\eta_c}{\gamma_M}\cdot 2.6797\cdot 10^{9}Pa = 1.929 \times 10^{3}\cdot MPa$$

$$v_{xysh} := 0.36236$$

25%

$t_{0.25sh} := 15mm$

33%

$t_{0.3sh} := 20mm$

50%

$t_{0.5sh} := 30mm$

Trailing edge

$$T_r := 200\frac{kg}{m^3}\,0.060m + 1920\frac{kg}{m^3}\cdot 0.060m = 127.2\frac{kg}{m^2}$$

$$\rho_{tr} := \frac{T_r}{(0.080m + 0.060m)} = 9.086 \times 10^{-10}\cdot\frac{tonne}{mm^3}$$

$$E_{xtr} := \frac{\eta_c}{\gamma_M}\cdot 3.5048\cdot 10^{10}Pa = 2.523 \times 10^{4}\cdot MPa$$

$$E_{ytr} := \frac{\eta_c}{\gamma_M}\cdot 1.2951\cdot 10^{10}Pa = 9.325 \times 10^{3}\cdot MPa$$

$$G_{tr} := \frac{\eta_c}{\gamma_M}\cdot 3.4827\cdot 10^{9}Pa = 2.508 \times 10^{3}\cdot MPa$$

$$v_{xytr} := 0.30638$$

25%

$t_{0.25tr1} := 17.5mm$

$t_{0.25tr2} := 13.1mm$

$t_{0.25tr3} := 6.1mm$

$t_{0.25tr4} := 3.5mm$

33%

$t_{0.3tr1} := 23.3mm$

$t_{0.3tr2} := 17.5mm$

$t_{0.3tr3} := 8.2mm$

$t_{0.3tr4} := 4.7mm$

50%

$t_{0.5tr1} := 35mm$

$t_{0.5tr2} := 26.3mm$

$t_{0.5tr3} := 12.3mm$

$t_{0.5tr4} := 7mm$

Shear web

$$S_w := 200\,\frac{kg}{m^3}\,0.080m + 1780\,\frac{kg}{m^3}\cdot 0.060m = 122.8\,\frac{kg}{m^2}$$

$$\rho_{sw} := \frac{S_w}{(0.080m + 0.060m)} = 8.771 \times 10^{-10}\cdot\frac{tonne}{mm^3}$$

$$E_{xsw} := \frac{\eta_c}{\gamma_M}\cdot 1.4146\cdot 10^{10}Pa = 1.019 \times 10^{4}\cdot MPa$$

$$E_{ysw} := \frac{\eta_c}{\gamma_M}\cdot 1.1874\cdot 10^{10}Pa = 8.549 \times 10^{3}\cdot MPa$$

$$G_{sw} := \frac{\eta_c}{\gamma_M}\cdot 9.1532\cdot 10^{9}Pa = 6.59 \times 10^{3}\cdot MPa$$

$$v_{xysw} := 0.48707$$

25%

$t_{0.25sw} := 21mm$

33%

$t_{0.3sw} := 28.7mm$

50%

$t_{0.5sw} := 43mm$

Loads acting on the deck

$L := 20m$ *Span length*

$w := \frac{4}{2}m = 2\,m$ *Width for half the bridge deck*

Width of the sparcap where the loads are assumed to be distributed, varies along the blade length.

$w_{spar1} := \frac{694mm + 617mm}{2}$ $w_{spar2} := \frac{617mm + 534mm}{2}$

$w_{spar3} := \frac{534mm + 472mm}{2}$ $w_{spar4} := \frac{472mm + 450mm}{2}$

Permanent Loads

Bridge deck: "COMPOSOLITE" from STRONGWELL

$w_{panel} := 604.3mm$

$m_{panel} := 11.2\frac{kg}{m}$

$w_{deck} := 2000mm$

$m_{deck} := \frac{m_{panel} \cdot w_{deck}}{w_{panel}} = 37.068\frac{kg}{m}$

$q_{deck} := m_{deck} \cdot g = 0.364 \cdot \frac{kN}{m}$

Surface

$h_{surface} := 5mm$

$q_{acrylate} := 22\frac{kN}{m^3}$ *Krav Brobyggande B.3.1.1*

$q_{surface} := q_{acrylate} \cdot h_{surface} \cdot w = 0.22 \cdot \frac{kN}{m}$

Polyurethane

$\rho_{poly} := 1.2 \cdot 10^{-3}\frac{kg}{cm^3} = 1.2 \times 10^{-9} \cdot \frac{tonne}{mm^3}$

$l_{poly} := 20cm$ $h_{poly} := 20cm$ $w_{poly} := 1.8m$ $n := 11$

$q_{poly} := \frac{\rho_{poly} \cdot g \cdot l_{poly} \cdot h_{poly} \cdot w_{poly} \cdot n}{L} = 0.466 \cdot \frac{kN}{m}$

Railing

$q_{railing} := 50g\frac{kg}{m} = 0.49 \cdot \frac{kN}{m}$

Total permanent load acting on the sparcap

The sparcap is divided into four areas since the thickness and width varies.

$$q_g := q_{deck} + q_{surface} + q_{railing} + q_{poly} = 1.54 \cdot \frac{kN}{m}$$

For the frequency analysis the loads where applied at the sparcap as densities. It is only the permanent loads that affects the fundamental frequency but it is important to also add the self weight from the bridge deck, acrylate, polyurethane and the railing. Therefore, the total permanent load was calculated and then applied as a density.

25%

$$\rho_{0.25gsc1} := \rho_{sc} + \frac{q_g}{w_{spar1} \cdot t_{0.25sc1} \cdot g} = 9.672 \times 10^{-9} \cdot \frac{tonne}{mm^3}$$

$$\rho_{0.25gsc2} := \rho_{sc} + \frac{q_g}{w_{spar2} \cdot t_{0.25sc2} \cdot g} = 1.139 \times 10^{-8} \cdot \frac{tonne}{mm^3}$$

$$\rho_{0.25gsc3} := \rho_{sc} + \frac{q_g}{w_{spar3} \cdot t_{0.25sc3} \cdot g} = 1.466 \times 10^{-8} \cdot \frac{tonne}{mm^3}$$

$$\rho_{0.25gc4} := \rho_{sc} + \frac{q_g}{w_{spar4} \cdot t_{0.25sc4} \cdot g} = 2.023 \times 10^{-8} \cdot \frac{tonne}{mm^3}$$

33%

$$\rho_{0.3gsc1} := \rho_{sc} + \frac{q_g}{w_{spar1} \cdot t_{0.3sc1} \cdot g} = 7.734 \times 10^{-9} \cdot \frac{tonne}{mm^3}$$

$$\rho_{0.3gsc2} := \rho_{sc} + \frac{q_g}{w_{spar2} \cdot t_{0.3sc2} \cdot g} = 9.044 \times 10^{-9} \cdot \frac{tonne}{mm^3}$$

$$\rho_{0.3gsc3} := \rho_{sc} + \frac{q_g}{w_{spar3} \cdot t_{0.3sc3} \cdot g} = 1.147 \times 10^{-8} \cdot \frac{tonne}{mm^3}$$

$$\rho_{0.3gc4} := \rho_{sc} + \frac{q_g}{w_{spar4} \cdot t_{0.3sc4} \cdot g} = 1.565 \times 10^{-8} \cdot \frac{tonne}{mm^3}$$

50%

$$\rho_{0.5gsc1} := \rho_{sc} + \frac{q_g}{w_{spar1} \cdot t_{0.5sc1} \cdot g} = 5.796 \times 10^{-9} \cdot \frac{tonne}{mm^3}$$

$$\rho_{0.5gsc2} := \rho_{sc} + \frac{q_g}{w_{spar2} \cdot t_{0.5sc2} \cdot g} = 6.665 \times 10^{-9} \cdot \frac{tonne}{mm^3}$$

$$\rho_{0.5gsc3} := \rho_{sc} + \frac{q_g}{w_{spar3} \cdot t_{0.5sc3} \cdot g} = 8.291 \times 10^{-9} \cdot \frac{tonne}{mm^3}$$

$$\rho_{0.5gc4} := \rho_{sc} + \frac{q_g}{w_{spar4} \cdot t_{0.5sc4} \cdot g} = 1.105 \times 10^{-8} \cdot \frac{tonne}{mm^3}$$

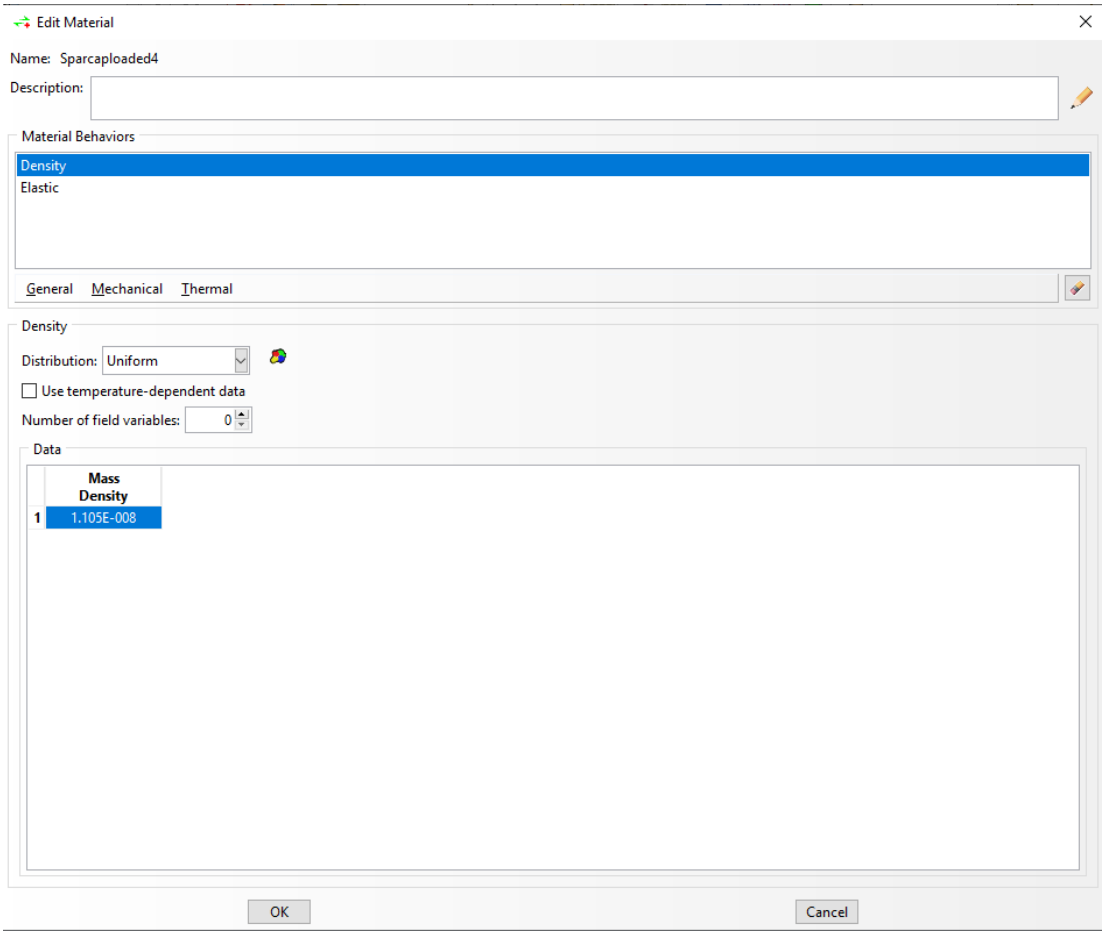

Figure 5: In the frequency analysis the permanent loads were applied as densities.

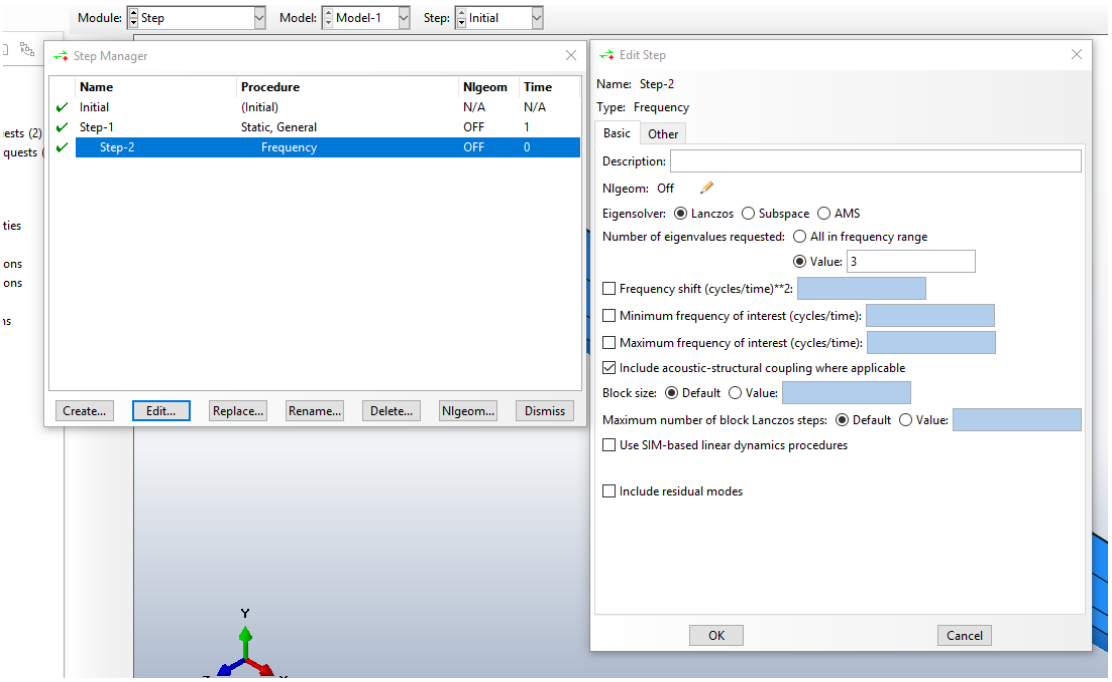

Figure 6: In the initial step the boundary conditions were applied. In Step-1 the permanent loads were applied and in Step-2 the frequency was calculated.

Variable Loads

Crowd load *SS_EN-1991_2_EN*

$$q_{fk} := 2\frac{kN}{m^2} + \frac{120\frac{kN}{m}}{L + 30m} = 4.4\cdot\frac{kN}{m^2} \qquad q_{fk} \le 5 \qquad (5.1)$$

$$q_{fksc} := q_{fk}\cdot w = 8.8\cdot\frac{kN}{m}$$

Load combinations SLS: SS-EN 1990/A1:2005

A.2.4.2: Frequent load combination: "The frequent combination of actions is recommended for the assessment of deformation."

$$G + \Sigma\psi_{1.SLS} \cdot Q$$

$\psi_{1SLS} := 0.4$ *Tab: A2.2*

Krav Brobyggande
TDOK 2016:0204
Version 3.0:
Vertikal defomation av variabel last får ej överskrida 1/400 av den teoretiska spännvidden. (B.3.4.2.2)
This means that the self-weight is not included in the control of defomation and hence it is only the variable load that is a part of this load combination.

$$q_{1.SLS} := \psi_{1SLS} \cdot \frac{q_{fksc}}{w_{spar1}} = 5.37 \times 10^{-3} \cdot MPa$$

$$q_{2.SLS} := \psi_{1SLS} \cdot \frac{q_{fksc}}{w_{spar2}} = 6.116 \times 10^{-3} \cdot MPa$$

$$q_{3.SLS} := \psi_{1SLS} \cdot \frac{q_{fksc}}{w_{spar3}} = 6.998 \times 10^{-3} \cdot MPa$$

$$q_{4.SLS} := \psi_{1SLS} \cdot \frac{q_{fksc}}{w_{spar4}} = 7.636 \times 10^{-3} \cdot MPa$$

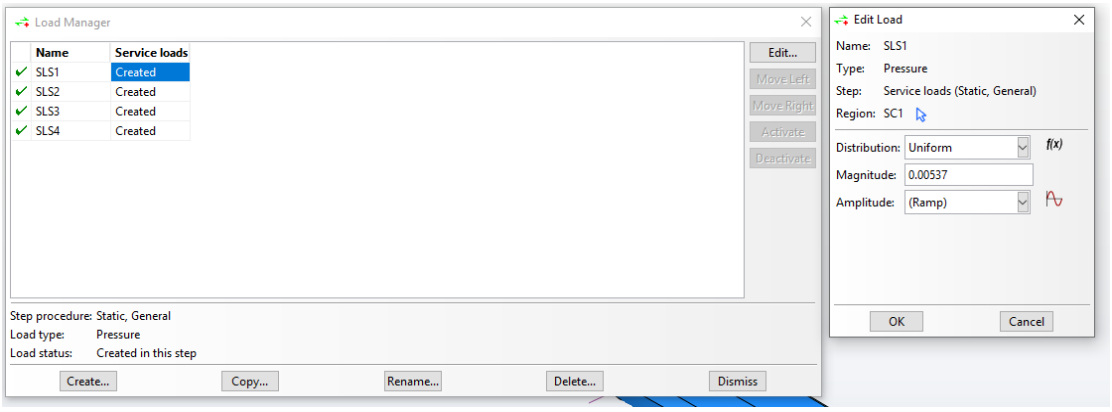

Figure 7: The variable load were applied at the four sparcaps. The boundary conditions were applied in the initial step whilst the variable load was applied in the next step.

Boundary conditions

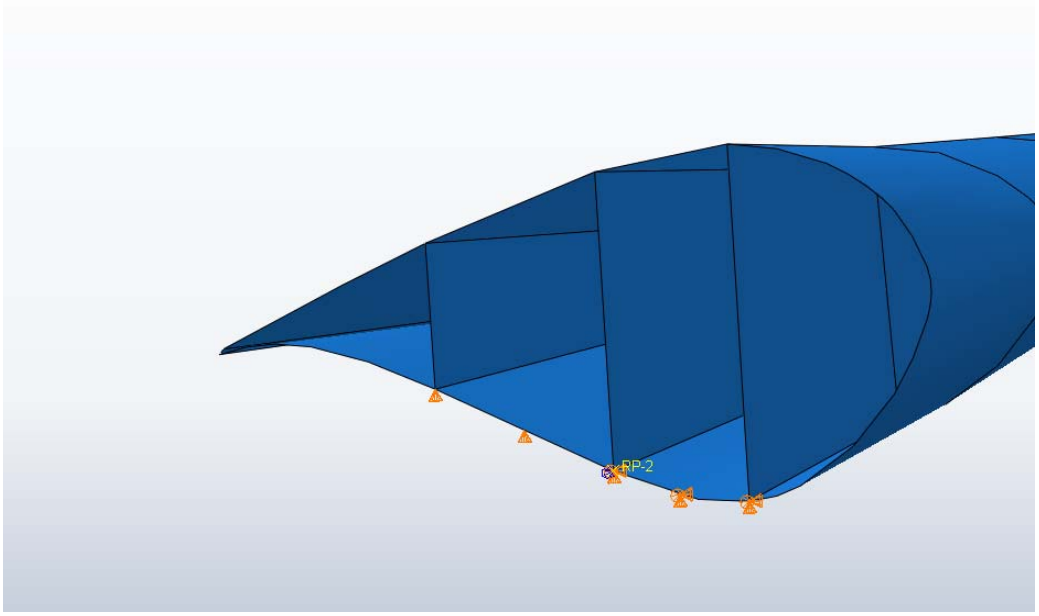

Figure 8: The boundary conditions in the bottom part of the thicker end was fixed in all directions but free to rotate. In the smaller end the bottom part was free to move in the longitudinal direction.

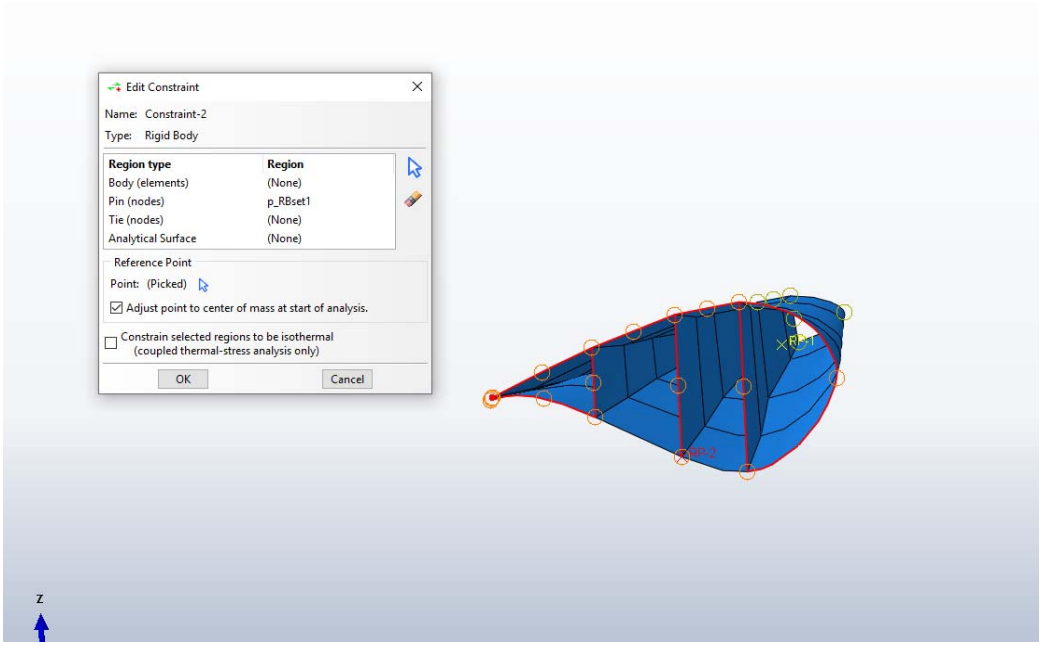

Figure 9: To avoid local buckling modes, the end is modelled as a rigid body with a tied constraint. The constraint is applied to all regions that is not modelled on the support, with a reference point in the middle shear web.

Mesh

In order to chose an adequate mesh size a convergence study were performed.

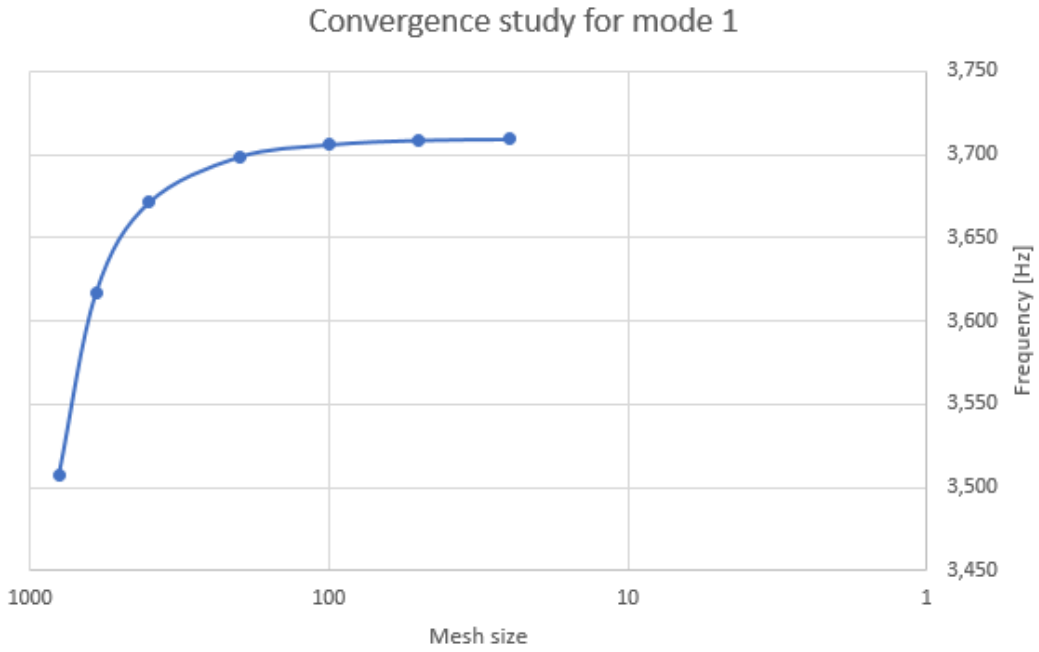

Figure 10: Convergence study for the frequency analysis. Same mesh was used for the deformation analysis as well.

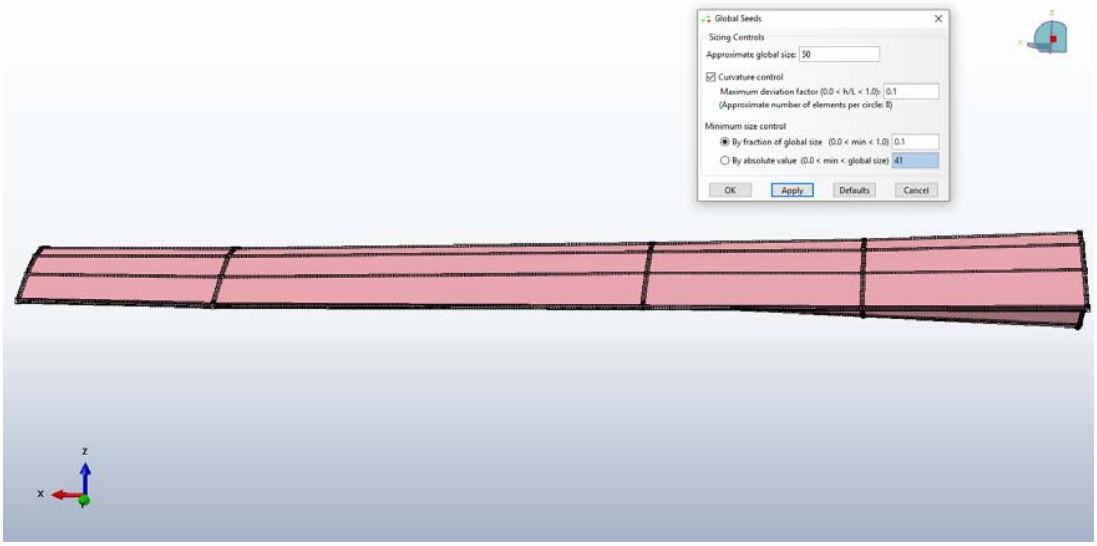

Figure 11: Generating approximate global element size 50.

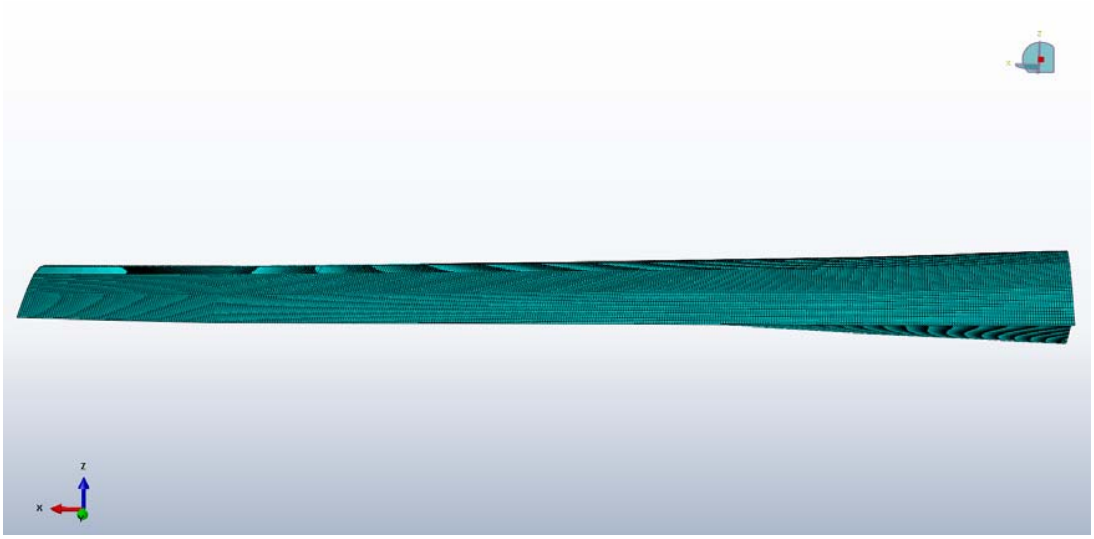

Figure 12: Shows the final mesh used in the analysis. The mesh is a Quad-dominated mesh with 83800 elements.

Verification of model

Total weight of the blade, areas obtained from Rhino. The verification is made from the blade with 50% of the total thickkness.

$A_{sc} := 21914099mm^2 \qquad A_{sw} := 50413233mm^2 \qquad A_{sh} := 82468854mm^2 \qquad A_{tr} := 32812856mm^2$

$$mass := A_{sc}\cdot\left(\frac{t_{0.5sc1} + t_{0.5sc2} + t_{0.5sc3} + t_{0.5sc4}}{4}\right)\cdot\rho_{sc} + A_{sw}\cdot t_{0.5sw}\cdot\rho_{sw} + A_{sh}\cdot t_{0.5sh}\cdot\rho_{sh} \cdots + A_{tr}\cdot\frac{\left(t_{0.5tr1} + t_{0.5tr2} + t_{0.5tr3} + t_{0.5tr4}\right)}{4}\cdot\rho_{tr}$$

$mass = 9.069 \times 10^3\,kg \qquad F_{blade} := mass\cdot g = 88.933\cdot kN$

$F_{reaction} := mass\cdot g + q_g\cdot L = 119.73\cdot kN$

Compared to BRIGADE/Plus:
117.02 kN

The deflection were also roughly calculated to verify the model.

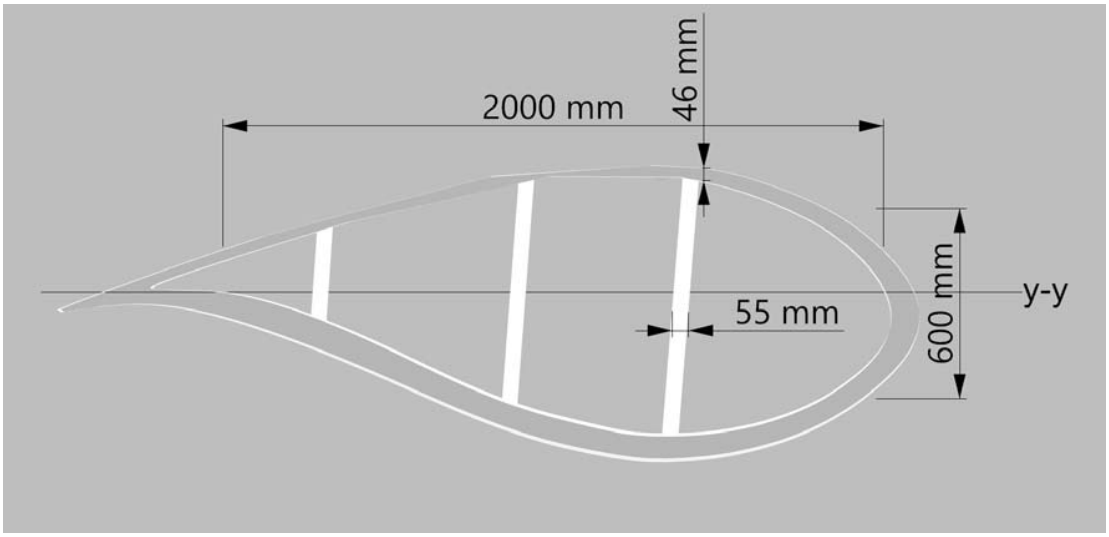

Figure 13: Shows the dimensions used to roughly calculate the moment of inertia.

$$I_{yy} := 3\,\frac{55mm\cdot(600mm)^3}{12}\ \ldots$$
$$+2\cdot\left[\frac{2000mm\cdot(46mm)^3}{12}+(2000mm\cdot 46mm)\cdot\left(\frac{600mm}{2}+\frac{46mm}{2}\right)^2\right]$$

$$I_{yy} = 2.22\times 10^{10}\cdot mm^4$$

Bear in mind that the moment of inertia is strongly dependent on where the cross section is taken and hence the model is also verified with the resultant forces.

$$E_{xsc} = 26.367\cdot GPa$$

$$\delta_{max} := \frac{5\psi_{1SLS}\cdot q_{fksc}\cdot L^4}{384\cdot E_{xsc}\cdot I_{yy}} = 12.529\cdot mm$$

Compared to BRIGADE/Plus: 12.77mm

D

Appendix: Test results from Anmet Poland

1. Results

Figure 1.1 below show photos of samples to be tested material.

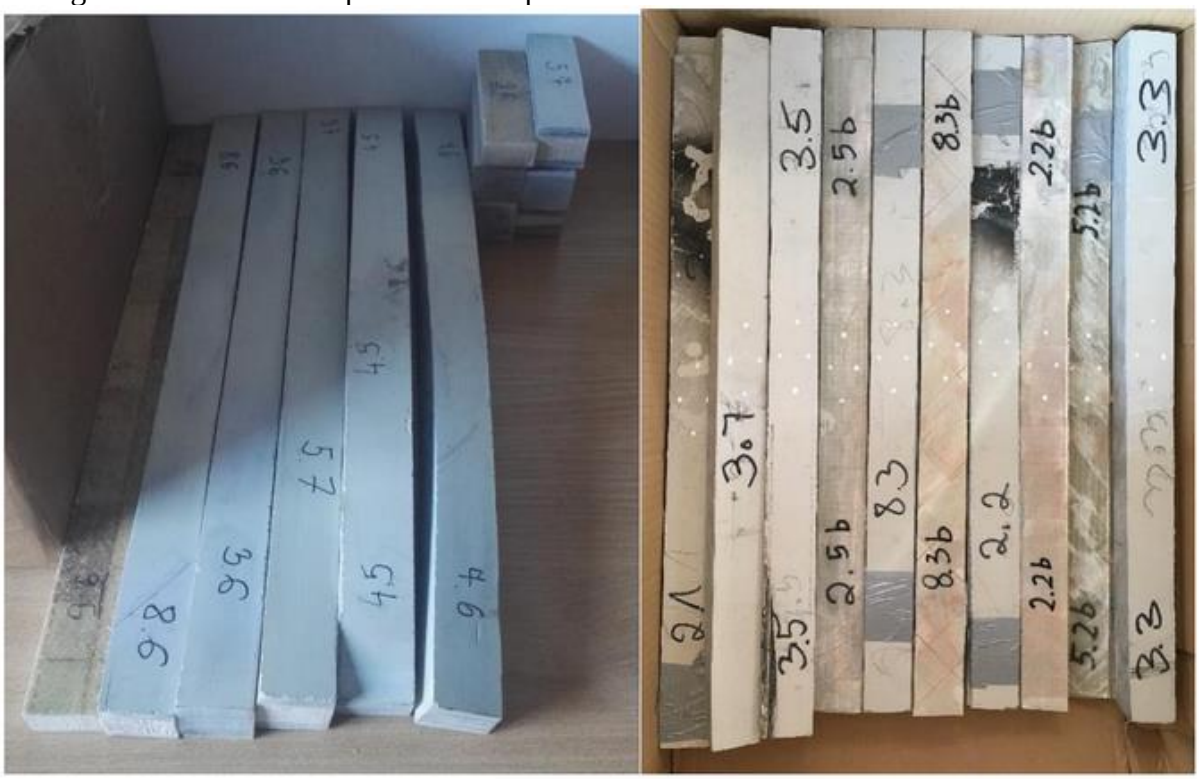

1.1. Samples intended for laboratory tests

1.1. Tensile strengh

1.1.1. Sample 3.6

The results obtained in the tensile test for sample 3.6 are shown in Table 1.1 and the graph of dependence load.

Tab. 1.1 Tensile test results for sample 3.6

No.	Thickness [mm]	Width [mm]	Max. strength [kN]	Endurance [MPa]	Deformation [%]	Modulus [GPa]	Poisson's ratio [-]
3.6	29,70	34,76	464,52	449,84	1,52	34,18	0,42
NOTES: Test without pads, damage near the jaws of the machine.							

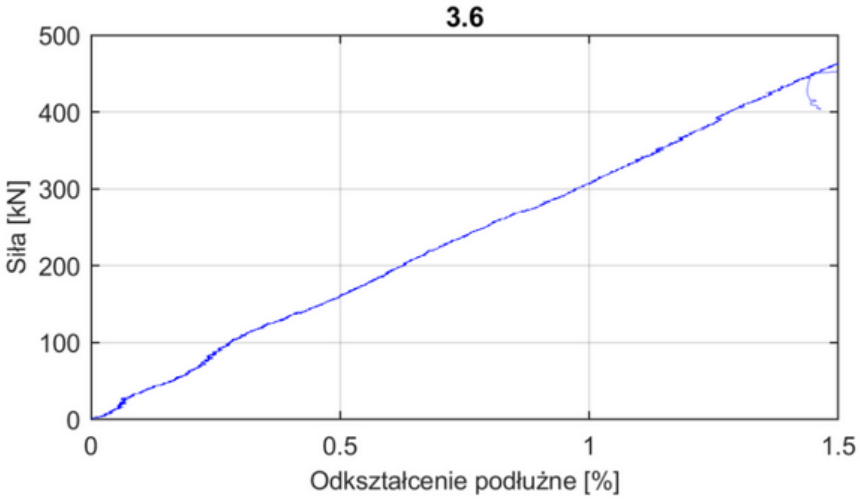

1.4. Load - longitudinal deformation for the sample 3.6

1.5. Form of sample destruction 3.6

1.1.2. Sample 4.5

The results obtained in the tensile test for sample 4.5 are shown in Table 1.2 and the graph of dependence load.

Tab. 1.2 Tensile test results for sample 4.5

No.	Thickness [mm]	Width [mm]	Max. strength [kN]	Endurance [MPa]	Deformation [%]	Modulus [GPa]	Poisson's ratio [-]
4.5	35,90	36,75	69,76	52,87	1,17	8,39	0,26
NOTES: Curved sample, clamped in jaws perpendicular to the reinforcement values, test without overlays.							

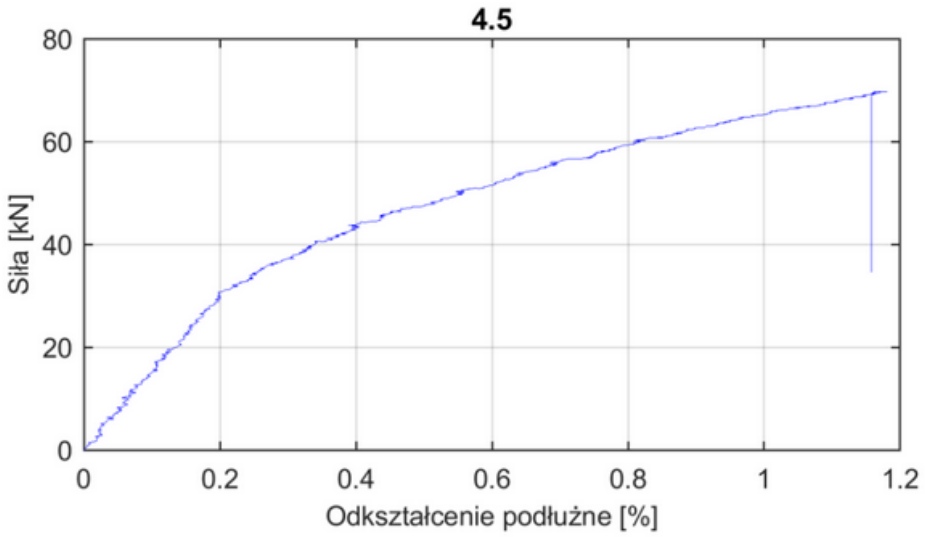

1.6. Load - longitudinal deformation for the sample 4.5

1.7. Form of sample destruction 4.5

1.1.3. Sample 5.7

The results obtained in the tensile test for sample 5.7 are shown in Table 1.2 and the graph of dependence load.

Tab. 1.3 Tensile test results for sample 5.7

No.	Thickness [mm]	Thickness of external laminates [mm]	Width [mm]	Max. strength [kN]	Endurance [MPa]	Deformation [%]	Modulus [GPa]
5.7	33,47	8,10+7,00	34,81	179,78	341,87	1,51	19,92
NOTES: Sample with interlayer material (balsa), filling material omitted in the analysis, examination without overlays, destruction by crushing in the jaws of the machine, the module was determined for the section 100-140 kN.							

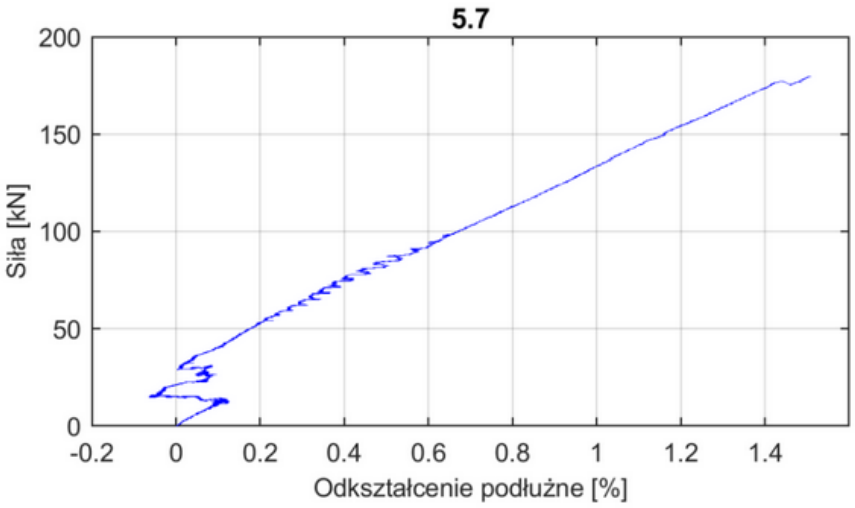

1.8. Load - longitudinal deformation for the sample 5.7

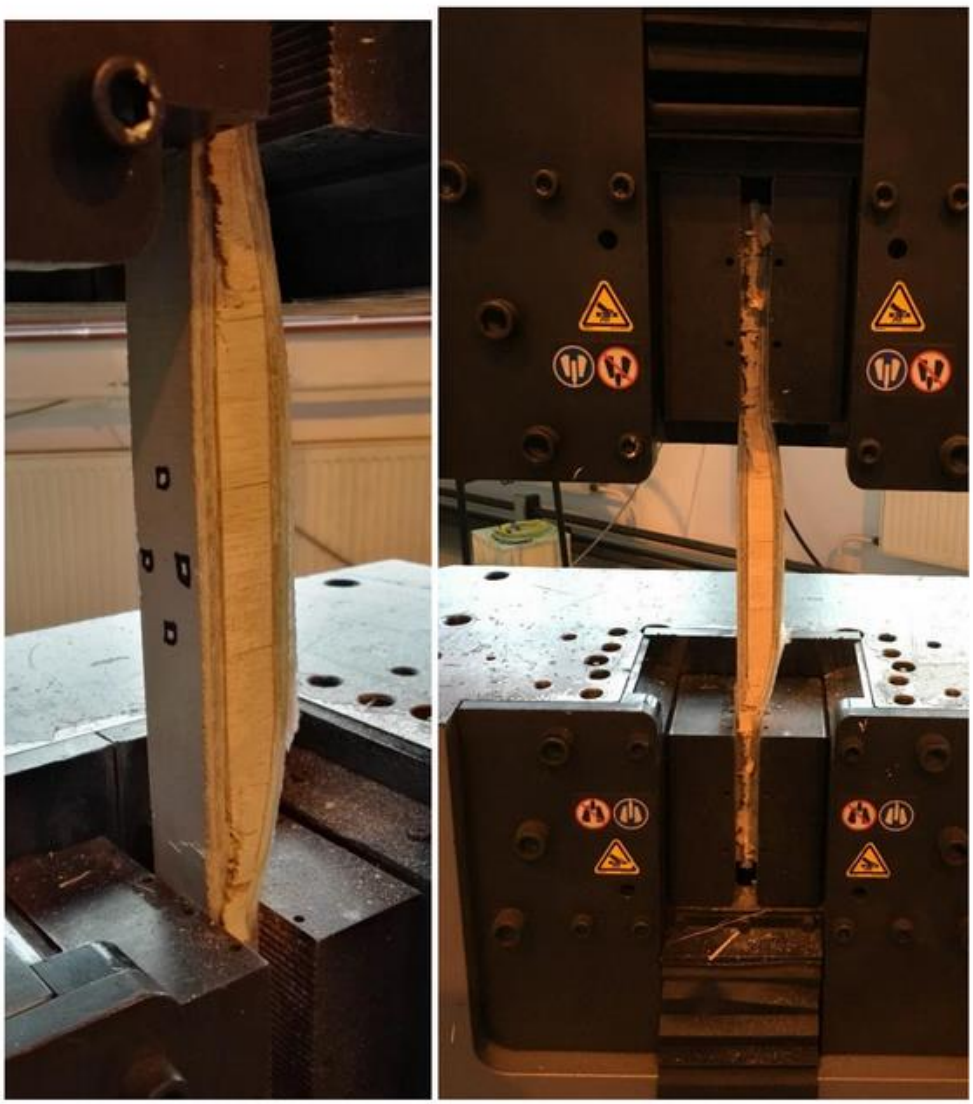

1.9. Form of sample destruction 5.7

1.2. Compression tests

The compression test was limited to two solid samples.

1.2.1. Sample 3.6

The results obtained in the compression test for sample 3.6 are shown in Table 1.7 while the form of sample destruction in Fig. 1.13.

Tab.1.7. Test results of compression test for sample 3.6

No.	Thickness [mm]	Width [mm]	Max. strength [kN]	Endurance [MPa]
3.6	31,26	35,31	417,90	378,60
NOTES: Test without pads, damage near the caliper.				

1.16. Form of destruction of sample 3.6 in the compression test

1.2.2. Sample 4.5

The results obtained in the compression test for sample 4.5 are shown in Table 1.8 while the form of sample destruction in Fig. 1.17.

Tab.1.7. Test results of compression test for sample 4.5

No.	Thickness [mm]	Width [mm]	Max. strength [kN]	Endurance [MPa]
4.5	31,49	35,77	350,07	310,79
NOTES: Test without pads.				

1.17. Form of destruction of sample 3.6 in the compression test